# The Taxonomy of the North American Species of *Parameletus* Bengtsson, 1908 (Ephemeroptera: Siphlonuridae), with Keys to Nymphs and Male Imagos

Steven K. Burian

Department of Biology, Southern Connecticut State University, 501 Crescent St., New Haven, CT USA 06515, burians1@southernct.edu

**Abstract**

In North America, the Holarctic genus *Parameletus* Bengtsson is widely distributed across the northern tier of the continent and parts of the Rocky Mountains. Four species occur in North America (*Parameletus chelifer*, *P. columbiae*, *P. croesus*, and *P. midas*) with *P. chelifer* having the greatest range and currently the only species of *Parameletus* detected broadly across the subarctic of Canada. In this paper, new detailed comparative descriptions are provided for nymphs and imagos. The nymph of *P. croesus* is described for the first time. A final instar nymph of *P. croesus* was positively associated with the male imago stage based on the observation of diagnostic characters of the male imago through the cuticle of the last instar nymph. New illustrated keys to male imagos and late instar nymphs are presented. New distribution records are presented and geographic variation in diagnostic characters of species is discussed. New information on the aquatic habitats of nymphs and the biology of species is presented.

Published online: November 1, 2017

## Introduction

Among the mayflies of higher latitudes (i.e., 50°–70°N ) of the Northern Hemisphere, species of the genus *Parameletus* Bengtsson are conspicuous, widespread, and ecologically important (McDunnough 1923, 1930, 1938, Edmunds 1952, 1957, Harper and Harper 1981, Söderstrom 1988, Söderstrom and Nilsson 1986, 1987, Giberson *et al.* 2007, and Tiunova 2008). The genus *Parameletus* was described from Sweden by Bengtsson (1908) and since then it has been the subject of many studies (Bengtsson 1909, Esben-Petersen 1916, McDunnough 1923, 1930, 1938, Traver 1935, Speith 1938, Daggy 1941, Edmunds 1952, 1957, Brinck 1957, Edmunds *et al.* 1976, Hubbard 1977, Söderstrom and Nilsson 1986, 1987, Studemann and Tomka 1991, Tiunova 2008, and Webb *et al.* 2012). Historically, the complex nomenclatural history of *Parameletus* produced much confusion as to the validity of the genus and its type species. Hubbard (1977) reviewed and clarified the nomenclature of *Parameletus* and *P. chelifer* (its type species) and thereby produced the current level of taxonomic stability for *Parameletus*. All previous synonyms for *Parameletus* were listed by Hubbard (1977) and there have been no new additions to his list. Despite stability in the genus name there have been continuing problems concerning the taxonomy of its species.

In North America species of the *Parameletus* are known mostly from the male imago, but this life stage is rarely collected. Currently 4 species of *Parameletus* are known from North America, 3 restricted to the Nearctic (*P. columbiae* McDunnough, *P. croesus* (McDunnough), and *P. midas* (McDunnough)) and 1 that is Holarctic (*P. chelifer* Bengtsson). Although the imagos of all 4 species and the nymphs of all but 1 species of North American *Parameletus* have been variously described and partially figured (McDunnough, 1923, 1938, Traver 1935, Spieth 1938, Daggy 1941, Edmunds 1952, Jensen 1966, Söderstrom and Nilsson 1986, and Tiunova 2008) the taxonomic treatments are incomplete and not comparable. There are no comprehensive keys to imagos or nymphs. Consequently, because the appropriate taxonomic tools were lacking, we know little about the life history, ecology, or distribution of *Parameletus* species.

The earliest account of *Parameletus* in North America was given by McDunnough (1923) where he described both *P. croesus* and *P. midas* in a single paper. Even though McDunnough (1923) did include basic outline drawings of the male genitalia of these species, the lack of detail greatly limited their usefulness. The species accounts of *P. croesus* and *P. midas* focused mostly on details of color and color patterns of male imagos with female imagos receiving similar, but briefer treatment. McDunnough (1930) later provided additional details of the nymph of *P. midas* and indicated that the reader should compare his figures of the gill and mouthparts of *P. midas* to those of *P. chelifer* presented by Ebsen-Petersen (1916). Unfortunately, McDunnough's figures (as well as those by Ebsen-Petersen) were too rudimentary to be used for any detailed comparison. Traver (1935) redescribed the male imago of *P. midas* and *P. croesus* (despite admitting that she was only able to study specimens of *P. midas*) and provided a key that relied on the use of pigmentation

of the forewing membrane to separate these species. Traver (1935) did provide figures of the wings and male genitalia of *P. midas.* Although figures of the wings seem quite accurate, her figure of the male genitalia of *P. midas* has some problems. Principally Traver's figure of the genitalia *P. midas* has 3 problems (1) the transparent inner edges of the lobes of the penes lobes were omitted, (2) the figure is presented from the dorsal perspective and shows paired blunt lobes crossing under the sharp inward curving paired spines; this is incorrect because the blunt lobes are actually ventral structures and should only be indicated as dotted lines dorsally, and (3) dorsally there appears to be 2 slender sharply pointed spines with diverging tips that arise near the base of the penes; these spines do not exist and what appears as spines are actually the thick edges of the large sharp inward curving spines of the dorsal surface of the penes.

Eight years after he described *P. croesus* and *P. midas,* McDunnough (1938) described *P. columbiae* based on imagos that were collected from a swarm above a glacial stream in British Columbia, Canada. In that same paper he also noted the first North American record of *P. chelifer* based on imagos collected from Churchill, Manitoba, Canada. In support of his earlier work McDunnough (1938) also provided much improved figures of the male genitalia of *P. chelifer* and *P. midas*. Although McDunnough's new figures for these species were much needed so was information on *P. croesus*, no new figures or details were presented. Until now this has been a problem concerning *P. croesus*, because except for the unpublished (and virtually unknown) figure of the male genitalia of *P. croesus* in Daggy's (1941) Ph.D. thesis on Minnesota mayflies, there were no detailed illustrations of its genitalia available for study.

The next major contribution to the study of North American *Parameletus* was made by Edmunds (1952, 1957) who reported on a population of *P. columbiae* that he discovered at altitude (~2100–2500 m ASL) in the Rocky Mountains of Utah. In his Ph.D. thesis, Edmunds (1952) redescribed the male and female imago and provided the first account of the nymph of *P. columbiae,* but none of these taxonomic accounts were ever published. Edmunds did however publish his observations of the life history of *P. columbiae* noting its remarkably short development time, 16–21 days at the Brighton, UT site (Edmunds 1957, Edmunds *et al.*1976). Despite not publishing some of his earlier taxonomic work, Edmunds' studies facilitated the survey of Idaho mayflies by Jensen (1966), wherein he reported additional new records of *P. columbiae*. Subsequently *P. columbiae* became the best studied of any species of *Parameletus* in North America, but because of the lack of knowledge of the other Nearctic species of *Parameletus* this contributed to a rather narrow view of the life history and habitat of the genus at that time. Details of the of life history and habitat of *P. columbiae* were presented by Edmunds *et al.*(1976) in a way that has frequently led to a misunderstanding of the entire genus in North America. Studies on the biology of the Holarctic species *P. chelifer* (Söderstrom and Nilsson 1987, Söderstrom and Johansson 1988, and Söderstrom 1988) clearly indicate a wider range of environmental tolerances and a more variable developmental period than what is known for *P. columbiae*. New data on the habitat of nymphs and estimates of development times are presented here for *P. midas*, *P. croesus,* and *P. chelifer.*

Jacobus and McCafferty (2002) briefly commented on the status of *P. croesus* based on their study of the types. They noted that even though *P. croesus* had not been collected for 75 years, it was premature to declare it extinct. This was a prudent decision, especially since Daggy (1941) collected a swarm of *P. croesus* in 1939, only 63 years earlier. Wing characters discussed by Jacobus and McCafferty (2002) for separating *P. croesus* from *P. midas* are now determined to be unreliable based on the study of additional specimens of these species. Webb *et al.* (2012) presented some data on *Parameletus* species as part of a larger project to quantify a portion of the regional species pool of the Canadian lower Arctic using DNA barcodes. The use of molecular marker sequences to assist in determining species has been a positive step toward addressing the problems of identifying species from life stages and material for which there are no useful traditional taxonomic keys. Webb *et al.* (2012) used the COI marker sequence to confirm the co-occurrence of *P. midas* and *P. chelifer* in samples from Churchill, Manitoba. Their consensus analysis of sequence divergence values also showed a strong association of samples of *P. midas* from Manitoba and New Brunswick with clear separation from samples of *P. chelifer*. The previous record of *P. midas* at the Churchill site (Harper and Harper 1981) had been somewhat suspect because it was far removed from what had been believed to the major part of the range of *P. midas* in eastern Canada, because there were no other sites known for the species between those two areas, and because the original adult material upon which the record was based could not be located for study. Kjærstad *et al.* (2012) briefly commented on the high degree of similarity in molecular marker sequences obtained for specimens of *P. chelifer* from Finmark region of Scandinavia and from Churchill, Manitoba, Canada. Their findings strongly support the true Holarctic status of *P. chelifer* and recognize the important genetic connection between Nearctic and Palearctic populations. The most recent treatment of Nearctic *Parameletus* was by Klubertanz (2016) who summarized the known distribution of the genus in Wisconsin, but did not include any new records for that region. Finally there are other publications that

include either brief taxonomic overviews of the genus (e.g., Burks 1953) or enigmatic distribution records without specifics (e.g., Edmunds *et al.* 1976); in most instances these treatments simply summarized what was already known about the genus and do not contribute any new information.

Despite all of the work done on North American *Parameletus* during the past 89 years, nymphs (the most frequently collected life stage) cannot be reliably identified to species. Moreover, the use of incomplete keys to nymphs has led to widespread misidentifications adversely affecting estimates of regional species diversity and inhibited new studies on the biology and ecology of the Nearctic species of *Parameletus*. To a lesser extent, incomplete and poorly illustrated keys for male imagos have also contributed to this problem. The focus of this study was to update and complete the taxonomy of the species of *Parameletus* in North America and produce new keys for nymphs and imagos. The distributions of all species are plotted and discussed. New information on the aquatic habitats, emergence times, and conditions are also presented.

**Materials and Methods**

Although it would have been desirable to obtain new reared material for all Nearctic *Parameletus* species, unfortunately this was not possible because of the difficulty in obtaining live nymphs for rearing. *Parameletus midas* was the only species for which a new series was obtained. Live nymphs of *P. croesus* were collected by Brigid O'Donnell in 2007 from Wisconsin, but she was unable to fully rear these specimens. Although none of O'Donnell's specimens fully emerged, one final instar male nymph was positively associated with the male imago of *P. croesus*. The association was made by the recognition of diagnostic characters of the male imago on the developing subimago visible through the cuticle of the last instar nymph, hence a complete association between the nymph and imago stage. Unequivocal diagnostic characters were the dark medial marks on the abdominal sterna of the male imago and the deep v-notched styliger plate. These characters were unmistakable through the nymphal cuticle and provide the same level of primary evidence of immature-adult association as if the specimen had fully emerged. Therefore it was not considered to be a tentative association. In addition, there were other secondary lines of evidence to support the association. First, nymphs of all other species of Nearctic *Parameletus* were known and morphological study of all nymphs from Wisconsin showed that they were different from those associated with all other known North American species. Second, no adults of any species except *P. croesus* have ever been collected in the region of Minnesota and Wisconsin. Third, all specimens of *Parameletus* nymphs studied from Wisconsin are morphologically congruent with the nymph associated by adult diagnostic characters to be that of *P. croesus*. Finally, with the intensity of entomological studies conducted in Wisconsin over the past 63 years by some of the most experienced aquatic entomologists in the United States (e.g., William Hilsenhoff), it is highly unlikely that if a different species of *Parameletus* was present that they would have failed to have found it (even if they didn't know what it was). All of these lines of evidence taken together strongly support the conclusion that all nymphs deemed morphologically congruent with the one specimen which was positively associated with the adult stage of *P. croesus* (by observation of adult diagnostic characters) were the nymphs of *P. croesus*.

Live nymphs of *P. midas* were collected from the Dead River, Maine, USA using a standard D-frame kick net, transferred to 500 ml plastic jars containing stream water from the collections site. Jars were aerated and slightly chilled for transport to the laboratory. In the laboratory nymphs were placed in large circular glass culture dishes (dia. ~ 23 cm) with emergent vegetation from the field site. Emergent vegetation placed in rearing dishes provided a natural surface for the final instar nymphs to crawl up (as do other siphlonurids) at the time of emergence. Each rearing dish was aerated with a small airstone and covered with a self-supporting domed mesh enclosure that allowed space for subimagos to fly away from the water. Water temperature in rearing dishes was maintained as close to 17°C as possible (field water temperature where black wing pad nymphs were collected ranged from 16.9–17.4°C). Subimagos were removed upon emergence to subimago boxes to make the final molt and associated nymphal exuviae were preserved in 80% alcohol and kept with each subimago until it molted. Imagos were preserved in 80% alcohol with the associated nymphal exuviae.

All specimens were observed for morphological characters, coloration, and color patterns under stereoscopic and compound light microscopes (up to 1000x magnification). Mouth and body parts of the nymphs were dissected in 80% alcohol and slide mounted in Hoyer's Mounting Media or Euparal®. Male genitalia were slide mounted for study and examined intact. Study of intact genitalia is important because subtle and membranous features are highly susceptible to distortion during and after slide mounting. Some of the type material was slide mounted by the original authors and studied in that form. Imago wings were also examined and measured intact. Standard terminology for adult anatomy and morphology was used (Kluge 1994). Standard terminology for nymphs given by Kluge *et al.* 1995 was used except for the names given to sclerotized supports for abdominal gills. All abdominal gills of *Parameletus*

nymphs have a sclerotized ventral strip with setae and a sclerotized mid-rib. These structures are identified as the fore costa (FC–ventral strip) and hind costa (HC–mid rib) by Kluge *et al.* 1995, but because of the similarity between these terms and the well-established name of the primary wing vein "costa" I have elected not to use them to avoid any confusion. The abbreviation PLPs is used to refer to the posterolateral projections of abdominal terga of nymphs and where necessary of a specific tergite (e.g., PLPs-tergite IX). Tarsal segments of legs of imagos are abbreviated as an uppercase "T" and a subscript denoting a specific segment number or range of segments (e.g., $T_1$ refers to tarsal segment 1). In the materials studied and appendix sections the abbreviation Nex refers to shed nymphal exuviae. Specimens were photographed using a Nikon D300s DSLR and the Nikon Camera Control Pro2® software. All measurements were made using a calibrated ocular micrometer (nearest 0.10 mm). Measurements were made from entire specimens and/or parts (not mounted on slides) that were held as flat as possible (without inducing distortion) using sections of broken glass microscope slides and coverslips. Conventions for standard measurements described by Hubbard (1995) were followed. Means and standard deviations (abbreviated as SD) were calculated for all continuous data. Lengths of the foreleg segments of the male imago were standardized to the length of the foretibia and expressed as ratios. These values represent percentages relative to the length of the foretibia. Description of colors and hues were kept as simple as possible with regard to common and standard color names. Eggs were dissected from a reared female imago in 80% alcohol. Eggs were carefully removed from the lower oviduct (to minimize differences possibly related to maturation) with a 2 $\mu$l adjustable micropipette, dehydrated in 100% propanol for 10 min. and mounted in Euparal®. Chorionic features of eggs were observed under phase contrast microscopy (400 and 1000x).

Although not comparable, basic descriptions of male imagos of *P. chelifer*, *P. columbiae*, *P. croesus*, and *P. midas* are available (McDunnough 1923, 1938, Traver 1935, Söderstrom and Nilsson 1986, and Tiunova 2008). For the 3 strictly North American, species adult descriptions have focused mostly on aspects of color and color patterns of male and female imagos. In addition, most of these descriptions were composed using terminology and color descriptions that are antiquated and difficult to interpret. To facilitate a clear and unambiguous understanding of these taxa new comparable descriptions using standard terminology and updated species diagnoses (with new figures) and morphometric data are presented here. Where possible specimens believed to show the least effects of long-term preservation in alcohol were used for descriptions and diagnoses. New comparative descriptions (with new figures) are presented for near final instar nymphs.

Specimen abbreviations and symbols: ♂ = male imago; ♀ = female imago; S♂ = male subimago; S♀ = female subimago; N♂ = male nymph; N♀ = female nymph; Nex = nymphal exuviae; **CNC** = Canadian National Collection, Ottawa, Ontario, Canada; **CSU** = Colorado State University, C.P. Gillette Museum of Arthropod Diversity, CO, USA; **FAMU** = Florida A&M University, Tallahassee, FL, USA; **FLBS =** Flathead Lake Biological Station Collection, University of Montana, Polson, MT, USA; **ILNHS =** Illinois Natural History Survey Insect Collection, Champaign, IL, USA; **MEIFW** = Maine Inland Fish & Wildlife, Bangor, ME (specimens from this source deposited with author); **NEL** = Northeast Ephemeroptera Laboratory, Department of Biology, Southern Connecticut State University, New Haven, CT, USA; **PERC** = Purdue Entomological Research Collection, Purdue University, West Lafayette, IN, USA; **SWRC** = Stroud Water Research Center, Avondale, PA, USA; **UAM =** University of Alaska Museum of the North, University of Alaska, Fairbanks, AK, USA; **UM** = University of Minnesota Insect Collection, University of Minnesota, St. Paul, MN, USA; **USGS-NAWQA** = United States Geological Survey, National Water Quality Assessment Program, National Water Quality Laboratory, Denver, CO, USA; **WDNR** = Wisconsin Department of Natural Resources, Ecological Inventory and Monitoring, Superior, WI, USA. Deposition of all specimens is with the institutions listed for each record. Latitude and longitude coordinates are given, where possible, in positive and negative decimal degree format. In some instances because of vague or incomplete original locality information coordinate pairs for a site were estimated using all available descriptive location data combined with remote inspection of general vicinity of sampling area using satellite imagery and information on the circumstances under which a sample was obtained. These estimates are denoted by an (*). All georeferenced specimen data for material studied are presented in a separate excel spread sheet (Append. 1) to facilitate use of these data in mapping programs and future biodiversity analyses. A separate excel spread sheet page is also provided for all records of Nearctic *Parameletus* previously published so these data can also be used for geo-spatial study (Append. 1). The literature cited section of the paper includes references for previously published records that occur in Append. 1. Species distribution maps were prepared using Simplemappr® (Shorthouse 2010).

## Material Studied

***Parameletus chelifer* Bengtsson, 1908**

*Material Examined.* **CANADA: Northwest Territories:** Horton River, Site 14 [68.47541N/ -128.634278W], D. Giberson, 23 Jul 2000, 1♂, 1♀ [NEL]; Horton River, Site 14 [68.47541N/ -128.634278W], D. Giberson, 24 Jul 2000, 5♂ [NEL]; Horton River, Site 29 [69.049639N/ -126.184833W], D. Giberson, 31 Jul 2000, 1♂,1♀ [NEL]; same, (PERC No. 0064691], same, 2♂, [PERC]; Thelon River, trib., Site 19 [64.179472N/ -102.616139W], D. Giberson & L. Purcell, 6 Jul 2002, 17N [NEL]; Thelon River, trib., Site 22 [64.184833N/ -102.318583W], D. Giberson & L. Purcell, 7 Jul 2002, 15N [NEL]; Tundra pond above Thelon River Site 27 [64.320333N/ -101.836417W], D. Giberson & L. Purcell, 8 Jul 2002, 26N [NEL]; **Nunavut:** Maguse River north of Arviat, swift flowing large river [61.298883N/ -94.080183W], D. Giberson, 10 Jul 2003, 1S♂, 1♀ [NEL]; Baker Lake, airport road, small pond at campground [64.315617N/ -96.053967W], D. Giberson, 14 Jul 2003, 14N [NEL]; **USA**: **Alaska**: Yukon-Koyukuk Co., Fort Yukon, above Arctic Circle [66.565367N/ -145.278597W*], C.W. Pagel, 17 Jul 1965, 1♂ [NEL]; Fairbanks North Star Co., Chatanika River, puddle near Elliot Hwy bridge, (UAM No. 50463) [65.084459N/ -147.725698W*], Sch. & Berg.(?), 6 Jun 1977, 2N [UAM]; Chatanika River, old channel (UAM No. 50467) [65.086376N/ -147.738764W*], Sch. & Berg. (?), 12 Jun 1973, 1N [UAM]; Chatanika River, old channel (UAM No. 50466) [65.086376N/ -147.738764W], Sch. & Berg.(?), 12 Jun 1973, 1N [UAM]; Chatanika River, old channel (UAM No. 50464) [65.095946N/ -147.680510W*], Sch. & Berg. (?), 23 Jun 1976, 15♀ [UAM]; Chena River, 2nd bridge (UAM No. 50484) [64.848259N/ -147.383583W*], Jink & Berg., 14 Jun 1972, 2♂ [UAM]; Salcha River, pipeline x-ing (UAM No. 50453) [64.485201N/ -146.663052W*], Sch. & Berg. (?), 22 Jun 1972, 1♂ [UAM]; Bethel Co., Holitna River (UAM No. 50458) [61.635231N/ -157.115829W*], Gar. & Berg. (?), 11 Jun 1976, 1♂ [UAM]; Holitna River (UAM No. 50461b) [61.635231N/ -157.115829W*], Gar. & Berg. (?), 26 Jun 1977, 1♂ [UAM]; Holitna River (UAM No. 50455) [61.635231N/ -157.115829W*], Gar. & Berg. (?), 30 Jun 1977, 1♂ [UAM]; Holitna River (UAM No. 50457), [61.635231N/ -157.115829*], Gar. & Berg. (?), 17 Jul 1977, 1♂ [UAM]; North Slope Co., Umiat, small rock bottomed stream, elev. 352' (PERC No. 0064686), [69.367277N/ -152.1416W*], C.M. White, 17 Jun 1964, 15N, [PERC]; **SWEDEN:** Abisko (estimated site edge of lake at Abisko–PERC No. 0064687) [68.354888N/ 18.840431E], Thienemann ? Jun 1936, 3N, 1Nex, [PERC].

***Parameletus columbiae* McDunnough, 1938**

*Material Examined.* **Holotype, CANADA: British Columbia:** Thompson-Nicola Co., Dunn Peak, North Thompson River, swarm over small glacial stream at 7000 ft. elev., (CNC No. 4289) [51.441757N/ -119.954675W*], J.K. Jacob, 10 Aug 1937, 1♂ [CNC].

*Other Material Studied*. **USA: Alaska:** Fairbanks North Star Co., Chatanika River, 0.8 miles below x-ing (13:00–14:00 hr.) sample C-B (UAM No. 50485) [65.081917N/ -147.734134W*], 12 Apr 1978, 3N [UAM]; Chena River, C-750, Qual. (UAM No. 50456) [64.848259N/ -147.383583W*], Sch. & Jin. (?), 8 May 1972, 20N [UAM]; Chena River, C-800, Qual. (UAM No. 50454) [64.848259N/ -147.383583W*], Sch. & Jin. (?), 8 May 1972, 1N [UAM]; Chena River, C-725, Qual. (UAM No. 50452) [64.848259N/ -147.383583W], Sch. & Jin.(?), 8 May 1972, 20N [UAM]; Bethel Co., Holitna River (UAM No. 50461a) [61.635231N/ -157.115829W*], Gar. & Berg. (?), 26 Jun 1977, 1♂ [UAM]; Holitna River (UAM No. 50460) [61.635231N/ -157.115829W*], Gar. & Berg. (?), 29 Jun 1977, 1♂ [UAM]; Holitna River (UAM No. 50459) [61.635231N/ -157.115829W*], Gar. & Berg. (?), 19–20 Jun 1976, 1♀ [UAM]; **Idaho:** Latah Co., 6 mi. north of Harvard (PERC No. 0064689) [46.982101N/ -116.670398W], G.B. White, 12 Jun 1964, 31♀ [PERC]; same, (PERC No. 0064688), same, 11♀ [PERC]; **Montana:** Flathead Co., Temporary pond at Nyack [48.439617N/ -113.804938W*], S. Chilcote, 13 Jun 2002, 5N [FLBS]; Small stream N. of 2-Lakes Creek, Gunsight Lake Trail, Glacier National Park [48.655035N/ -113.662708W*], N.P. Colager (?), 19 Jul 1997, 7♂, 4♀ [FLBS]; **Utah:** Salt Lake Co., Brighton, Silver Lake [40.603466N/ -111.588268W*], G.F. Edmunds Jr., 2 Jun 1947, 3N [FAMU]; same (ILNHS No. 12373), 23 Jun 1947, 1♂ [ILNHS]; same (ILNHS No. 12373), 2 Jun 1947, 17N [ILNHS].

***Parameletus croesus* (McDunnough, 1923)**

*Material Examined.* **Holotype**, **CANADA: Ontario:** Ottawa Division, Ottawa (CNC No. 522) [45.389755N -75.711848W*], J.H. McDunnough, 22 May 1922, 1♂ [CNC].

*Other Material Studied*. **USA: Minnesota:** Pine Co., St. Croix River, at ferry between Pine City, MN and Grantsburg, WI [45.823431N/ -92.764246W], R.H. Daggy, 26 May 1939, 8♂ [UMN]; **Wisconsin:** Marinette Co., Menominee River, right bank, about 85ft dnstr. from Hwy JJ bridge and ~2.9 miles dnstr. of Grand Rapids Dam [45.325784N/ -87.663235W*], S. Rheaume, 23 May 1995, 2N [USGS-NAWQA]; same, B. O'Donnell, 13 May 2007, 8N [NEL]; Burnette Co., St. Croix River, Seven Islands, 0–3ft. depth, swift, sand, & gravel [45.83979N/ -92.750617W*], R.A.

Lillie, 6 May 1992, 1N [WDNR]; same, St. Croix River, Seven Islands, drop-off, sand, rock, debris, 12492018 (PERC No. 0064690), same, 1N [PERC]; Outagamie Co., Wolf River, Shiocton, below Hwy 54 [44.44283N/ -88.588162W*], R.A. Lillie, 6 May 1993, 1N [WDNR]; same, 011994047-89 (PERC No. 0064685) same, 7N [PERC].

***Parameletus midas* (McDunnough, 1923)**

*Material Examined.* **Holotype, CANADA: Ontario:** Ottawa Division, Ottawa (CNC No. 523), [45.389755N -75.711848W*], J.H. McDunnough, 29 May 1922, 1♂ [CNC]; **Paratype, Ontario**, Ottawa Division, Ottawa (CNC No. 523) [45.389755N/ -75.711848W*], J.H. McDunnough, 29 May 1922, 1♂ [CNC].

*Other Material Studied*. **CANADA: New Brunswick:** Gloucester Co., Nepisquit River, Hwy 360 (Middle Landing) [47.440943N/ -65.705252W*], B. Kondratieff & R. Bauman, 17 Jun 1993, 1♂ [CSU]; **Newfoundland (Labrador):** Minipi Drainage, L4 [52.604899N/ -61.162381W*], D. Larson & D. Butt, 26 Jun 1983, 3N [NEL]; same, 28 Jun 1983, 2N [NEL]; **Quebec:** Minganic, Côte-Nord Region, Thunder River (Rivière-au-Tonnerre)[50.28091N/ -64.74834W*], W.J. Brown, 16 May 1930, 3♂ [CNC]; same, 19 Jun 1930, 4♂(reared), 4♀ [CNC]; same, 19 Jun 1930, 5♂ [CNC]; same, 19 Jun 1930, 8Nex [CNC]; same, 21 Jun 1930, 1♂ [CNC]; same, 23 Jun 1930, 5♂ [CNC]; Saquenay, Rivière Pigou, above Tr. 138, elev. 075 ft AMSL [50.2825N/ -65.641944W], D.H. Funk, 6 Jul 1984, 1S♂, 1Nex [SWRC]; **USA: Maine:** Aroostook Co., Machias River, Site 26 [46.5348N/ -68.6128W], M. Duron & M. Neal, 29 May 2004, 1N [MEIFW]; Machias River, sedge meadow within 1 mile below Grassy Landing (T10 R7 Wels/ T11 R7 Wels) [46.557908N/ -68.592197W], B. Swartz, 8 Jun 2005, 1N [MEIFW]; Franklin Co., South Branch Dead River, Eustis (UTM 19T 0384938 5001167) [45.154645N/ -70.463786W], M. Seibenmann, 3 Jun 2009, 11N [NEL]; South Branch Dead River, Eustis, cove on north shore nr. Cove Brk., north of Stratton, elev. 351 m [45.154583N/ -70.463767W], S.K. Burian, 30 May 2008, 1S♂,3 S♀, 2Nex [NEL]; same, 30 May 2008, 20♂,28♀, 7S♂, 11 S♀ 13N, 61Nex [NEL]; Washington Co., Narraguagus River, Rt. 9 [44.842212N/ -68.069674W*], B. Kondratieff & R. Bauman, 2 Jun 1998, 1♂ [CSU].

1) ***Parameletus*** immature aquatic stage (nymph) with large single lamellate gills on abdominal segments 1 – 7; segment 2 of labial palps with thumb-like projection (indicated by arrow).

2

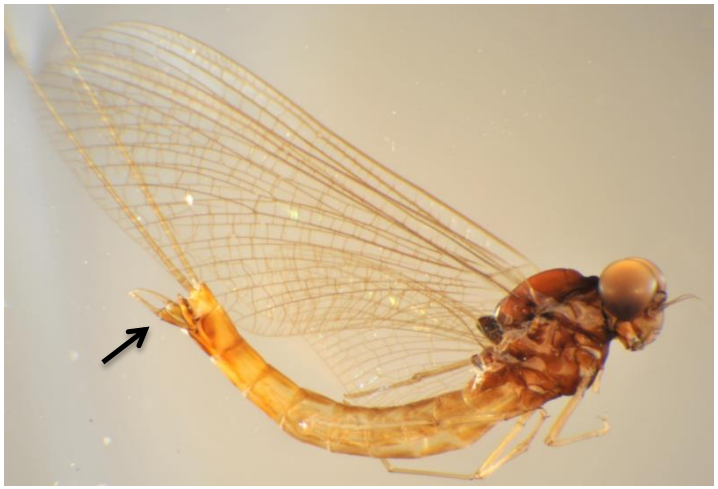

1') ***Parameletus*** mature terrestrial stage (imago) with clear wing membranes (although some staining may be present wings don't appear gray or opaque), fully formed genitalia present for male (as indicated by arrow). Subimagos are not keyed.

5

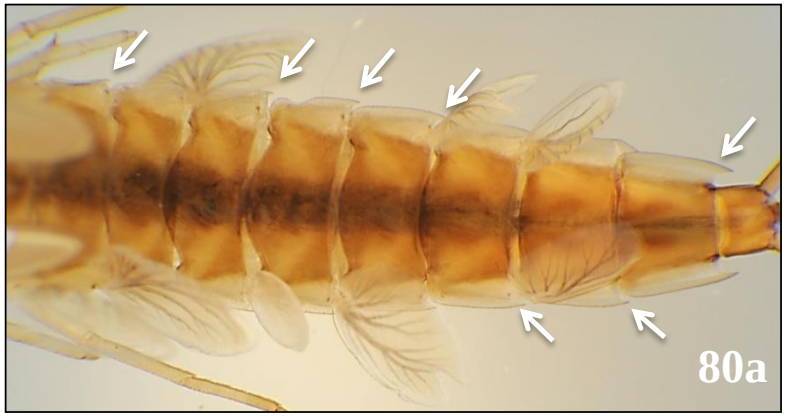



2) Distinct sharp PLPs on abdominal terga I - IX (Figs. 80a,b as indicated by arrows).

***P. croesus*** (McDunnough)

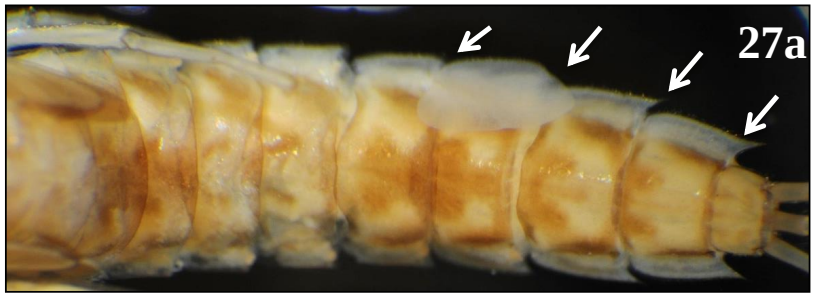



2') Distinct sharp PLPs restricted to abdominal terga VI – IX (Fig. 27a,b), small to minute sharp PLPs can sometimes be present on tergite V of some species.

3

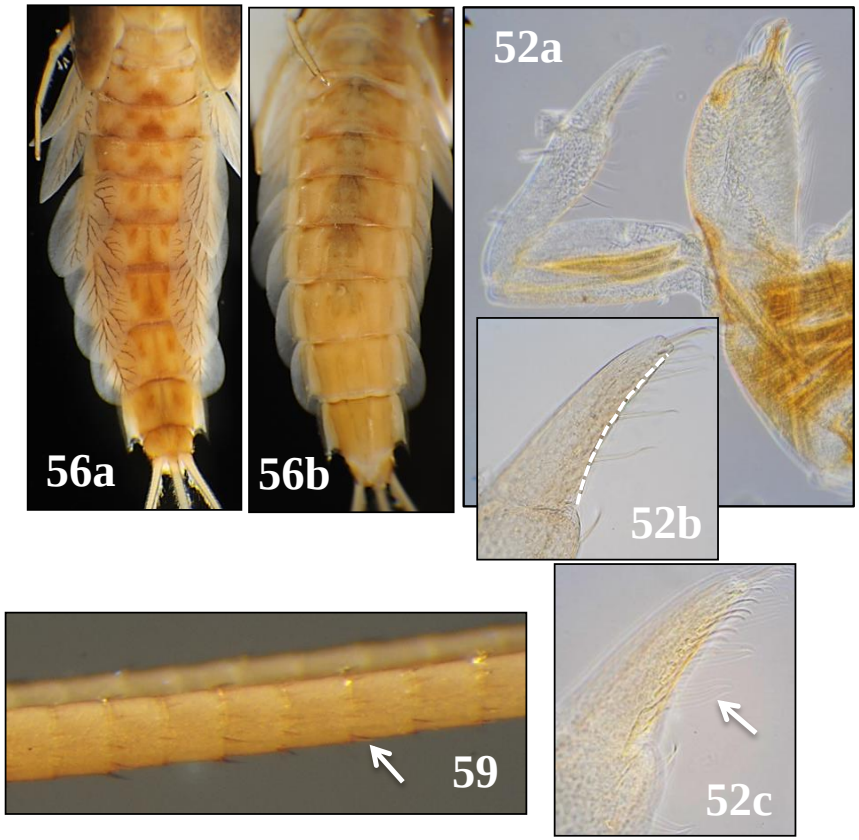


3) Color pattern of abdominal terga as in Figs. 56a,b composed of submedian paired oval marks and median dark stripe that connects to a triangular brown mark on the posterior margin of terga II – VIII; no extensive brown shading over medial marks; Cerci with long thin setae at outer lateral edges of most annuli (Fig. 59); segment 3 of maxillary palp with inner surface concave making segment seen crescent-shaped (indicated by dotted line), ventral edge of this segment with 16 – 18 closely spaced long thin setae in row that extends to base of segment (Figs. 52a – c).

***P. columbiae*** McDunnough

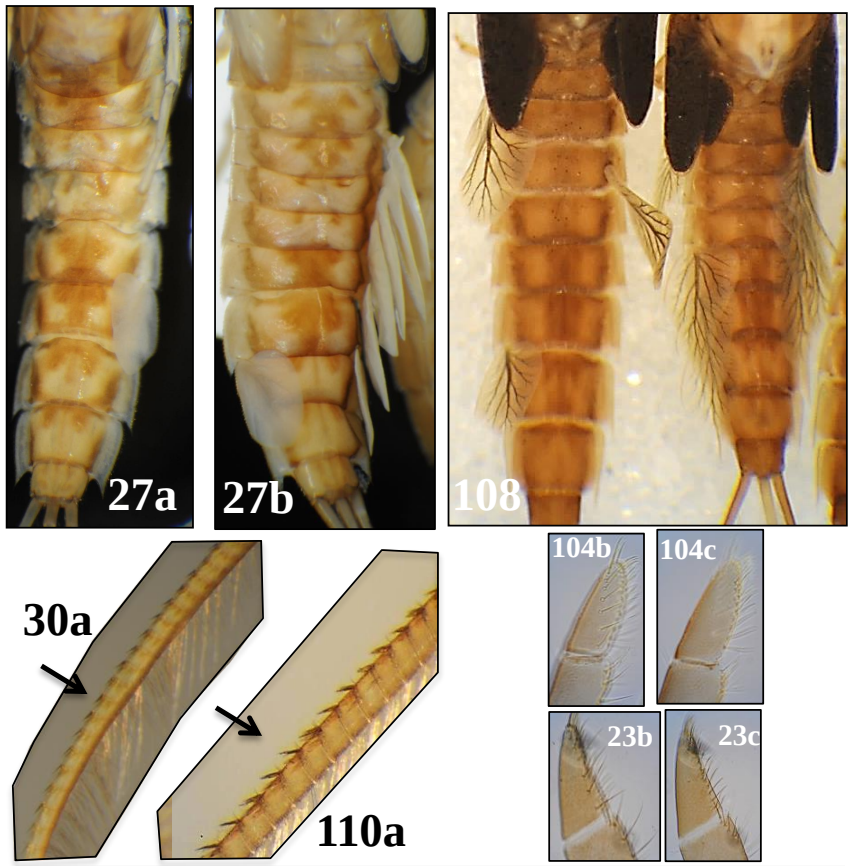


3') Color pattern of abdominal terga not as above, pattern of medial marks over shaded with brown on abdominal terga VI – VIII as in Figs. 27a,b, 108; cerci with either large flat setae or short flat setae with divided tips on lateral posterior edges of most annuli (Figs. 30a,110a); segment 3 of maxillary palp not distinctly crescent shaped, inner surface of segment 3 either not concave (Figs. 104b,c) or at most slightly concave (Figs. 23b,c) and setae on ventral edge of segment 3 usually fewer than above.

4


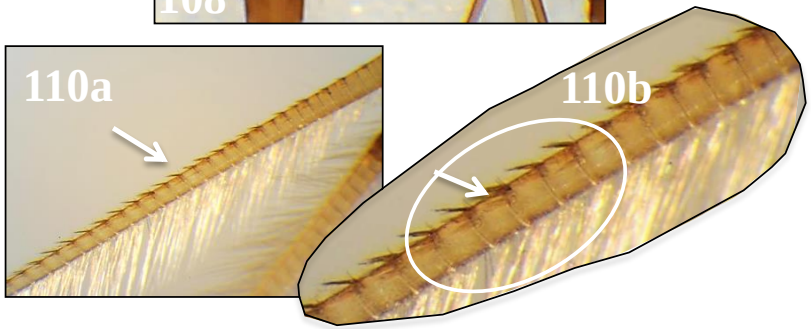


4) Abdominal color pattern as in Fig. 108, with paired median marks on terga VI – VII over shaded with brown forming a wide brown median stripe; lateral edges of tergite X with small light brown spine-like setae that similar to background color of tergite; cerci with groups of 4 – 6 large flat setae with either straight pointed tips or tips divided into multiple points on the outer lateral posterior edges of most annuli (Figs. 110a,b).

***P. midas*** (McDunnough)

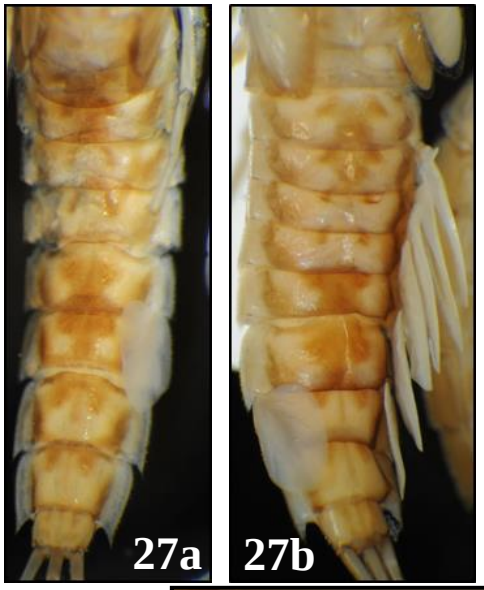


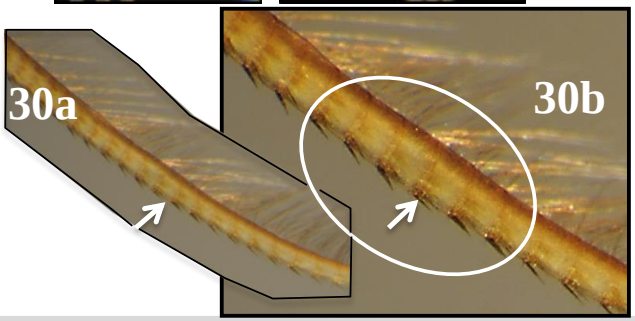


4') Abdominal color pattern as in Figs. 27a ,b, with paired median marks on terga VIII – VI over shaded with brown on tergite VI forming a large brown mushroom-shaped spot, similar shading on tergite VII produces more slender version of a mushroom-shaped spot, but brown median stripe is sometimes weakly connected to brown band along posterior margin; over-shading is less extensive on tergite VIII; lateral edges of tergite 10 with 2 – 4 brown spine-like setae that are much darker than the background color of tergite; cerci with groups of 3 – 4 short flat setae with tips mostly divided into 3 points (middle point often larger than others) on the outer lateral posterior edges of most annuli (Fig.s 30a,b).

***P. chelifer*** Bengtsson





5) Posterior margin of styliger plate with deep v-shaped median notch (Fig. 68); genitalia as in Figs. 67a,b; abdominal sterna with broad dark brown medial mark (Fig. 65c).

***P. croesus*** (McDunnough)

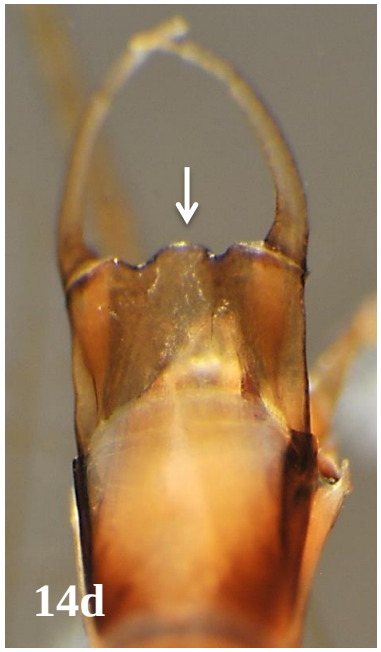



5') Posterior margin of styliger plate smoothly curving between forceps bases or with a distinct rectangular or rounded median process or with a slight median notch (Figs. 14d, 89a); genitalia not as above; abdominal sterna variably marked with spots and merging lateral bands, but not as above.

6




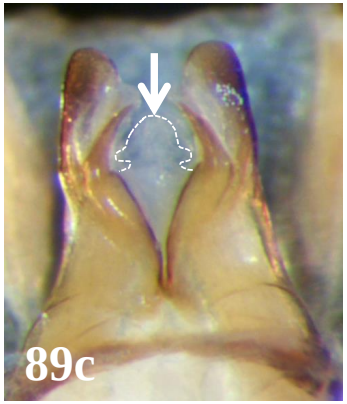


6) Penes of male genitalia with broadly rounded tips that have many small stout setae (Figs. 89a – c), large rounded tips separated by a gap as wide or wider than the width of one large lobe, dorsal median spines distinctly curved inward and ventral spines straight and about as long as penes and usually not visible from dorsal perspective; posterior margin of styliger plate with either a smoothly curving edge between the forceps bases or with a slight median notch (Figs. 89a, 90c).

***P. midas*** (McDunnough)

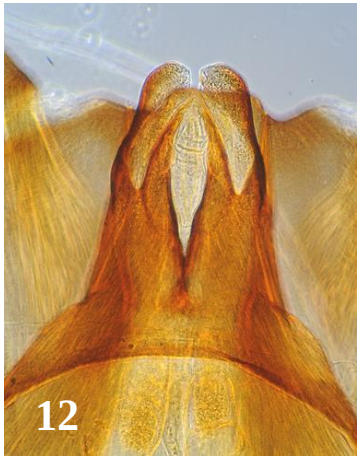



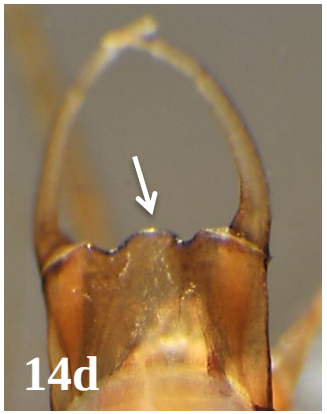


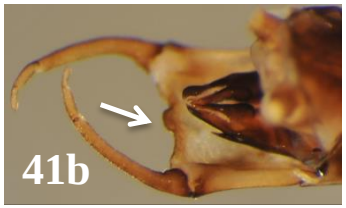


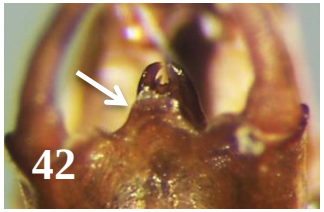


6') Male genitalia not as above with tips of penes narrow and curved inward appearing pincher-like or tips broad, but only separated by a narrow gap (Figs. 12, 39); dorsal and ventral spines not curving inward and tips of ventral spines visible from dorsal perspective; posterior margin of styliger plate with either a low and slightly rounded or distinctively rectangular median process (Figs. 14d, 41b, 42)

7




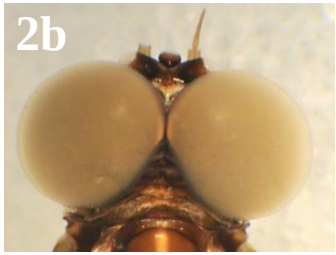


7) Penes of male genitalia sclerotized with broadly rounded tips and many small stout setae (Figs. 12, 13), large rounded tips are separated by a gap much smaller than the width of one large lobe of the penes (tips often appear to meet); dorsal median spines only slightly curved inward at tips and tips bifid; ventral spines straight and sharp about the same length as the dorsal spines and tips of ventral spines are not hidden by penes; compound eyes meet along the dorsal midline of head (Figs. 2a,b).

***P. chelifer*** Bengtsson



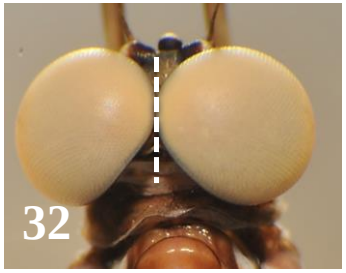


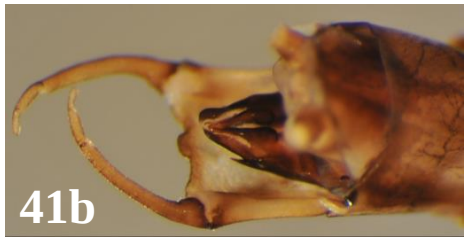


7') Penes of male genitalia) sclerotized with narrowed tips that curve inward appearing pincher-like (Figs. 39, 40, 41b), dorsal surfaces of tips with many small stout setae; dorsal median spines broad with bifid tips with u-shaped gap between the points, outer point is broad compared to the inner point and can be blunt whereas the inner point is always sharp; ventral spines straight and pointed and do not reach the tips of the penes, ventral spines are not hidden by penes; compound eyes distinctly separate along the dorsal midline of head if only by a narrow gap (Fig. 32).

***P. columbiae*** McDunnough

## Systematic Accounts

### *Parameletus chelifer* Bengtsson, 1908 (Figs. 1–30)

***Male Imago*** (in alcohol). Body length: 8.83–16.00 mm (11.97±2.10, mean±SD, n=14). Body medium to dark brown (Figs. 1a–c). Long term preservation in alcohol causes fading and more amber tint to brown color (Fig. 1a, 2a).

***Head.*** Background color medium brown shaded with dark grey. Bases of ocelli dark brown, occasionally almost black. Compound eyes large and semiturbinate with lower portion greyish blue, large upper portion of compound eyes meet dorsally along midline of head (Figs. 2a,b). Antennae uniform light brown. Frons with median keel produced to sharp point ventrally, cuticle below antennal sockets marked with broad dark brown streaks that end about halfway to margin of frons (Fig. 3). Lateral and medial margin of frons semi-transparent with brown shading.

***Thorax.*** Dorsal and lateral aspect as in Figs. 2a,b, 4. Sclerotized areas mostly dark brown, in some places lighter amber brown. Membranous cuticle white to cream colored. Thickened edges of nota and sutures much darker than background color, ranging from dark brown to almost black. Pronotum mostly obscured by large upper part of compound eyes. Shape of pronotum trapezoidal with broadly curved anterior margin. Posterior margin medially indented to accommodate anterior part of mesonotum. Pronotum background color medium to dark brown with some tints of grey on some specimens. Mesonotum medium brown with lighter yellow-brown areas along parascutellum (PSL). Antelateroparapsidal suture (ALPs) dark brown and blend into darker lateral areas of submedioscutum (SMS), which is mostly brown. Posterior scutal protuberance (PSp) and posterior medial parts of medioscutum (MS) dark brown (Figs. 2a,b). Scuto-scutellar impression (SSLi) pale yellow-brown. Center and edges of scutellum (SL) usually dark brown, but sometimes center area of SL pale similar to SSLi. Dorsally mesonotal suture (MNs) seems straight and with anteronotal transverse impression (ANi) and anteronotal protuberance (ANp) forms distinctive outline on anterior of MS (Figs. 2a,b, 4). Area within outline often much lighter yellow-brown compared to rest of MS. Metanotum mostly medium brown with similar dark edges of more heavily sclerotized areas as seen on the mesonotum. Pale yellow areas occur at margins of metanotum, as on mesonotum. Metanotal infrascutellar (ISL) areas dark brown. Metanotal SL with light brown center region and dark brown edges, as occurs on mesonotum (Figs. 2a,b, 4).

**W*ings.*** Forewing length: 9.92–12.91 mm (10.99±0.95, n=14). Forewing membrane transparent and unpigmented, except for opaque stigmatic region between costa and subcosta veins and subcosta and radius$_1$ veins (Figs. 5a,b). Major longitudinal veins brown, radial and medial vein groups darker than costa and subcostal veins. All major longitudinal veins fade to pale white at wing base. All discal crossveins lighter than longitudinal veins. Most crossveins of costa/subcosta interspace single with 1–2 crossveins merging near wing apex. CuA vein joined to hind margin by series of about 8 sinuate crossveins (1 or 2 merge with short marginal intercalary veins near edge of hind margin). About 5 unattached marginal intercalary veins occur alternately between sinuate crossveins, sometimes only 1 unattached intercalary vein present. Hind wing membrane unpigmented as in forewing (Fig. 5b). Major longitudinal veins and discal crossveins pigmented as described for forewing. Brown color of major longitudinal veins extends to wing base, only basalmost part of costa pale in contrast to forewing. Hind wing MP vein not forked. Costal projection evident only as slight arching of costa near wing base.

***Legs.*** Ranges, means, and ratio values of segments of forelegs as follows: Femur 2.20–3.00 mm, (2.63 [1.07], n=10 ) (mean [median of ratio to tibia], sample size), Tibia 1.92–2.76 (2.42 [1.00], n=10), $T_1$=1.16–1.68 (1.46[0.60], n=10), $T_2$=1.28–1.82 (1.59[0.66], n=10), $T_3$= 1.30–1.96 (1.64[0.67], n=10), $T_4$=1.00–1.60 (1.28[0.53], n=10), $T_5$=0.72–1.04 (0.85 [0.34], n=10). Legs yellow-brown, femora with slightly more brown than other segments (Figs. 6, 7). Foretibiae and $T_1$ of foretarsi with blunt spine-like knobs (Fig. 6). Ventral apical spine on mid and hind tarsal segments $T_1$–$T_4$, ventral edges with several small dark spines. Forelegs with 5 distinct tarsal segments and joints between all segments. Mid and hind legs with only 4 distinct tarsal segments, segment $T_1$ fused to the tibiae. Segment $T_1$ fuses to tibiae during development to subimago (5 distinct tarsal segments of imago legs can be seen through cuticle of last instar nymphs).

***Abdomen.*** Background color yellow-brown, with medium brown shading on both terga and sterna (Figs. 8–11b). Intersegmental membranes of abdominal segments and membranes of pleural areas yellow to semi-transparent white. Terga III–V with dark brown paired medial crescent shaped marks near anterior margin. Terga I–II with diffuse dark brown shading over area of paired medial marks reducing distinctiveness of marks, on some individuals paired marks blend with background color forming single large medial mark. On terga VI–IX paired medial marks become elongated into paired streaks almost reaching posterior margins of terga. Anterolateral corners of terga pale yellow (Figs. 8–10a, 11a). Lateral areas of terga I–IX with distinctive dark brown streaks, occasionally streaks merge with narrow brown band at posterior of terga. Tergite X lacks lateral brown streaks, but has large dark brown medial spot often darker than

marks on terga I–IX. Sterna I–IX with centers shaded medium brown (Figs. 10b, 11b). Lateral edges of sterna adjacent to pleural fold margined with thin dark brown line. Outline of 4 "ghost" spots (i.e., spot with detectable outline, but no evidence of color) present on sterna I–IX. Pattern of ghost spots, 2 smaller medial circular spots flanked by 2 larger "coma" shaped spots. Sternite IX with distinctive dark brown lateral steaks, streaks occasionally meet along anterior margin. Membrane between base of styliger plate sternite IX transparent (Figs. 11b, 14a, 14b). Genitalia as in Figs. 12–14a–d, forceps light brown and 4 segmented, but basal segment only weakly sclerotized on its dorsal surface and has no distinct joint with second segment. Posterior margin of styliger plate with rounded median projection, shape of median projection varies from low rounded hump to rectangular form. Median projection does not protrude beyond flanking raised edges of posterior margin and usually is less than or equal to about one third width of posterior margin. Dorsal and ventral medial surfaces of styliger plate pale compared to lateral areas and forceps bases. Penes as in Figs. 12, 13, tips do not extend beyond the posterior margin of the styliger plate. Large sclerotized lobes of penes almost meet medially on intact specimens. Dorsal aspect of slide mounted genitalia (undistorted) as in Figs. 14b,c.

***Caudal Filaments.*** Caudal filaments as in Fig. 15, cerci light brown from base almost to tips. Junctions of annuli pale. Terminal annuli slightly darker than others. Median terminal filament vestigial.

***Female Imago*** (in alcohol). Body length: 9.33–13.80 mm (11.54±1.34, mean±SD, n=15). Body color medium brown as in Figs. 16a,b, 17.

***Head.*** Base color of head pale yellow, much lighter than male imago. Vertex with 2 dark longitudinal stripes posterior to lateral ocelli, stripes do not reach postoccipital suture. Compound eyes small and lateral in position. Lateral ocelli larger than median ocellus, bases of lateral ocelli dark brown. Median ocellus recessed into depression in frons and base dark brown. Antennae light brown. Frons with median keel extending from median ocellus to ventral margin, dark brown streaks across frons below antennal sockets meet at medial keel. Ventral edge of frons yellow-brown, similar to parts of vertex.

***Thorax.*** Dorsal and lateral aspect as in Figs.17a,b, general color and structural features similar to that of male imago. Shape and color of pronotum as in Fig. 17b. Meso- and metanotum with extensive pale areas adjacent to PSL and on pleural region around wing bases. Background color of dorsal surface of SMS and SL yellow-brown, but middle and lateral areas of SL on meso- and metanotum medium brown. No extensive blackish brown areas on pterothorax.

***Wings.*** Forewing length: 12.16–14.83 mm (13.61±0.76, n=16). Wing membrane color, as well as color and placement of major longitudinal veins as noted for male imago. Occasionally some individuals vary, with some anterior longitudinal veins dark to medium brown and posterior longitudinal veins tan to yellow-brown.

***Legs.*** Legs yellow-brown, femora tend to have more brown than other segments. Ventral apical spine on mid and hind tarsal segments $T_1$–$T_4$, ventral edges with several small dark spines. Tarsi of all legs with four distinct tarsal segments. Tarsal segment $T_1$ of all legs fused to tibiae. Segment $T_1$ fuses to tibiae during development to subimago (5 distinct tarsal segments of imago legs can be seen through cuticle of last instar nymphs).

***Abdomen.*** Background color yellow-brown, shaded with medium brown on both terga and sterna (Figs. 16a,b, 17a,b). Lateral color pattern as in Figs. 16a,b, 17a. Dorsal and ventral color patterns as in Figs. 17b,c. Terga I–X with paired crescent shaped submedian pale spots margined with dark brown. Pale median line margined with brown occurs on terga VI–X. Diffuse area of slightly darker brown shading occurs medially between pale spots, brown shading most distinctive when segments viewed laterally (Fig. 17b). Dark lateral streaks occur on all terga, dark lateral streaks broader and more distinctive than on male imago (Fig. 16b). Dark lateral streaks usually stop at posterior of each segment and do not extend dorsally along posterior margins of terga. Color and markings of sterna as in Figs. 17c,d. Shape and appearance of genital openings on sternite VII and color of sternite VIII as in Fig. 17d. Posterior margin of sternite IX varies from broadly rounded to bluntly pointed (Fig. 17d).

***Caudal Filaments.*** Caudal filaments similar in length and appearance to those of male imago.

***Nymph*** (in alcohol, well developed or dark wing pad stage). Body length ♂: 6.92–12.50 mm (9.87±2.09, mean±SD, n=14); Body length ♀: 6.79–11.00 mm (9.05±1.78, n=7); Tergite VII ratio width:length ♂: 1.86–2.93 (median=2.41, n=14); Tergite VII ratio width:length ♀: 0.78–0.88 (median=2.50, n=5); PLPs-tergite IX (width) ♂: 0.08–0.18 mm (0.14±0.053 n=14); PLPs-tergite IX (width) ♀: 0.10–0.16 mm (0.14±0.02, n=7); PLPs-tergite IX (length) ♂: 0.20–0.36 mm (0.28±0.05, n=14); PLPs-tergite IX (length) ♀: 0.24-0.37 mm (0.30±0.05, n=7).

***Mouthparts.*** **Labrum:** Labrum somewhat rectangular with widest point about halfway along lateral edge (Fig. 18a). Medial part of anterior margin extending onto ventral surface as an under-turned lip (Figs. 18a,b). Anterior dorsal surface with many long, hair-like setae and long, thick setae concentrated over median area of under-turned lip (Fig. 18c). Most large hair-like setae have finely branched edges and curve over anterior

margin forming brush of setae. Ventral surface with group of about 5 long sharp setae lateral to medial pads of shorter hair-like setae (Fig. 18d). **Labium:** Glossae and paraglossae with numerous fine hair-like setae on dorsal and ventral surfaces (Fig. 19a). Joint at base of glossae and paraglossae aligned on each side of midline of labium. Together both joints form an angle of ~60° in relation to midline of labium. Labial palps 3 segmented, segment 3 broad and apically rounded. Inner apical margin of segment 3 slightly indented, with an irregular row of long sharp setae (Figs. 19b,c). Segment 1 broad and slightly shorter than lengths of segments 2 + 3. Thumb-like process of segment 2 about one third length of segment 3, often only about one quarter length of segment 3 (Fig. 19c). Thumb-like process of segment 2 set apart from segment 3 by u-shaped gap (Fig. 19c). **Hypopharynx:** Lingua rectangular (Fig. 20), somewhat broader than long. Anterior margin with slightly v-shaped indentation flanked by pair of low rounded lobes making surface appear slightly crenulated. Outer corners of lingua rounded and have long fine setae. Sides of lingua slightly convex. Superlinguae broadly rounded with many long thin setae (Fig. 20). **Right Mandible:** Anterior margin between molars and incisors relatively smooth with only few minute surface denticles (Fig. 21a). Bases of incisors usually positioned above anterior margin, occasionally deep cleft between incisors extends slightly below edge of anterior margin (Fig. 21b). Incisors curved inward from their bases. Many long sharp setae occur on dorsal apical corner below molar surface. One row of setae on dorsal surface of innermost incisor. Prostheca present, brush-like portion extends across much of anterior margin (Fig. 21a). Large pointed or truncated pre-molar projection (Fig. 21a). **Left Mandible:** Ventral edge of outermost incisor with small bifid accessory tooth, occasionally tooth may be worn down (Fig. 22a). Ventral surface of innermost incisor with row of setae. Anterior margin between incisors and molars relatively smooth as on right mandible, but raised area present about halfway between base of incisors and molars (Fig. 22b). Prostheca present and extends almost to molars (Fig. 22c). **Right Maxilla:** Galea-lacinia with apex rounded, upper edge smoothly curving to meet apical cluster of canines (Fig. 23a). Crown of galea-lacinia with row of 9–10 large pectinate setae and 1–2 long sharp setae (Fig. 23e,f). Apex of galea-lacinia with 3 canines and 3 large dentisetae flanked by 2 rows of long thin setae with finely serrate edges. Maxillary palp 3 segmented with segments 1 and 2 subequal in length. Apex of segment 2 broad, but not more than 1.7x width of its base at joint with segment 1 (Fig. 23a). Segment 1 with scattered large bi-serrate setae on ventral surface and 1–2 similar setae on dorsal surface. Segment 3 apically rounded with straight to slightly concave inner margin (Fig.23a–c). Dorsal surface of segment 3 with row of 8 widely spaced long setae extending from base to tip of segment (Fig. 23b). Ventral surface of segment 3 with irregular double row of 10–12 closely spaced setae (Fig. 23c). Apex of segment 2 with short row of 4 long setae (similar to setae on segment 3), row of setae meet similar setae on segment 3 forming functional single row from segment 2 to segment 3. Setae along inner edge of segment 2 mostly restricted to apical half of segment.

***Legs*. Foreleg:** Dorsal surface of femora with median row of large bi-serrate setae (Fig. 24a). Dorsal edge of femora with an irregular double row of large spine-like setae and long bi-serrate setae. Ventral edge of femora with irregular rows of spine-like and bi-serrate setae (Fig. 24a). Ventral apical edge of femora extends as conical projection with rounded apex. Tibiae lack tibiopatellar suture. Tibiae longer than tarsi except in final instar nymphs when length of tarsi exceeds tibiae to accommodate developing legs of imago. Ventral edge tibiae with numerous large bi-serrate (Figs. 24b,c), especially near tibial-tarsal joint. Ventral edge of tarsi with mixture of large bi-serrate and spine-like setae that extend to base of claw (Figs. 24a,d). **Foreclaw:** Claws slender tapering uniformly from base to apex, no abrupt change in shape along transition from the wider basal portion to apex (Figs. 25a,b). Denticles small to minute, restricted to basal quarter of the claw. Denticles occur in 2 parallel patches at base of claw (Fig. 25a).

***Gills*. Mid-Gills (3–5):** Gills subcordate type (Figs. 26a). Gill membranes not pigmented, but appear slightly darker over central trachea. Ventral sclerotized edges of gills with double row of large finely bi-serrate setae along inner surface. Scattered large spine-like setae occur along outer part of edge (Fig. 26b). Ventral sclerotized edges about one third length of gill lamellae, longer on gills 6 and 7. Secondary trachea of gill usually branch symmetrically from central main trachea (Fig. 26c). Secondary trachea on mid-gills usually with 3 long ventral branches and 4 long dorsal branches (gills 6, 7 have fewer). Widely spaced small hair-like setae occur along outer margin of gills. Trachea uniformly pigmented. Sclerotized mid-ribs present on all gills. Mid-ribs extend dorsally about one third length of gill lamellae. Mid-ribs not pigmented (Fig. 26c).

***Abdomen.* Abdominal Color Pattern:** Paired medial brown marks present near anterior margins of all terga. On terga VI–VIII paired medial marks often shaded over with brown. Triangular brown marks present on terga VI–IX, bases of triangular marks located along posterior margins. Apices of triangular marks on terga VI–IX extend medially. On tergite VI paired anterior spots over shaded with brown forming brown mushroom shaped medial mark (Figs. 27a,b). Paired anterior brown spots merge with brown median stripe on tergite VII,

stripe widens near posterior margin of tergite. Lateral brown triangular marks on tergite VII connect to base of median stripe at posterior margin. Same pattern of marks repeated on tergite VIII, but median stripe usually does not reach posterior margin. On terga II–IV brown marks fade into diffuse spots. **Setae on Posterior Margin of Abdominal Terga:** Short medial row of 10–12 stout spine-like setae on posterior edge of terga VIII–X. Spine-like setae on terga VIII–IX located at extreme edge of sclerotized cuticle (Fig 28). Frequently spine-like setae on terga VIII–IX darker than surrounding cuticle, occasionally spine-like setae match background color exactly appearing absent. When visible, spine-like setae appear as fixed spinules. Occasionally scattered stout spine-like setae occur on posterior margin of tergite VII, but none occur on terga I–VI. Two to 4 stout spine-like setae (similar to setae on posterior margin of tergite IX) occur along edges of the tergite X. **Setae on Surface of Abdominal Terga:** Many small hair-like setae broadly distributed over surface of abdominal terga. Scattered spine-like setae (shorter than on posterior margins of terga VIII–X) occur on terga among more numerous finer setae. All surface setae transparent or light yellow-brown. **Setae on Surface of Abdominal Sterna:** Same basic arrangement of setae described for terga applies to abdominal sterna. No spine-like setae present along posterior edges of sterna. **Setae on Lateral Margins of Terga and PLPs-tergite IX:** Lateral margins and PLPs-tergite IX with double row of stout spine-like setae and many thin hair-like setae. Fewer spine-like setae occur on PLPs-terga VII –VIII with no consistent number or pattern of setae. **PLPs-terga V - IX:** Distinct sharp PLPs on terga VI–IX, inconspicuous small to minute PLPs on tergite V, none on tergite IV. PLPs-tergite V weakly pointed or blunt. Shape of PLPs-tergite IX varies from straight to slightly diverging and may curve upward at tips. PLPs-tergite IX long relative to length of tergite X, usually reaching to or past midpoint of tergite X (Figs. 27a,b). **Left Paraproct:** About 24 thin spine-like setae and 10 large stout setae cover about two thirds of surface. Setae mostly concentrated in middle of paraproct and along inner apical edge (Fig. 29).

***Caudal Filaments*:** Cerci and median terminal filament yellow-brown. Cerci with long fine hair-like setae along inner edges, hair-like setae overlap similar setae from outer edges of median terminal filament. Annuli of cerci with groups of 4–5 short flat setae with tips divided into 3 points (median point longer than lateral points). Groups of short flat setae occur along edges of annuli and overlap proceeding annulus (Figs. 30a,b). Groups of short flat setae begin near base of cerci and continue almost to tips. Apical annuli lack groups of short flat setae. Dark brown color of short flat setae makes annuli appear to have brown bands.

***Diagnosis*. Imagos:** Male imagos of *P. chelifer* can be separated from those of other North American species of *Parameletus* by following characters (1) distinctive structure of penes and associated styliger plate (Figs. 12–14a–d), (2) general brown color of abdominal terga and sterna and lack of distinctive color patterns as occurs on other species (Figs. 8–11a, b), and (3) far north distribution with southern range limit about 58° N (Fig. 111a). Female imagos can tentatively be separated from those of other species by (1) distinctive dark brown coloration of thorax and abdomen (Figs. 16 a,b, 17a–c), (2) distinctive structure of genital openings and associated color of abdominal sterna VII and VIII (Fig. 17d), and (3) far north distribution with southern range limit about 58° N (Fig. 111a). Southernmost part of range *P. chelifer* overlaps range of *P. midas,* but much darker females of *P. chelifer* should be distinct from much lighter colored females of *P. midas*.

***Diagnosis.* Nymphs**: Nymphs of *P. chelifer* can be separated from those of other North American species of *Parameletus* by the following characters: (1) unique color patterns on abdominal terga (Figs. 27a,b), (2) groups of short, flattened setae on outer edges of cerci with tips divided into 3 points (Figs. 30a,b), (3) broad rectangular shape of lingua of hypopharynx (Fig. 20), (4) relatively smooth anterior margin of right mandible between prostheca and molars (Fig. 21a,b), (5) shape of maxillary palps, specifically segment 3, which has straight to slightly concave inner margin (Figs. 23a–c ), (6) dorsal surface of segment 3 of maxillary palp with row of 8 long widely spaced setae extending from base to tip of segment (Fig. 23b) and ventral surface of segment 3 with irregular double row of 10–12 closely spaced setae (Fig. 23c), (7) paraproct with most surface setae localized to middle area and apical edge and only about 10 large stout setae (Fig. 29), (8) tarsal claws shaped as in Figs. 25a,b, with patch of cuticular denticles relatively broad and distributed over half of total claw length, and (9) abdominal gills 3–5 with large straight central trachea as in Fig. 26, gradually tapering toward apex of gill lamellae.

***Comments on Character Variation*. Imagos:** Although many individuals studied seemed to be medium brown with slight reddish tint, specimens from far northern Canada were dark brown with reddish tints (Figs. 1b,c, 10a,b). In addition, specimens from northern Canada had dark brown lateral streaks on sternite IX that were much wider compared to lighter colored specimens. However, the brown streaks on these darker specimens did not encroach any further onto the posterior margin of sternite IX than occurred on more lightly pigmented

specimens from Alaska.

Diagnostic characters of *P. chelifer* male imagos were stable between Alaska and NWT populations. Although not of diagnostic value, there were noticeable differences in body size and intensity of brown body color between these populations. Even though sample sizes did not meet the requirements for parametric statistical tests, the mean body size of specimens from Alaska, 13.21 mm (n=6), and the mean body size of specimens from the NWT, Canada, 10.50 (n=6), were noticeably different. In addition the smaller specimens from Canada had generally darker brown abdomens and some areas of the mesothorax.

All female imagos examined, except one, were collected from Alaska and all were collected on the same date from a single site (perhaps even part of a single large emergence). Unfortunately the long period of preservation in alcohol caused these specimens to be extensively faded and some have even become transparent in places. Only the more recently collected specimen from NWT of Canada retained what was considered to be representative color. This specimen was used for figures of the female imago. Structurally the Alaskan and Canadian specimens were quite similar. Color of the Canadian specimen generally seemed to match the description given by Söderstrom and Nilsson (1986) except for the abdomen, which they describe as being dull brownish white. The abdomen, as in Figs. 16a,b, 17a–c, was mostly brown and only had limited pale areas between some of the darker shaded zones. The structure and coloration of the female genital sterna (Fig. 17d) seemed to be the same as noted by Söderstrom and Nilsson (1986).

**Nymphs:** Nymphs of *P. chelifer* seemed to have varying degrees of difference in some diagnostic characters. Most differences were mainly in relation to size of individuals and apparent developmental stage. Body shape, color pattern, and shape of maxillary palp segment 3 varied widely among early instar nymphs up to about the mid-point in development (i.e., judged by wing pad size where moderate to large wing pads indicated an individual had achieved or past the mid-point of development). Nymphs with moderate to large wing pads were relatively consistent in the expression of diagnostic characters. Chief among these were color patterns on abdominal terga. The distinctive brown mushroom shaped marks on terga VII–VIII combined with the paired submedian spots and brown lateral streaks made *P. chelifer* nymphs distinctive among the Nearctic *Parameletus*. The use of the presence of sharp PLPs on terga VII–IX, as described by Söderstrom and Nilsson (1986) was not sufficient to reliably separate *P. chelifer* nymphs from those of *P. midas*. Nearctic *P. chelifer* had sharp PLPs on terga VI–IX and small to minute PLPs on tergite V. The same PLPs characters occurred on *P. midas*. In addition to this problem, some *P. midas* nymphs had restricted brown shading on terga VI and VII causing the brown median band to somewhat resemble the marks on *P. chelifer* nymphs.

If abdominal color patterns were not definitive for making a determination, the structural features of setae on the outer edges of cerci and mouthparts will work. Perhaps the most difficult among structural characters to interpret were the shape of tarsal claws, area of claw denticles, and the form of gill trachea. Tarsal claw characters were subtle and difference in claw shape and denticles could be the result of damage and regrowth. Therefore, a single claw should not be used as a stand-alone decision character for a species determination. Generally nymphs of *P. chelifer* seemed to have fewer denticles on tarsal claws than those of *P. midas*. In addition, abdominal gills were quite susceptible to damage. Abrasion, turbulence, and predators cause gills to be lost or damaged. Mayfly gill morphology can also vary across the range of a species (Burian 1995) with differences likely the result of individual exposure to the rigors of different conditions for growth and development (e.g., pond conditions vs. those of the margins of large river channels).

Lastly, the length of the PLPs-tergite IX relative to the length of tergite X used by Jacobus *et al.* (2014) to separate nymphs of *P. chelifer* from those of *P. columbiae*, with *P. chelifer* reported to have long PLPs-tergite IX extending to or past the midpoint of tergite X and of *P. columbiae* having shorter PLPs-tergite IX only reaching about the midpoint of tergite X, was determined to be unreliable as a diagnostic or key character. In many instances it was extremely difficult to get an accurate measurement of the length of PLPs-tergite IX relative to the length of tergite X (even when specimens were held flat using pieces of glass slides). Measurements of nymphs of *P. columbiae* (mostly from Utah and Alaska) showed that most had PLPs-tergite IX long enough to reach to or beyond the midpoint of tergite X.

***Biology and Habitat.*** The biology and life history of *P. chelifer* has been extensively studied in Sweden (Brinck 1957, Olsson and Söderström 1978, Söderström and Nilsson 1987, Söderström and Johansson 1988, Söderström 1988, and Kjærstad *et al.* 2012), but no detailed studies have been conducted in any other part of its vast Holarctic range. Recent general comments on the biology of *P. chelifer* by Bauerfeind and Soldán (2012) indicate that they seem to accept all the past work as universally applicable across the entire range and only reference the life history differences observed for the Nearctic species *P. columbiae* (Edmunds *et al.* 1976). Much more work needs to be done on *P. chelifer* to determine if the behaviors and developmental differences observed in northern Europe are universal

or perhaps become modified according to local habitat and climatic variables. Far northern Holarctic species, such as *P. chelifer*, potentially could be sentinel species for climatic changes that are predicted to occur more rapidly in the Arctic than other areas if their life histories are well known. For example, data on development presented by Olsson and Söderström (1978) showed that in Sweden, *P. chelifer* nymphs required about 55 days to complete development from nymphs to the adult stage. In Canadian Lower Arctic, however, development may only take about 40 days. This estimate of a shorter development time was made based on the presence of newly hatched early instar nymphs in samples collected the fourth week of June and imagos collected toward the end of July. Although this estimate is only a crude first approximation, it indicates that a full and detailed life history study is needed to determine if this seemingly shorter developmental period is real. Finally even though this type of life history data is preliminary, it at least hints at possible differences between North American and northern European populations that could be responding in different ways to prevailing thermal conditions.

One aspect of the biology of *P. chelifer* nymphs of northern Europe that seems to be consistent in North America is their behavior to move from larger rivers into small side channel backwaters and small (sometimes seasonal) streams that connect to pools or wetlands (Olsson and Söderström 1978). In far northern Canada *P. chelifer* nymphs were collected by Donna Giberson from 2000–2004 from a wide range of habitats such as tundra pools, poorly connected seep/pool systems, and shallow permanent ponds. Many of these habitats were close, or connected, to large rivers with wide channels that likely inundated these peripheral areas during seasonal high flows. Marginal aquatic habitats in the Canadian Lower Arctic may offer similar advantages to developing nymphs as discovered in Sweden, but it requires further studies to say this with any certainty.

Although much has been learned about the ecology of *P. chelifer* nymphs in Sweden, habitat details from other parts of the range have been lacking. From 2000–2004, a study of aquatic insect diversity across the Central Barrens area of the lower Canadian Arctic obtained water quality and qualitative habitat data for several sites where *P. chelifer* (nymphs and/or imagos) were collected (per. comm. Donna Giberson). These data are summarized in Table 1.

Specific habitat data were not available for specimens of *P. chelifer* examined from Alaska, but locality label data did allow for a coarse inspection of those areas via Google Earth®. All Alaskan specimens where collected on or next to large river channels. The channel widths (measured using Google Earth®) near what were believed to be the collecting locations varied from 20–45m. The Yukon River at Fort Yukon and the Holitna River south of its confluence with the Kuskowkwin River were > 200m. Unfortunately site specific details for these specimens were lacking, but in one instance, nymphs were collected from a "mud puddle" adjacent to the Chatanika River suggesting that they were likely in similar marginal and flood plain habitats as observed in northern Canada and Sweden.

***Distribution.*** *Parameletus chelifer* is the only Holarctic species of *Parameletus* and thereby had the largest global range. Kjærstad *et al.* (2012) reported that the difference in molecular marker sequence divergence between Finmark populations of *P. chelifer* and those of Manitoba, Canada was extremely small. Thus *P. chelifer* showed little genetic difference across much of its Holarctic range. In North America, current records show the range *P. chelifer* to include much of the lower Arctic of Canada, ranging west from Hudson Bay across Nunavut, Northwest Territories, and the Yukon to the interior of Alaska in the United States (Fig. 111a, Append. 1). The east-west range of *P. chelifer* spans about 65° of longitude (i.e., from 95°W–160°W). The southern edge of the range runs through northern Manitoba, Saskatchewan, and Alberta. Currently there are no records for British Columbia and the far northern part of Quebec, despite both areas having suitable habitats for nymphs.

Table 1. Summary of water quality metric for *Parameletus chelifer* sites in the Northwest Territories and Nunavut, Canada. Data from aquatic insect surveys conducted over four summers from 2000–2003 (per. comm. Donna Giberson).

| | | | Water Quality Metrics | | | |
|---|---|---|---|---|---|---|
| Site | Date | Site No. | pH | Spec. Cond. ($\mu$S·cm$^{-1}$) | Temp. (°C) | D.O. (ppm) |
| NWT: Horton River | 23 Jul 2000 | 14 | ** | ** | 12.0 | 8.7 |
| NWT: Horton River | 31 Jul 2000 | 29 | 8.3 | 200 | 20.0 | 8.0 |
| NWT: Trib. To Thelon River | 6 Jul 2002 | 19 | 6.0 | 20 | 14.0 | ** |
| NWT: Trib. To Thelon River | 7 Jul 2002 | 22 | 5.7 | 50 | 9.0 | ** |
| NU: Tundra Pond above Thelon River | 8 Jul 2002 | 27 | 6.0 | 10 | 15.0 | ** |
| NU: Baker Lake Area, Pond | 14 Jul 2003 | 20 | 7.4 | 540 | 13.0 | ** |
| NU: Arviat Area, Maguse River | 10 Jul 2003 | 6 | 6.0 | 10 | 12.0 | ** |

**No data

***Parameletus columbiae* McDunnough, 1938 (Figs. 31–59)**

***Male Imago*** (in alcohol). Body length: 10.16–13.83 mm (11.95±1.42, mean±SD, n=10). General body color brown, some areas darker and some with reddish tints (Figs. 31a–c).

***Head.*** Background color light yellow-brown, heavily shaded with dark grey (Figs. 32, 33). Bases of ocelli dark brown. Compound eyes large and semiturbinate with upper portions meeting along dorsal midline of head. Large upper parts of compound eyes cover most of head, only small part of posterior of head capsule visible. Lower portion of compound eyes blueish grey. Basal segments of antennae brown, apical segments of flagella pale yellow-brown. Frons below lateral ocelli and bases of antennae marked with dark brown as in Fig. 33. Frons below lateral ocelli elongated with medial keel and straight ventral edge (Fig. 33).

***Thorax.*** Dorsal and lateral aspects as in Figs. 32, 34. Most sclerotized areas dark brown, some areas blackish brown. Membranous cuticle white to cream colored. Thickened edges of nota and pleural sutures with darkest color. Posterior half of pronotum visible dorsally. Pronotum medium brown with extensive grey shading, on some specimens pronotum mostly dark grey. Mesonotum mostly brown to dark brown with few light yellow-brown areas (Figs. 32, 34). Pale white to cream colored areas along PSL. ALPs dark greyish-brown and distinct from darker brown lateral areas of SMS. PSp and posterior medial parts of MS and ISL dark brown, almost black (Figs. 32, 34). SSLi light brown. Center and edges of mesonotal SL dark brown. Dorsally MNs appears slightly curved and together with ANi and ANp forms distinctive outline on MS (Fig. 32). Area within outline often much lighter yellow-brown than rest of MS (Figs. 32, 34). Metanotum mostly dark brown with darker edges of more heavily sclerotized areas as seen on mesonotum. Metanotal SL with same dark brown to black edges as occurs on mesonotum SL (Figs. 32, 34).

***Wings.*** Forewing length: 10.16–12.50 mm (11.00±0.73, mean±SD, n=10). Forewing membrane transparent and unpigmented except for opaque area of stigmatic region between the costa and subcosta veins and subcosta and radius$_1$ veins (Fig. 35a). All major longitudinal veins, most crossveins, and marginal veins medium to dark brown. All major longitudinal veins fade to white at wing base. Most crossveins of costa/subcostal interspace single with only a few merging near wing apex. CuA vein joined to hind margin of wing by series of about 8 sinuate crossveins that do not merge with marginal intercalary veins. Variable number (~4–6) unattached marginal intercalary veins can occur alternately between sinuate crossveins. Occasionally 2 marginal veins occur together in same space (Fig. 35a). Hind wing membrane unpigmented as in forewing (Fig. 35b). Major longitudinal veins and discal crossveins pigmented as described for forewing. Brown color of major longitudinal veins extends to wing base. Basalmost part of costa pale. MP vein not forked. Costal projection evident only as slight arching of costa near wing base.

***Legs.*** Ranges, means, and ratio values of segments of male forelegs as follows: Femur 2.24–2.84 mm, (2.45 [1.05], n=9 ) (mean [median of ratio to tibia], sample size), Tibia 2.12–2.67 (2.42 [1.00], n=9), $T_1$= 1.12–1.58 (1.31[0.53], n=9), $T_2$=1.26–1.75 (1.52[0.60], n=9), $T_3$= 1.28–1.83 (1.59[0.63], n=9), $T_4$= 1.00–1.50 (1.24[0.48], n=9), $T_5$= 0.76–0.92 (0.82 [0.36], n=9). Forelegs dark brown (Fig. 36a). Mid and hind legs yellow-brown, femora tend to have slightly more brown than other segments (Figs. 31a, 37). Foretibiae and $T_1$ of tarsi with blunt spine-like knobs (Fig. 36b). Ventral apical spine on mid and hind tarsal segments $T_1$–$T_4$ (Fig. 37), ventral edges with several small dark spines (Fig. 37). Forelegs with five distinct tarsal segments. Mid and hind legs with only 4 distinct tarsal segments, basal segment $T_1$ fused to tibiae. Segment $T_1$ of mid and hind legs fuses to tibiae during development to subimago (5 distinct tarsal segments of imago legs can be seen through cuticle of last instar nymphs). Fused joint between tibiae and tarsal $T_1$ marked by difference in color of cuticle (Fig. 37).

***Abdomen.*** Background color pale yellow-brown, shaded with medium reddish brown on both terga and sterna (Figs. 38a–c). Membranous cuticle between abdominal segments and along pleural areas semi-transparent white or pale yellow-brown. Anterior margin of terga II–X with paired medial dark brown crescent shaped marks (Figs. 38a,b). Tergite I with diffuse dark brown shading over paired medial marks making marks less distinct. On some individuals paired marks blend together with background color forming medial large brown mark. Anterolateral corners of terga pale yellow (Figs. 38a,b). Lateral areas of terga I–IX with distinctive dark brown streak. Lateral streak merges dorsally into narrow brown band along posterior margins of terga. Brown bands of posterior margins of terga merge with medial brown line that extends anteriorly between paired submedian spots (Fig. 38a). Tergite X with large brown medial spot that merges with slightly darker paired submedian spots, marks on tergite X darker than marks on terga I - IX. Tergite X lacks lateral brown streaks. Dark trachea below cuticle of terga enhance overall darker color of segments (Figs. 38a,b). Occasionally on specimens where cuticular color has faded because of preservation parallel bands of muscle tissue below cuticle become visible and tend to obscure paired submedian spots, as well as other color features. Background color of sterna reddish brown (Fig. 38c). Sterna I–IX with center areas

mostly brown. Anterior edges of sterna white. Lateral edges of sterna adjacent to pleural fold often margined with thin dark brown line (Fig. 38c). Paired submedian brown dashes and 2 small brown spots evident within brown background color on sterna I–IX. Spots smaller and occur close to middle of sterna, longer dashes anterior and lateral to spots (Fig. 38c). On sterna VII–VIII dashes become more like horizontal dashes (Fig. 38c). Genitalia as in Figs. 39, 40, forceps brown and 4 segmented. Basal segment of forceps only weakly sclerotized on dorsal surface and has no distinct joint with second segment (Figs. 40, 41a,b). Posterior margin of styliger plate with rectangular median projection that protrudes beyond flanking edges of posterior margin of styliger plate. Rectangular median projection usually one quarter to one third width of posterior margin (Figs. 41b, 42). Dorsal and ventral medial surfaces of styliger plate pale compared to lateral areas adjacent to base of forceps (Fig. 41b). Forceps bases dark brown, dark brown bands extend from bases diagonally along edges of styliger plate. Penes as in Figs. 39, 40, 41b, tips do not reach beyond posterior margin of styliger plate. Large lobes of penes have pincher-like appearance and almost meet on intact specimens (Figs. 41b, 42). Dorsal medial spines have distinct bifid tips (Fig. 39).

***Caudal Filaments.*** Caudal filaments as in Fig. 43, cerci light brown. Basal quarter of caudal filaments usually dark brown, mid-section somewhat lighter. Apical annuli light brown. Annuli of darker part of filaments with pale bands at joints (Fig. 43). Median terminal filament vestigial.

***Female Imago*** (in alcohol). Body length: 9.16–14.17 mm (12.07±2.00, mean±SD, n=5). General body color pale to medium brown (Figs. 44, 45a), thorax much lighter compared to that male imagos.

***Head.*** Base color of head light yellow-brown, but extensively shaded with dark grey. Vertex with 2 dark longitudinal stripes arising from bases of lateral ocelli, stripes converge posteriorly meeting at postoccipital suture. Compound eyes small and lateral in position. Lateral ocelli and median ocellus similar in size. Bases of lateral ocelli with narrow dark blackish brown band. Median ocellus recessed into depression on frons, base dark brown. Antennae light brown. Frons with median keel extending from median ocellus to ventral margin. Ventral edge of frons yellow-brown, similar to lighter parts of vertex.

***Thorax.*** Dorsal and lateral aspect as in Figs. 44, 45a,b, general structural features similar to those of male imago, but overall color much lighter. Most large sclerotized areas beige to sand color with dark brown sutures. Pronotum as in Fig. 45a, grey infused over lighter background color similar to vertex of head. Meso- and metanotum with pale yellow or white areas adjacent to PSL and pleural region around wing bases. ANi medium brown, distinctly darker than adjacent areas of mesonotum. Dorsal anterior part of MS beige. SL of mesonotum medium brown and ISL dark brown. Mid-dorsal area of SL and ISL of metanotum similar to that of mesonotum. Lateral areas of SL light brown. Female pterothorax lacks blackish brown color, darkest areas of color occur on ISL of meso- and metanotum (Figs. 44, 45a).

***Wings.*** Forewing length: 10.16–12.50 mm (12.04±1.40, mean±SD, n=4). Wing membrane color, as well as color and placement of major longitudinal veins as noted for male imago. Forewing CuA vein joined to hind margin by series of 6–7 sinuate crossveins, none merge with marginal intercalary veins. Unattached marginal intercalary veins (~3–4) can occur alternately between sinuate crossveins.

***Legs.*** All legs yellow-brown, tarsi tend to have slightly more brown than other segments. Legs with four distinct tarsal segments and 1 basal segment fused to tibiae. Tarsal segment $T_1$ fused to tibiae, no tarsal joint present. Ventral apical spine on mid and hind tarsal segments $T_1$–$T_4$, ventral edges with several small dark spines. Tarsal segment $T_1$ fuses to tibiae during development to subimago (5 distinct tarsal segments of imago legs can be seen through cuticle of last instar nymphs).

***Abdomen.*** Background color beige to pale yellow-brown, shaded with medium reddish brown on both terga and sterna (Figs. 45a,b, 46a,b). Lateral color pattern as in Figs. 44, 46b. Range of dorsal and ventral color patterns as in Figs. 45a–c, 46a–c. Tergite I mostly brown, submedian spots absent. Terga II–X with paired crescent-shaped submedian brown spots and medial triangular spots (Fig. 45a). Dark brown triangular marks with base on brown band along posterior margin of terga. Brown lateral streaks on all terga, streaks most distinctive near posterolateral corners of terga (Figs. 45a, 46a). Anterolateral areas of terga mostly white or cream colored. Lateral appearance of genital openings on sternite VII and color of sternite VIII as in Fig. 46a. Shape of posterior margin of sternite IX as in Figs. 45c, 46c.

***Caudal Filaments.*** Caudal filaments similar in appearance and length to those of male imago.

***Nymph*** (in alcohol, well developed or dark wing pad stage). Body length ♂: 7.25–9.83 mm (8.27±0.83, mean±SD, n=13); Body length ♀: 8.16–12.17 mm (9.34±1.60, n=7); Tergite VII ratio width:length ♂: 2.11–2.93 (median=2.73, n=13); Tergite VII ratio width:length ♀: 2.05–2.93 (median=2.63, n=5); PLPs-tergite IX (width) ♂: 0.10–0.20 mm (0.12±0.03 n=13); PLPs-tergite IX (width) ♀: 0.12–0.16 mm (0.14±0.02, n=7); PLPs-tergite IX (length) ♂: 0.16–0.27 mm (0.20±0.03, n=13);

PLPs-tergite IX (length) ♀: 0.18–0.28 mm (0.23±0.03, n=7).

***Mouthparts*. Labrum:** Labrum somewhat rectangular with widest point about half way along lateral edge (Fig. 47a). Dorsal surface relatively flat, not distinctly arched. Numerous widely spaced long thin setae on dorsal surface, but setae near anterior edge of labrum packed closely together (Fig. 47b). Medial part of anterior edge extending onto ventral surface, appearing as an under-turned lip. Under-turned lip narrow (Figs. 47c). Ventral surface of labrum with 2 groups of long sharp setae lateral to dense patches of fine setae. **Labium:** Glossae and paraglossae with numerous small thin setae arranged in dense brush-like patches on apical third of each lobe (Figs. 48a,b). Apical edges of glossae with small patches of short stout setae surrounded by finer setae. Glossae and paraglossae large relative to prementum. Joint at based of glossae and paraglossae aligned on either side of midline of labium. Together both joints form an angle of 60º–65° in relation to midline of labium (Fig. 48a). Labial palps 3 segmented. Segment 1 with several large stout setae on dorsal surface, but only small scattered hair-like setae occur along anterior edge of dorsal surface (Fig. 48a). Ventral surface of segment 1 with several broadly distributed long thin setae. Segment 1 subequal to length of segments 2+3. Segment 2 with thumb-like process extending about one third length of segment 3. Margin of thumb-like process with 3 long thin setae directed inward toward paraglossae and several small hair-like setae. Outer dorsal surface of segment 2 with 2 irregular rows of large thin setae similar to setae on dorsal surface of segment 1. Segment 3 with apex broadly rounded, apical edge forms a sharp corner at junction with inner edge (Figs. 48b,c). Inner apical surface of segment 3 not distinctly indented. Dorsal surface of segment 3 with an irregular row of about 6 long thin setae. Inner apical surface of segment 3 only slightly concave (Figs. 48b,c) with row of short setae along ventral edge. Row of short setae does not quite reach base of segment 3. **Hypopharynx:** Lingua square, anterior margin with shallow v-shaped notch (Fig. 49a). Fine hair-like setae occur across dorsal surface and apically, tips of setae extend beyond anterior margin. Corners of lingua lack long thin setae. Superlinguae with outer lobes broadly rounded and many long thin setae (Fig. 49b). Apical edges of superlinguae with about 14 long setae widely spaced along outer part of apical edge, but much more closely spaced along inner part of apical edge. Innermost surface of each lobe of superlinguae with dense brush of shorter hair-like setae. **Right Mandible:** Anterior margin between molars and incisors mostly free of surface features (rarely few minute surface denticles present on some individuals) appearing smooth (Fig. 50a). Molar surface relatively short with only about 9 large rounded teeth visible above rows of brush-like setae present on outer edge of molar surface (Fig. 50b). Pre-molar projection conical with pointed apex (Fig. 50a). Incisors arise almost perpendicular to anterior margin and do not curve inward from their bases (although tips do curve inward slightly). Notch between incisors extends below edge of anterior margin. Innermost incisor with row setae on ventral surface. Cluster of long setae occurs below outer corner of molars. Prostheca present with brush portion reaching about halfway across anterior margin (Fig. 50a). **Left Mandible:** Anterior margin between molars and incisors straight (Fig. 51a). Anterior margin mostly smooth, rarely few minute surface denticles occur on some individuals. Molar surface short with only about 9 rows of teeth (Fig. 51b). Postmolar projection (below horizontal rows of teeth) broad and conical with apex rounded. Ventral apical edge of outer group of incisors with single accessory tooth with pointed tip (Fig 51c). Area of brush-like fine setae adjacent to molar surface, tips of setae do not extend above anterior margin of mandible. **Right Maxilla:** Galea-lacinia broad with apex rounded to apical group of canines (Fig. 52a). Crown of galea-lacinia with 8 large pectinate setae and 4 long thin setae with finely serrate tips (Figs. 52a,d). Apex of galea-lacinia with 3 large canines and 3 large dentisetae below apex. Largest dentisetae closest to canines (Fig. 52e). Dentisetae flanked by 2 rows of long thin setae (~19 per row) with finely serrate edges. Rows of long thin setae extend from dentisetae to base of galea-lacinia. Near base of galea-lacinia small cluster of 2–3 small setae. Maxillary palps 3 segmented (Fig. 52a). Ventral surface of segment 1 with staggered row of 5–6 long sharp setae near outer edge, about 5 long thin setae directly on outer edge and 5–6 similar setae on inner edge. Segment 1 only slightly longer than segment 2 and segment 2 widest at junction with segment 3 and narrowest at junction with segment 1 (Fig. 52a). Ventral edge of segment 2 with row of about 5 long thin setae that extend up to junction with segment 3. Ventral surface of segment 2 with row of 7–8 long thin setae that extends to inner apical corner of segment. Ventral setae of segment 2 closely spaced near apical corner and connect up to closely spaced row of setae on ventral edge of segment 3. Tip of segment 3 rounded, inner edge distinctly concave, appearing semilunar or crescent shaped (Figs. 52b,c). Dorsal surface of segment 3 with row of about 6 widely spaces long, thin setae (Fig. 52b). Ventral surface of segment 3 with row of 16–18 closely spaced long thin setae that meet row of similar setae on segment 2 at junction between segments (Fig. 52c).

***Legs*. Foreleg**: Dorsal and ventral surfaces of femora with staggered rows of long sharp setae (Fig. 53a). Middle of dorsal surface relatively free of setae. Middle of ventral surface with few large sharp setae near coxa. Tibiae and

tarsi subequal in length (except for last instar nymphs where tarsi elongate relative to tibiae to accommodate developing legs of imago (Fig. 53a). Dorsal edge of tibiae and tarsi relatively free of setae, only few scattered hair-like setae present (Fig. 53b,c). Ventral edge of tibiae and tarsi with long sharp setae and stout finely bi-serrate setae (Figs. 53b,c). Tibiae lack tibiopatellar suture. Setae on inner surface of tarsi arranged in 2 roughly parallel rows, setae in rows occur in small groups with gaps between groups. **Foreclaw:** Foreclaw slender and uniformly tapered from base to apex (Figs. 54a,b). Small to minute denticles usually on basal quarter of claw, but occasionally denticles can cover one third claw. Extent of denticle patches can vary from right to left foreclaw (Fig. 54b). Denticles organized into 2 patches separated by narrow space with no denticles. Because foreclaw mostly free of denticles, when viewed with moderate to low magnification claw can appear to lack denticles (Fig. 54a).

***Gills.*** **Mid-Gills (3–5):** Gills broad, slightly more oval than typical subcordate form (Fig. 55a). Mid-gills with rounded apices (Fig. 55a), but posterior gills 5–7 have slightly more pointed apices. Basal dorsal edges of gill lamellae straight, not appearing as lobe-like flap. Most gills with 2–3 ventrally directed secondary tracheal branches off main gill trachea, 4 secondary tracheal branches usually occur dorsally. Gill membrane mostly unpigmented except over major trachea where it is slightly darker than surrounding surface. All trachea uniformly pigmented yellow-brown (Fig. 55a). Numerous small hair-like setae along outer margin of gills. Ventral sclerotized edge narrow with single row of large bi-serrate setae interspersed with small thin setae similar to, but longer than setae along outer margin of gill (Fig. 55b). Ventral sclerotized edge extends half to one third length of gill lamellae. Sclerotized mid-rib present on all gills, but weakly pigmented. Mid-ribs extend dorsally from gill bases no more than one fifth length of gill lamellae (Fig. 55c).

***Abdomen.*** **Abdominal Color Pattern:** Abdominal color pattern composed of paired submedian brown spots and thin dark median stripe that merges with brown band along posterior margin of terga (Figs. 56a,b). Laterally faint brown triangular patches connect to brown posterior band. Lateral markings fade extensively on anterior abdominal segments. Tergite X with paired brown stripes. No brown shading over paired submedian spots on terga. Sterna pale yellow with faint paired brown marks on sterna II–IX and arched posterior brown band on sterna II–VI as in Fig. 56b. **Setae on Posterior Margin of Abdominal Terga:** Posterior margin of terga VII–IX with scattered short stout setae similar to those on surface of terga, but no obvious row of large dark spine-like setae. Rarely 5–6 small dark stout setae occurred widely spaced along posterior margin of tergite IX and/or terga VII and VIII. **Setae on Surface of Abdominal Terga:** Surfaces of terga covered with numerous small short hair-like setae and scattered short stout setae. **Setae on Surface of Abdominal Sterna:** Surfaces of sterna covered with numerous small short hair-like setae and scattered short stout setae similar to terga. In addition to general surface setae, dense clusters of short setae occur near posterior margins of sterna I–V. Setae in clusters appear as small brushes when viewed laterally. **Setae on Lateral Margins of Terga and PLPs-tergite IX:** Lateral margins mostly with small short hair-like setae and scattered small stout setae, large spine-like setae absent. Lateral margins of tergite IX roughly parallel to midline of body, only early instars seem to slightly deviate from this (Fig. 57). **PLPs-tergite IX**: Short relative to length of tergite X, only reaching to about midpoint of tergite X (Fig.57). Shape of PLPs-tergite IX variable, tips can be thick or thin and projections either straight or flare outward. Inner margin of PLPs-tergite IX smoothly curved or slightly sinuate. **PLPs-terga V - IX:** Distinct PLPs on terga VI–IX. Small to minute PLPs rarely occur on tergite V of some nymphs. **Left Paraproct:** Surface with about 26 long sharp setae broadly distributed over middle of paraproct. Cluster of about 6 large sharp setae occur on inner apical edge (Fig. 58).

***Caudal Filaments.*** All caudal filaments yellow-brown (Fig. 59). Dense fringe of long setae arises from both side of medial terminal filament and overlap similar fringes of setae from inner edges of cerci. Simple spine-like setae uniformly spaced along outer edges of all but apical annuli (Fig. 59). Outer lateral corners of annuli at midpoint of cerci with groups of 2–3 long thin setae, because color and fine structure setae often blend into background appearing absent. Median terminal filament with few scattered stout setae on dorsal midline of some annuli.

***Diagnosis*. Imagos:** Male imagos of *P. columbiae* can be separated from those of other North American species of *Parameletus* by following combination of characters (1) distinctive structure of penes and associated styliger plate (Figs. 39–41a,b, 42), (2) generally darker brown color of thorax and abdomen with distinctive reddish brown dorsal and lateral marks and contrasting pale anterolateral corners of terga (Figs. 38a–c), and (3) mostly northern and montane distribution that extends from Alaska south along the Rocky Mountains to northern Utah (Fig. 111b). Female imagos can be tentatively separated from those of other North American species of *Parameletus* by (1) distinctive dark brown color of abdomen with its pattern of dorsal and lateral marks similar to those of male imago (Figs. 44–46a–c), color of female thorax not as deeply pigmented as abdomen,

(2) distinctive color of abdominal sterna as in Figs. 45b, 46b and specifically sterna VII and VIII with regards to structure and appearance of genital openings (Figs. 45c, 46c), and (3) mostly northern and montane distribution that extends Alaska south along the Rocky Mountains to northern Utah (Fig. 111b).

***Diagnosis.*** **Nymphs**: Nymphs of *P. columbiae* can be separated from those of other North American species of *Parameletus* by the following combination of characters: (1) unique color pattern on abdominal terga (Figs. 56a,b), (2) presence of only thin spine-like setae on outer edges of cerci (Fig. 59), (3) maxillary palp segment 3 with distinctly concave or semilunate inner margin (Fig. 52b) and inner surface with 16–18 closely spaced setae (Fig. 52c), (4) lingua of hypopharynx square and anterior margin with v-shaped notch (Fig. 49a), (5) shape of apex of labial palp segment 3 with outer edge smoothly rounded to sharp corner where outer edge meets inner margin (Fig. 48c), (6) left paraproct with few large spine-like setae, scattered over surface (Fig. 58), (7) tarsal claws shaped as in Fig. 54a, with patches of small to minute denticles restricted to base of claws (denticles often so small as to appear absent), (8) abdominal gills 3–5 with poorly developed ventral sclerotized edges and mid-ribs (Figs. 55a,b), (9) abdominal gills 3–5 broad with rounded apices, generally gills more oval than typical subcordate form (Fig. 55a), and (10) lateral margins of abdominal segment 9 roughly parallel to midline of body (Fig. 57).

***Comments on Character Variation*. Imagos:** No consistent alternate color morphs of the male imago were observed among material available for study. However, among the more recently collected specimens there was a distinct difference in the amount of dark shading on the abdomen, suggesting the possibility of local differences that may be reflective of small scale habitat conditions and/or local population variation. Diagnostic characters were consistent among all male imagos studied. The more recently collected material from Montana agreed well with the holotype and older material from Alaska. Center and edges of mesonotal SL were consistently dark brown, lacking occasional pale areas that occur on some *P. chelifer* imagos. Fewer discal crossveins occur in the hind wings of *P. columbiae* compared to those of *P. chelifer*. The shape of the median projection on the posterior edge of the styliger plate showed the most variation among genital characters. The median projection varied from a well-defined rectangular shape to one that had more rounded corners and was somewhat trapezoidal. The lower, rounded form on some individuals was little different from that observed on some specimens of *P. chelifer*. Despite the overlap in this character between *P. columbiae* and *P. chelifer*, the structure of the penes was consistently different between the two species.

Although few female imagos were available for study, primary diagnostic characters were consistent. Female imagos were lighter brown with more distinctive patterns of dorsal, ventral, and lateral spots and marks compared to male imagos. Among the specimens studied, the most variable abdominal color pattern was associated with the genital openings between sterna VII and VIII. The most consistent pattern for genital segments was a diffuse dark brown band along the edge of sternite VII. On some individuals this brown band was narrower and less diffuse. The general reddish hue of abdominal sterna was also consistent.

**Nymphs:** Nymphs of *P. columbiae* were morphologically quite different from those of other Nearctic species of *Parameletus*. The unique color pattern of abdominal terga was certainly the most definitive character for determining nymphs of *P. columbiae*; faint but visible evidence of the pattern is observable even on specimens that have been preserved in alcohol for several decades. The brown marks on abdominal sterna were also unique, but much less resilient to long term exposure to alcohol. Structural characters seem to work best on mid-instar and latter instar nymphs, but such features as the shape the apex of segment 3 of the labial palp and shape of the maxilla and segment 3 of the maxillary palp also worked for small nymphs that hadn't reached the mid-point of development. Comparatively, setae along the middle of the anterior margin of the labrum were thinner and the under-turned lip narrower than observed on *P. midas* or *P. chelifer*. Another subtle difference in mouthparts between *P. columbiae*, *P. chelifer* and *P. midas* was the setae at the base of the galea-lacinia. On maxillae of *P. columbiae* a cluster of small equal length setae occur near the base of the galea-lacinia. This differed from nymphs of *P. chelifer* and *P. midas* where a single long setae occurs in the same position. Unfortunately these setae were damaged on several specimens thus limiting their usefulness as a reliable and resilient diagnostic character. Tarsal claw characters showed some variability from right to left on a single individual, but the slender form of the claw with few, minute denticles was relatively consistent. Abdominal gills had a unique shape and poorly developed sclerotized ventral edges and mid-ribs. Outer margins of gills had many small hair-like setae, noticeably more than observed for other Nearctic species of *Parameletus*. Abdominal terga VII–IX had scattered short stout setae similar to those on surface of terga, but there was no obvious row of large dark spine-like setae as described for *P. chelifer* and *P. midas*. Finally, the lateral margins of abdominal tergite IX were roughly parallel to the body midline on even the smallest specimens studied, but the position of sharp tips

of the PLPs of this segment did vary. The position of the sharp tips of PLPs varied from straight (paralleling the midline of the body) to distinctly diverging (away from the midline) and PLPs tips were also bent dorsally on some specimens. Sometimes the position of the tips of the PLPs can bias the interpretation of the lateral margin producing a slight optical illusion that the entire edge diverges and not just the tips.

***Biology and Habitat.*** Almost everything that is known about the life history of *P. columbiae* comes from the studies of Edmunds (1952, 1957) on the population at Silver Lake, Brighton, UT, USA. The synopsis of the life history for the genus *Parameletus* given by Edmunds *et al.* (1976) is that of *P. columbiae* even though the species is not specifically mentioned by name. Details of the habitat of nymphs presented by Edmunds *et al.* (1976) were also taken directly from the earlier work (Edmunds 1952, 1957) on *P. columbiae*. In the pond and associated forest wetland of the high elevation Silver Lake site, development was observed to take from 16–22 days (Edmunds 1957). This is the briefest developmental period known for any of the Nearctic species of *Parameletus*. The reason for such a rapid development from nymph to imago has been explained by the rapid changes in available habitat where development, reproduction, and oviposition must be completed before suitable habitats dry up (or mostly dry up) as spring rapidly progresses into early summer at high altitude (~2651m AMSL). If *P. columbiae* only occurred in high elevation ponds and wetlands this would seem a likely reason, but *P. columbiae* also occurs at low elevations across the interior of Alaska where seasonally flooded wetlands and shallow flood plain pools persist longer in the spring and early summer. In these habitats perhaps a greater advantage to a fast life cycle is predator avoidance and less competition for food. Considering this alternative possibility for the benefit of a fast life cycle, did the short development time evolve first in response to habitat pressures and later proved to be adaptive for predator avoidance and reduced competition or did it evolve first as a mechanism to avoid predators and lessen competition and later proved to be adaptive in shorter lived marginal habitats at high elevation, possibly enhancing survival during the last glacial maxima? To begin to address these questions more life history information is needed on the low elevation populations of *P. columbiae*.

Currently the only other study on the biology of *P. columbiae* was done by Gilpin and Brusven (1970). They observed *P. columbiae* nymphs at 5 sites on the St. Maries River, Idaho and examined their gut contents to determine food habits. They reported that about 70% of the gut contents of nymphs were detritus and 20% the Xanthophyte (Stramenopiles clade) *Bumilleria* sp. The remainder was mostly composed of unidentifiable algae and vascular plant fragments.

***Distribution.*** *Parameletus columbiae* has the greatest latitudinal range all of the Nearctic *Parameletus*. The southernmost range point occurs at Brighton, Utah, USA (~ 40° N) and the northernmost point at the Chatanika River, Alaska, USA (~65°N). The current distribution essentially follows the spine of the Rocky Mountains between these points (Fig. 111b, Append. 1). *Parameletus columbiae* is also the only other Nearctic species of *Parameletus* whose range extensively overlaps that of *P. chelifer*. The co-occurrence of *P. columbiae* and *P. chelifer* in Alaska suggests that both species should be present in suitable habitats in the Yukon, northern British Columbia, and Alberta where currently there are no records for these taxa.

***Parameletus croesus* (McDunnough, 1923) (Figs. 60–82)**

***Male Imago*** (in alcohol). Body length: 10.00–12.33 mm (11.17±0.86, mean±SD, n=7). Body mostly brown (Figs. 60a,b), but mesonotum mostly greyish brown (i.e., similar to ~50% French Grey tint).

***Head.*** Background color pale yellowish brown. Small areas of grey posterior to bases of lateral ocelli and on vertex (Figs. 61a–c). Bases of ocelli dark brown (occasionally appearing almost black). Compound eyes large and semiturbinate with lower portion shaded greyish blue (Fig. 62a). Large upper part of compound eyes barely meet along dorsal midline of head or separated by extremely narrow gap (Figs. 61a–c). Antennae uniform light brown (Fig. 62a). Frons with median keel produced ventrally to sharp point, surface of frons directly below antennal sockets light brown (Fig. 62a). Thin dark brown lines extend from medial corners of lateral ocelli toward medial keel of frons. Posterior lateral edges of frons dark brown (Fig. 62a). Frons extends ventrally well below head (Fig. 62a). Posterior of head mostly obscured by compound eyes (Fig. 61c).

***Thorax.*** Dorsal and lateral aspect as in Figs. 61a,b, 62b. Sclerotized areas mostly light brown, but grading to slightly darker brown in some places. Membranous cuticle white to cream colored. Thickened edges of nota and sutures dark brown to almost black (Figs. 61a, 62b). Anterolateral corners of pronotum largely obscured by compound eyes, but middle and posterolateral corners of pronotum visible. General shape of pronotum trapezoidal, posterior margin indented medially to accommodate anterior part of mesonotum. Pronotum background color light brown with areas of medium to dark brown laterally. Posterior edge of pronotum margined with dark brown (Figs 61a,b). Mesonotum greyish brown with lighter

pale yellow to white areas along PSL (Figs. 61a,b). ALPs medium brown appearing distinct from mostly greyish brown SMS (Figs. 61a,b). PSp and posterior edges of MS dark brown (Figs. 61a,b, 62b). SSLi pale compared to darker parts of MS. Center and edges of SL usually dark amber-brown. ISL regions and SL have darkest brown shading (Figs. 61a,b, 62b). Dorsally MNs appears straight and together with ANi and ANp forms distinctive outline on MS (Figs. 61a,b, 62b). Area within outline often much lighter yellow-brown compared to surrounding MS (Fig. 61a,b). Metanotum with similar coloration as on mesonotum. Metanotal SL and ISL dark brown. Margins of metanotum pale yellow-brown (Fig. 61b, 62b).

***Wings.*** Forewing length: 9.16–10.83 mm (10.09±0.50, mean±SD, n=8). Forewing membrane with slight yellowish tint (Fig. 63b), overlap of forewing and hind wing membranes near wing bases makes tint much more distinctive. Stigmatic area between costa and subcosta veins and subcosta and radius$_1$ veins opaque (Fig. 63b). All major longitudinal veins, most crossveins, and marginal veins medium to dark brown. All major longitudinal veins fade to white at wing base. Most crossveins of costa/subcosta interspace single veins with only few merging near wing apex. CuA vein joined to hind margin by series of about 6 sinuate crossveins. Alternately, between sinuate crossveins 3–5 unattached marginal intercalary veins can occur (Fig. 63b). Occasionally 1 sinuate crossvein may merge with short marginal intercalary veins. Hind wing membrane pigmented as in forewing (Fig. 63c). Major longitudinal veins and discal crossveins of hind wing pigmented as described for forewing. All major longitudinal veins brown to wing base except costa, basalmost part of costa pale (Fig. 63c). Costal projection only evident as slight arching of costa near wing base (Fig. 63c).

***Legs.*** Ranges, means, and ratio values of segments of male forelegs as follows: Femur 2.12–2.60 mm, (2.43 [1.15], n=10 ) (mean [median of ratio to tibia], sample size), Tibia 2.00–2.26 (2.42 [1.00], n=10), $T_1$= 1.16–1.44 (1.25[0.59], n=10), $T_2$=1.12–1.50 (1.29[0.62], n=10), $T_3$= 1.12–1.60 (1.34[0.64], n=10), $T_4$= 0.92–1.28 (1.10[0.50], n=10), $T_5$= 0.60–0.96 (0.80 [0.39], n=10). All legs yellow-brown, forefemora and tibiae tend to have slightly more brown than other segments (Figs. 64a–c). Foretibiae and tarsal segment $T_1$ with blunt spine-like knobs (Fig. 64b). Edges of segments at joints of tibiae and tarsi margined with dark brown (Fig. 64b,c). Color on forelegs most intense at joints and much less intense on mid and hind legs. Ventral apical spine on mid and hind tarsal segments $T_1$–$T_4$, ventral edges with several small dark spines. Forelegs with 5 distinct tarsal segments, but mid and hind legs have only 4 distinct tarsal segments. Tarsal segment $T_1$ of mid and hind legs fuses to tibiae during development to subimago (5 distinct tarsal segments of imago legs can be seen through cuticle of last instar nymphs). Fused joint between tibiae and tarsal segment $T_1$ marked by difference in cuticle color.

***Abdomen.*** Background color white to pale yellow shaded with medium brown on terga and sterna (Figs. 65a–c, 66a–c). Membranous cuticle between abdominal segments and along pleural areas semi-transparent white to pale yellow (similar to ivory). Terga II–X with dark brown paired submedial, elongate marks (Figs. 65a,b, 66b). On tergite X paired submedial marks tend to broaden near posterior margin becoming less distinctive (Figs. 65a, 66b, 68). On tergite I paired submedial marks fuse with broader area of dark brown shading. Anterolateral corners of terga white or pale yellow (Figs. 60b, 65b). Pale anterolateral areas of terga connect across anterior margin creating pale band (Figs. 65b, 66b). Pale median streak between paired submedian dark marks, pale streak meets anterior pale band (Figs. 65b, 66b). Lateral areas of terga I–IX with distinctive dark brown streak that extends length of terga. Dark lateral streaks merge dorsally forming narrow brown band along posterior edge of terga (Fig. 65b). Tergite X lacks lateral brown streaks Sterna background color pale yellow-white or white, similar to terga. Lateral edges of sterna adjacent to pleural fold white to pale yellow (Fig. 65c).Sterna II–VII with distinctive rectangular dark brown center (Fig. 65c). Sternite VIII has similar large brown central mark, but mark narrows to acute point at anterior margin (Fig. 65c). Sternite IX with large brown v-shaped mark, apex of v-shaped mark along anterior margin of sternite IX, apex seems to merge with base of central dark mark on sternite VIII (Fig. 65c). Tips of v-shaped mark extend to posterior corners of sternite IX. Center of sternite IX pale yellow, similar to base of styliger plate (Fig. 65c). Styliger plate yellow-brown to brown, membrane at posterior margin where styliger plate articulates with sternite IX transparent (Fig. 65c). Posterior margin of styliger plate with deep v-shaped notch (Fig. 65c, 66c, 68). Dorsal and ventral medial surfaces of styliger plate pale compared to lateral areas anterior to forceps bases. Genitalia as in Figs. 67a–e, forceps 4 segmented, segments 2–4 light brown. Forceps segment 1 dark brown and dorsal surface weakly sclerotized. No distinct joint between segments 1 and 2 of forceps. On some specimens collected while swarming styliger plate was flexed downward at 90° angle to penes (Fig.67c). Penes as in Figs. 67a,b, tips do not extend beyond posterior margin of styliger plate. Dorsally, sclerotized lateral lobes have long paired spines next to bifid tips of penes (Figs. 67a,e). Ventral surface of penes with eversible membranous pouches, each with rounded apical portion and curved finger-like apical lobes (Figs. 67b–e). Membranous pouches of penes not apparent on specimens with styliger plate held in horizontal position relative to abdomen (Fig. 69). Membranous pouches of

penes difficult to discern when genitalia slide mounted (Fig. 67b).

***Caudal Filaments.*** Caudal filaments as in Fig. 70. First fifteen annuli of cerci dark brown, remainder uniform light brown. Beyond dark brown basal annuli, joints between remaining annuli ringed with dark brown (Fig. 70). Median terminal filament vestigial.

***Female Imago***. No specimens were available for study.

***Nymph*** (in alcohol, well developed or dark wing pad stage). Body length ♂: 9.66–12.66 mm (11.61±1.69, mean±SD, n=3); Body length ♀: 10.00–12.80 mm (11.28±1.60, n=8); Tergite VII ratio width:length ♂: 1.79–2.45 (median=2.42, n=3); Tergite VII ratio width:length ♀: 1.83–2.83 (median=2.17, n=5); PLPs-tergite IX (width) ♂: 0.10–0.12 mm (0.11±0.01 n=3); PLPs-tergite IX (width) ♀: 0.08– 0.12 mm (0.11±0.02, n=8); PLPs-tergite IX (length) ♂: 0.14–0.22 mm (0.18±0.04, n=3); PLPs-tergite IX (length) ♀: 0.11–0.20 mm (0.16±0.03, n=8).

***Mouthparts.*** **Labrum:** Labrum as in Fig. 71a, with maximum width at outer corners of anterior margin. Posterior margin of labrum (at clypeolabral suture) much shorter than anterior margin. Dorsal surface of labrum with pronounced raised areas on either side of midline, from lateral perspective labrum appears triangular in cross section (Fig. 71c). Anterior surface of raised areas with many long thin setae and smaller hair-like setae arranged in brush-like pads (Figs. 71b,c). Surface of labrum between raised areas slightly depressed, long thin setae occur across shallow medial depression (Figs. 71a,b). Color of raised areas lighter compared to dark brown of surrounding surface of labrum. Medial area of anterior margin extending onto ventral surface as broad under-turned lip (Fig. 71b). Anterior margin usually appears nearly straight with only a slight median indentation on some specimens (Figs. 71a,b). Ventral surface of labrum with long sharp setae lateral to medial pads of shorter hair-like setae, long sharp setae directed inward. **Labium:** Glossae and paraglossae with numerous fine hair-like setae on both dorsal and ventral surfaces (Fig. 72a). Joint at base of glossae and paraglossae aligned on either side of midline of labium. Together both joints form an angle of ~60° in relation to midline of labium (Fig. 72a). Labial palps 3 segmented with segment 1 larger and longer than segments 2 + 3. Many long thin setae occur along posterior edge of segment 1. Segment 3 tapers to narrowly rounded apex. Dorsal surface of segment 3 with 2 rows of long thin setae closely spaced along upper edge of slightly concave inner surface (Fig. 72b). Lower edge of segment 3 with closely spaced row of numerous short fine setae (Fig. 72c). Thumb-like process of segment 2 about half length of segment 3, usually not separated from segment 3 by u-shaped gap (Figs. 72a,c). **Hypopharynx:** Lingua rectangular, broader than long. Anterior margin of lingua slightly concave. Outer corners of lingua rounded with clusters of long fine setae that transition to row of short hair-like setae across middle of anterior margin (Fig. 73). Sides of lingua slightly convex. Superlinguae broadly rounded with many long thin setae. Inner edges of superlinguae with uniform row of shorter hair-like setae. **Right Mandible:** Anterior margin between molars and incisors relatively rough with many minute surface denticles (Fig. 74a). Bases of incisors often above anterior margin. Incisors often curved slightly inward (Fig. 74b). Dorsal apical corner below molars with many long setae. Row of setae on dorsal surface of innermost incisor. Prostheca present, brush-like portion about three quarters length of anterior margin (Fig. 74b). Molar surface large with rounded pre-molar. **Left Mandible:** Ventral edge of outermost incisor without small bifid accessory tooth (Fig. 75a). Ventral surface of innermost incisor with row of setae. Anterior margin between incisors and molars relatively rough (as on right mandible) with many minute surface denticles (Fig. 75b). Anterior margin relatively flat with no distinct raised area near molar surface (Fig. 75c). Molar surface with 12–13 individual toothed surfaces (Fig. 75d). Prostheca present and about half length of anterior margin (Fig. 75c). **Right Maxilla:** Galea-lacinia broad and apically rounded, crown with 7 thick pectinate setae and 5 long finely bi-serrate setae (Figs. 76a,e). Apex of galea-lacinia with 3 canines and 3 large dentisetae with coarse serrations (Fig. 76e). Dentisetae flanked by 2 rows of about 19 long thin finely serrate setae (Fig. 76e). Rows of long thin finely serrate setae terminate as single row of about 5 long thin hair-like setae. Maxillary palp long (total length ~1.22 mm) and 3 segmented. Segment 1 somewhat cylindrical and slightly longer than segment 2 (Fig. 76a). Segment 1 lacks scattered large bi-serrate setae on dorsal surface, but scattered long thin setae occur along both inner and outer edges. Segment 2 with few scattered thin setae along outer edge, most setae occur along inner edge. Cluster of setae on inner apex of segment 2 near joint with segment 3 (Fig. 76d). Dorsal inner edge of segment 2 with row of 7 long thin setae. Ventral surface of segment 2 with row of 12 closely spaced long thin setae that extends from segment apex to about its midpoint where setae become widely spaced. Segment 3 with broadly rounded apex and without any flattened or concaved inner surface (Fig. 76b). Dorsal surface of segment 3 with row of about 10 long thin setae that meet row of similar setae on segment 2 (Fig. 76b). Ventral surface of segment 3 with closely spaced row of about 27 long thin setae (Fig. 76c) that meet row of similar setae on segment 2 (Fig. 76d).

***Legs.*** **Foreleg:** Dorsal and ventral edges of femora with many stout sharp setae (Fig. 77a). Middle of dorsal surface lacks stout setae, but middle of ventral surface with 2–3 irregular rows of stout sharp setae. Tibiae lacks

tibiopatellar suture, dorsal and ventral edges with many stout sharp setae. Ventral apical area of tibiae with dense patch of large bi-serrate setae (especially near joint with tarsi) (Figs. 77a,b). Dorsal surface of tarsi with scattered stout sharp setae, scattered hair-like setae, and bi-serrate setae (Fig. 77a). Ventral edge of tarsi with 2 irregular rows of numerous bi-serrate setae (Fig. 77a,c). Tarsi shorter than tibiae. **Foreclaw:** Apical section, where claw begins to taper up to apex, short. Base of foreclaw with 2 patches of small to minute denticles (Fig. 78). Smaller nymphs have more slender gradually tapering claws, whereas larger more well developed nymphs have more robust claws with distinctly short apical sections.

***Gills.*** **Mid-Gills (3–5):** Apex of gills broadly rounded, general shape of gill lamellae rounder than typical subcordate gill form (Fig. 79a). Deep indentation at base of dorsal edge of gills causing part of dorsal edge to appear flap-like (Fig. 79c). Pattern of gill trachea distinctly dendritic with secondary trachea branching irregularly from main trachea (Figs. 79a,c). Outer margin of gills with widely spaced small hair-like setae. Ventral sclerotized edges with 2–3 staggered rows of large bi-serrate setae (Fig. 79b). Ventral sclerotized edges extend about half length of gill lamellae mid gills and greater than half the length of lamellae on gills 6 and 7 (Figs. 79a,b). Sclerotized mid-ribs present, but small usually reduced to faintly pigmented or unpigmented strip adjacent to gill insertions on all gills (Fig. 79c).

***Abdomen.*** **Abdominal Color Pattern:** Paired brown submedian oval spots occur on anterior of terga II–VII, spots elongated on terga VIII–X (Figs. 80a,b). Anterior submedian marks variably shaded with brown on most terga. Median brown shading greatest on terga IV–VII. Submedian spots and brown shading diffuse on terga I–IV. Sublateral dark brown triangular marks occur on terga I–VIII and as dark lateral streaks on tergite IX. Dark lateral marks merge across posterior edge of terga I–VIII (Fig. 80b) Ventrally, anterior of sterna with only faint paired submedial marks. Male nymphs at or near final instar show dark medial marks of subimago sterna through cuticle of sterna V–IX (Fig. 80c). **Setae on Posterior Margin of Abdominal Terga:** No spine-like setae on posterior margins of abdominal terga. **Setae on Surface of Abdominal Terga:** No large spine-like setae on surface of terga, but many short stout setae broadly distributed over surface of terga. Setae on terga slightly darker than brown background color of cuticle. **Setae on Surface of Abdominal Sterna:** No large spine-like setae on abdominal sterna, but many short stout setae more or less uniformly distributed over surface of sterna. Setae on sterna similar in color to yellow-brown background color of cuticle. **Setae on Lateral Margins of Terga and PLPs-tergite IX:** Few short stout setae occur along lateral margins of terga and PLPs-tergite IX, no large setae or hair-like setae present. **PLPs-tergite IX:** Short not extending beyond midpoint of tergite X, on some specimens PLPs-tergite IX only one third length of tergite X (Fig. 80a). **PLPs-terga I–IX:** Distinct PLPs present on terga I–IX. Small, but sharp PLPs on terga I–III. Large and sharp PLPs on terga IV–IX (Fig. 80a). **Left Paraproct:** Surface uniformly covered with short spine-like setae and some scattered hair-like setae (Fig. 81).

***Caudal Filaments.*** Caudal filaments brown with white tips. Cerci with fringe of long brown setae along inner edges that overlaps fringe of similar setae from outer edges of median terminal filament (Fig. 82a). Outer posterolateral edges of annuli of cerci with group of 4–5 long thick setae (some with divided tips) (Figs. 82a,b). Basal and apical annuli of cerci lack groups of large thick setae, all other annuli have such setae.

***Diagnosis*. Imagos:** Male imagos of *P. croesus* can be separated from those of other known North American species of *Parameletus* by following combination of characters (1) distinctive structure of penes and styliger plate (Figs. 67a–e, 68), (2) abdominal color pattern composed of contrasting brown marks with conspicuous lighter areas of pale yellow both on terga and sterna (Figs. 60b, 65 –66), and (3) restricted distribution across southern Ontario, Wisconsin and Minnesota (Fig. 111c). Female imagos were not studied, but comments provided by McDunnough (1923) indicate that color patterning of body (presumably which includes both thorax and abdomen) were similar to that of male imago and wing membranes lacked amber tint observed in male imago.

***Diagnosis.*** **Nymphs**: Nymphs of *P. croesus* can be separated from those of all other North American species of *Parameletus* principally by the following combination of characters: (1) presence of sharp PLPs on abdominal terga I–IX (Fig. 80a), (2) shape of labrum with raised setaceous dorsal surface (Figs. 71a–c), (3) shape and length of maxillary palp, specifically shape of segment 3 (Figs. 76a–d), (4) shape of apex of segment 3 of labial palps, with apex narrowly rounded (Figs. 72a–c), (5) color pattern on abdominal terga and sterna (Figs. 80a–c), (6) rough anterior margin of right mandible between prostheca and molars (Fig. 74a), (7) abdominal gills 3–5 broadly rounded subcordate form, with rounded apices (Fig. 79a), (8) abdominal gills 3–5 with large lobe-like flap near base of dorsal edge (Fig. 79a), (9) abdominal gills 3–5 with ventral sclerotized edge half of length of gill lamellae (Figs. 79a,b), (10) left paraproct with relatively few small spine-like setae distributed evenly across surface (Fig. 81), and (11) tarsal claws shaped as in Fig. 78, with apical portion short relative to length of claw.

***Comments on Character Variation*. Imagos:** No alternate color morphs were observed among specimens studied. Only slight differences in the color of the thorax and abdomen were observed, but these could easily be the result of how specimens were preserved (i.e., pinned vs. alcohol). The styliger plate on the holotype was dark brown, similar to the color of abdominal terga, but specimens preserved in alcohol had much lighter brown styliger plates. Perhaps the most notable color difference between the holotype and Minnesota specimens was the presence of brown pigment surrounding crossveins between the subcosta and radius veins. The lack of pigmentation in the Minnesota specimens could easily be the result of long term preservation in alcohol. In addition there were fewer discal crossveins in the hind wing of *P. croesus* compared to hind wings of *P. chelifer*. Another interesting aspect of the morphology of *P. croesus* was the presence of membranous pouches associated with the penes. Specimens of *P. croesus* collected by Daggy (1941) while they were swarming over the St. Croix River between Minnesota and Wisconsin had the styliger plate flexed down relative to the horizontal position of the abdomen and membranous pouches exposed. Some specimens in the same sample had the styliger plate positioned horizontally relative to the abdomen and on these individuals the membranous pouches were not exposed. This suggests that the pouches were eversible and may have only been deployed when needed during swarming. Membranous pouches such as these have not been observed on any other Nearctic siphlonurid and could be unique among all *Parameletus* species. New material will be necessary to further investigate this unusual character. Despite differences noted above, all primary diagnostic characters were consistent between the specimens collected from Minnesota and the holotype of *P. croesus*.

**Nymphs:** Nymphs of *P. croesus* had the widest suite of structural diagnostic characters of all the Nearctic *Parameletus*. Because the majority of diagnostic characters do not depend on color patterns, they were highly resistant to damage and problems concerning preservatives, making species determinations more accurate. Although all specimens studied were from Wisconsin, they invariantly had sharp PLPs on all abdominal terga. A bonus color character was observed on recently collected male nymphs from Wisconsin. The unique coloration of the abdominal sterna of the male imago was visible through the cuticle of a final instar male nymph. This bonus character was important in positively associating the nymph of *P. croesus* with the adult stage. Gill characters were useful, but could be problematic if gills were damaged or lost. The enlarged flap-like lobe at the base of the dorsal surface of most gills is discernible even on nymphs that had not reached the mid-point of development. Tarsal claw shape and minute denticles were useful, but exhibited a small amount of individual right to left variability in shape. Claw denticles seemed to be slightly larger and fewer in number than on other Nearctic species of *Parameletus*. Surface features of the right mandible and left paraproct require careful dissection and slide mounting to view properly, but also seemed to show little difference across specimens studied. Lastly, the maxillary palp was long compared to palps of other North American species of *Parameletus*. In addition, the base of the galea-lacinia of *P. croesus* had a cluster of 5 short hair-like setae, which was different from the single long setae present in this position on *P. midas* and *P. chelifer*.

***Biology and Habitat.*** It is now apparent that all of the records *P. chelifer* nymphs published for the State of Wisconsin (Lillie 1995) were actually *P. croesus*. Some general water quality data provided by Lillie (1995) for the St. Croix and Wolf Rivers (where he collected *Parameletus* nymphs) is all the habitat-specific information available for *P. croesus*. Unfortunately data provided by Lillie (1995) spans the entire sampling period from 1991–1993 and therefore can't be associated to a particular month or year. In May of 2007, *P. croesus* nymphs were collected from submerged vegetation along the Menominee River, which forms the border between Wisconsin and Michigan north of Marinette, WI. Although several well developed late instar nymphs were collected, no aquatic habitat data was recorded. Data from the USGS NAWQA data base (per. comm. Robert Hood) for the collection date in 1995 (when a nymph of *P. croesus* was collected during the NAWQA survey) and for the next water-year nearest the 2007 sample are presented in Table 2. Regional climatic records were available for maximum, minimum, and mean monthly air temperatures for 2003 and 2007, but it was not possible

Table 2. Summary of water quality metric for *Parameletus croesus* site on the Menominee River, Marinette County, Wisconsin. Data USGS NAWQA database.

| | | Water Quality Metrics | | | |
|---|---|---|---|---|---|
| USGS Site | Date | pH | Spec. Cond.($\mu$S·cm$^{-1}$) | Temp. (°C) | D.O. (ppm) |
| WI: 04067500 | 23 May 1995 | 8.0 | 185 | 15.5 | 10.0 |
| WI: 04067500 | 20 May 2003 | 7.8 | 145 | 14.9 | 11.7 |

to predict what water temperatures would have been for 2007 just from recorded air temperatures. However in May in northern Wisconsin, it is unlikely that the mean monthly water temperature could exceed the mean air temperature; working from this premise and using the monthly climatological summary for Marinette, WI (GHCND:USC00475091) the estimated water temperature for May 2007 at the sampling site was > 0°C ≤ 13.71°C.

***Distribution.*** Current collection records show that *P. croesus* had the smallest range for any of the Nearctic species of *Parameletus* (Fig. 111c, Append. 1). The only Canadian record was from the type locality (Ottawa) and no new specimens have been reported from that site. The male imagos collected by Daggy (1941) on the St. Croix River, which forms the border between Minnesota and Wisconsin, suggests that the species likely occurs in suitable habitats in other parts of Minnesota. In Wisconsin the previous records (Lillie 1995) of *Parameletus* nymphs (now known to be *P. croesus*) showed the species was not restricted to a single drainage, but broadly occurred across the middle and northern parts of the State. Therefore it is reasonable to believe that *P. croesus* should occur similarly in Minnesota and across southern Ontario (perhaps even just north of the Great Lakes). Although the current records indicate a relatively small range, the types of *P. croesus* were collected in Ottawa at about the same time as were the types of *P. midas* (i.e., only 7 days apart); it is therefore reasonable to assume that both have similar environmental tolerances. Thus extrapolating from what is known about the range of *P. midas* it seems likely that *P. croesus* should have a larger range.

***Parameletus midas* (McDunnough, 1923) (Figs. 83–110)**

***Male Imago*** (in alcohol). Body length: 8.42–11.33 mm (9.90±0.86, mean±SD, n=32). Body color yellow-brown (Fig. 83).

***Head.*** Base color pale yellow with scattered areas of dark grey on vertex and across occiput (Figs. 84a–c). Bases of ocelli brown with narrow black band (Fig. 84d). Compound eyes large and semiturbinate with lower portion greyish blue (Fig. 85a). Large upper parts of compound eyes barely meet along dorsal midline of head or separated by narrow gap (Figs. 84a,b). Antennae uniform light yellow-brown, scape and pedicel slightly darker. Frons with median keel (Figs 85a,b). Frons below antennal sockets marked with dark brown streaks that end about halfway to ventral margin (Fig. 85b), lower part of surface yellow.

***Thorax.*** Dorsal and lateral aspect as in Figs. 84a,b. Sclerotized areas mostly yellow-brown, in some places beige. Membranous cuticle pale yellow or white. Thickened edges of nota and sutures ranging from amber to dark brown (Fig. 85b). Anterior pronotum mostly obscured by upper part of compound eyes, but median, posterior, and lateral corners visible (Figs. 84a,b). Shape of pronotum trapezoidal with broadly curved anterior margin to accommodate posterior of head capsule. Posterior margin medially indented to accommodate anterior of mesonotum. Pronotum pale yellow-brown and marked with grey producing speckles and thin grey lines. Posterior margin of pronotum dark brown. Mesonotum yellow-brown with lighter beige areas anterior to MNs and yellow-brown areas along PSL (Fig. 84a). ALPs dark brown and distinct against mostly yellow-brown SMS. PSp and posterior medial parts of MS yellow-brown (Fig. 84a). SSLi beige, edges of SL and lateral areas of ISL brown (Fig. 84a). Dorsally, MNs appears straight and together with ANi and ANp forms distinctive outline on MS (Figs. 84a). Area within outline often much lighter yellow-brown or beige compared to surrounding MS. Metanotum mostly yellow-brown, but edges and heavily sclerotized areas dark brown as on mesonotum. Metanotal SL with dark brown edges and light brown center (Figs. 84a, 85c). Metanotal ISL dark brown, similar to mesonotum.

***Wings.*** Forewing length: 8.75–11.00 mm (10.13±0.68, mean±SD, n=24). Forewing membrane tinted with light amber (Figs. 86a,b). Stigmatic region between costa and subcosta veins and subcosta and radius$_1$ veins opaque. Major longitudinal veins brown, radial and medial vein groups darker than costa and subcostal veins. All major longitudinal veins pigmented to wing base except costa, which fades to pale yellow at basal crossvein. Forewing discal crossveins brown. Several crossveins of outer costa and subcosta interspaces merge together near apex of forewing (Fig. 86a). CuA vein of forewing joined to hind margin by series of about 8 sinuate crossveins (1 or 2 merge with short marginal intercalary veins near hind margin). Two to 3 groups of anastomosed marginal intercalary veins occur between outermost sinuate crossveins (Fig. 86a). Occasionally 1 or 2 small unattached marginal veins may be present. Hind wing membrane pigmented as in forewing (Fig. 86b). Major longitudinal veins and discal crossveins brown as in forewing. Color of major longitudinal veins extends to wing base. Numerous discal crossveins between major longitudinal veins, MP vein of hind wing not forked (Fig. 86b). Costal projection evident only as slight arching of costal margin near wing base.

***Legs.*** Ranges, means, and ratio values of segments of male forelegs as follows: Femur 2.00–2.68 mm, (2.33 [1.06], n=17 ) (mean [median ratio to tibia], sample size), Tibia 1.80–2.50 (2.20 [1.00], n=17), $T_1$= 0.88–1.60 (1.22[0.56], n=17), $T_2$=1.26–1.75 (1.52[0.61], n=17), $T_3$=

1.00–1.53 (1.59[0.58], n=17), $T_4$= 0.76–1.28 (1.01[0.47], n=17), $T_5$= 0.52–0.76 (0.67 [0.30], n=17). Legs light yellow-brown (Fig. 87a). Forefemora with narrow brown bands adjacent to apical joints with tibiae and basal joints with trochanters (Fig. 87b). Mid and hind tibiae and respective tarsi with edges of segments at joints margined with dark brown (Fig. 87c,d). Foretibiae and segment $T_1$ of tarsi with blunt spine-like knobs (Fig. 87a). Ventral apical spine on mid and hind tarsal segments $T_1$–$T_4$, ventral edges with 1–3 small dark spines (Figs. 87c,d). Forelegs with 5 distinct tarsal segments, but mid and hind legs have only 4 distinct tarsal segments. Tarsal segment $T_1$ of mid and hind legs fuses to tibiae during development to subimago (5 distinct tarsal segments of imago legs can be seen through cuticle of last instar nymphs). Fused joint between tibiae and tarsal segment $T_1$ marked by difference in cuticle color.

***Abdomen.*** Background color varies from pale yellow (similar to ivory) to yellow-brown, lighter color darkened with medium brown on lateral and posterior margins of terga and in some places on sterna (Figs. 88a–f). Membranous cuticle between abdominal segments and along pleural areas semi-transparent white (Fig. 88b). Terga usually lack any distinct brown medial marks (Fig. 88c), but occasionally some brown pigment occurs medially over area of each heart chamber of underlying dorsal vessel on terga II–IX. Medial brown pigment on terga appears as short, brown medial streak (Figs. 88e). Most of anterior half of terga II–IX pale yellow (Fig. 88c). Terga I–IX with dark brown lateral band that extends from posterolateral corners along lateral margins almost to anterolateral corners. Lateral brown bands usually interrupted near anterolateral corners by yellow streak (Figs. 88b,c,e). Anterolateral corners of terga II–IX with small areas of brown. Posterior margins of terga I–IX with brown band that connects with lateral brown areas at posterolateral corners of terga (Figs. 88b,c,e,f). Tergite X mostly light yellow-brown, lacks lateral brown bands and posterior brown band typical of other terga. Background color of sterna pale yellowish-white. Center of sternite I mostly brown. Centers of sterna II–VI light yellow-brown with 2 diffuse medial brown spots (Fig. 88d). Stena VII–VIII mostly yellow-brown with faint darker brown shading laterally. Lateral edges of sterna adjacent to pleural fold margined with pale yellow or appear white (Fig. 88b). Sterna I–VIII occasionally with short brown steaks along pleural fold (Fig. 88d). Sternite IX with dark brown shading lateral to base of styliger plate. Center and posterior margin of sternite IX yellow-brown (Fig. 88d). Abdominal segment IX flared-out posteriorly with sharp PLPs directed away from midline of body (Fig. 88c). Genitalia as in Figs. 89a–c, forceps 4 segmented, pale yellow to yellow-brown. Dorsal surface of basal segment of forceps weakly sclerotized with poorly developed joint with segment 2 (Figs. 89a,b). Posterior margin of styliger plate mostly straight or with slight median indentation, but no medial projection (Figs. 89a,b, 90c). Penes as in Figs. 89a–c, tips of lateral lobes do not extend beyond posterior margin of styliger plate (Figs. 90a–d). Large sclerotized lateral lobes roughly parallel, rounded tips do not meet (Figs. 89b,c, 90c,d). Inner edges of large sclerotized lobes membranous as in Figs. 89b,c. Paired dorsal spines curved inward, similar spines on ventral surface straight (Figs. 89a–c). Membranous projection extends medially from ventral surface of penes. Tip of membranous projection visible dorsally between inner edges of large lateral lobes of penes (Fig. 89c).

***Caudal Filaments.*** Caudal filaments as in Fig. 91, cerci either light yellow-brown with annuli ringed with dark brown or cerci uniform light brown from base to about thirteenth annulus where darker color fades to light brown or beige from there to tips, annuli ringed with dark brown (Fig. 91). Median terminal filament vestigial.

***Female Imago*** (in alcohol). Body length: 8.42–11.16 mm (9.76±0.72, mean±SD, n=22). Body color yellow-brown (Figs. 92a, 93a,b, 94a, 95a, 96a).

***Head.*** Base color light yellow, but extensively shaded with grey dots and lines producing speckled or grainy appearance. Vertex with 2 dark stripes arising from bases of lateral ocelli and converging toward occiput, but remain separate to terminus near postoccipital suture (Fig. 93a). Compound eyes small and positioned laterally on head. Lateral occelli and median ocellus similar in size, bases shaded with blackish brown. Median ocellus recessed into depression in frons. Antennae scape and pedicel light brown, flagellum pale. Frons with median keel, area below antennae shaded with dark brown from edges of compound eyes to median keel. Lower edge of frons yellow (Fig. 92a).

***Thorax.*** Dorsal and lateral aspect as in Figs. 92a, 93a,b, 95a, 96a, general morphology similar to that of male imago, but overall color much lighter. Most large sclerotized areas beige to sand colored with sutures and thickened edges dark brown. Pronotum light yellow shaded with grey (Fig. 93b). Posterior margin and lateral edges of pronotum with darkest color. Lateral areas of meso- and metanotum adjacent to PSL white. Pleural region around wing bases pale yellow to white. SSLi of meso- and metanotum darker brown compared to lighter colored surrounding areas of raised cuticle. Dorsal anterior part of MS beige (Fig. 93b). SL of mesonotum beige with brown tints, ISL dark brown (Fig. 93b). Mid-dorsal area of SL and ISL of metanotum similar to that of mesonotum. Lateral areas of SL light brown. No extensive blackish brown areas on female pterothorax, darkest areas of color appear on ISL and below wing bases (Figs. 92a, 93b).

***Wings.*** Forewing length: 8.50–11.00 mm (9.46±0.61, mean±SD, n=21).
Wing membrane lightly tinted with amber. Color and placement of major longitudinal veins same as noted for male imago (Figs. 93a, 95a, 96a). CuA vein joined to hind margin of forewing by series of 7–8 sinuate crossveins, several of which merge with short marginal intercalary veins. Most small marginal veins merge together, but some unattached marginal intercalary veins can occur alternately between sinuate crossveins.
***Legs.*** Base color yellow-brown, tarsi and ventral edges of femora tend to have slightly more brown than other leg segments. Apical edges of tibiae and tarsi with thin dark brown line (Figs. 92a, 93c). Ventral apical spine on mid and hind tarsal segments $T_1$–$T_4$, ventral edges with several small dark spines. All legs with four distinct tarsal segments and 1 indistinct fused basal segment (i.e., $T_{1)}$. Tarsal segment $T_1$ fuses to tibiae during development to subimago (5 distinct tarsal segments of imago legs can be seen through cuticle of last instar nymphs).
***Abdomen.*** Background color beige to pale yellow-brown, shaded with dark brown on both terga and sterna (Figs. 93b,c, 94a,b, 95b). Lateral color pattern as in Figs. 92a, 93a, 95a, 96a,b. Dorsal and ventral color patterns as in Figs. 94a,b. Terga II–IX mostly light yellow-brown, but small area of dark brown pigment occur medially over area of heart chamber of dorsal vessel beneath cuticle of each segment. Tergite I with median brown mark that merges with brown shading along anterior margin. Tergite X completely lacks median brown mark present on other terga (Fig. 93b). Terga I–IX with distinctive dark brown lateral bands that extend about half length of lateral margin, dark brown band interrupted by small pale yellow or white streak (Figs. 92a, 93a, 95a, 96a). Posterior margins of terga I–IX with brown band. Posterior brown band merges with brown posterolateral corners of terga. Tergite X lacks posterior brown band (Fig. 93b). Anterior margins and anterolateral areas of terga mostly cream colored or white. Shape and appearance of genital openings on sternite VII and coloration of sternite VIII as in Figs. 92b,c, 93c, 94b, 95b,c, 97a,b. On some specimens paired sclerotized copulatory pouches marked with dark brown (Figs. 92b,c, 97a,b). On other specimens copulatory pouches were not marked. Posterior margin of sternite IX as in Figs. 94b, 95c.
***Caudal Filaments.*** Caudal filaments similar in appearance and length to those of male imago (Fig. 98).

***Nymph*** (in alcohol, well developed or dark wing pad stage). Body length ♂: 6.58-10.33 mm (8.29±1.11, mean±SD, n=15); Body length ♀: 8.00-10.08 mm (9.45±0.74, n=9); $T_7$ ratio width:length ♂: 1.63–2.67 (median=2.11, n=11) [Nex $T_7$ ratio width:length ♂: 1.90–2.95 (median=2.05, n=7)]; $T_7$ ratio width:length ♀: 1.80–2.74 (median=2.35, n=9) [EXU $T_7$ ratio width:length ♀: 2.05–2.33 (median=2.23, n=4)]; PLPs-tergite IX (width) ♂: 0.06–0.14 mm (0.09±0.02 n=15); PLPs-tergite IX (width) ♀: 0.08–0.14 mm (0.09±0.02, n=9); PLPs-tergite IX (length) ♂: 0.16–0.30 mm (0.22±0.04, n=15); PLPs-tergite IX (length) ♀: 0.18-0.30 mm (0.24±0.04, n=9).
***Mouthparts.*** **Labrum:** Labrum rectangular with widest point about halfway along lateral edge (Fig. 99a). Medial part of anterior margin extending onto ventral surface, appearing as an under-turned lip (Figs. 99a). Anterior margin of labrum with numerous long, thick setae (much more abundant than hair-like setae) with tips curved over edge of anterior margin forming brush-like band (Figs. 99b,c). Dorsal surface of labrum with many long, hair-like setae (Fig. 99d). Ventral surface with groups of long sharp setae lateral to pads of shorter hair-like setae. **Labium:** Glossae and paraglossae with numerous fine hair-like setae on both dorsal and ventral surfaces (Fig. 100a). Joint at base of glossae with prementum not aligned with joint at base of paraglossae with prementum. Angle of joint of glossae to midline of labium ~60º. Angle of joint of paraglossae to midline of labium ~85–90º. Labial palps 3 segmented, segment 3 broad and apically rounded with an irregular row of long sharp setae along inner surface (Fig. 100b). Thumb-like projection of segment 2 about one third to one half length of segment 3 and set apart from segment 3 by u-shaped gap (Fig. 100c). **Hypopharynx:** Lingua rectangular, outer corners rounded with long fine setae and anterior margin broadly concaved (Fig. 101). Superlinguae with broadly rounded lateral lobes, each with many long thin setae (Fig. 101). **Right Mandible:** Anterior margin between incisors and molars rough (Fig. 102a), with many minute surface denticles. Base of incisors deeply cleft with division extending below line of anterior margin (Fig. 102b). Incisors project straight from anterior edge of mandible. Prostheca present, brush-like portion extends about halfway across anterior margin (Fig. 102a). Molar surface large with pointed pre-molar. **Left Mandible:** Dorsal edge of outer incisor with small accessory peg-like tooth (Fig. 103a). Anterior margin rough with many minute surface denticles and slight raised area near molars (Figs. 103a,b). Prostheca present, brush-like portion extends about two thirds length of anterior margin. **Right Maxilla:** Maxillary palp 3 segmented with segments 1 and 2 subequal in length. Segment 2 widened apically, but not more than 1.5x width of its base at joint with segment 1 (Figs. 104a,d). Segment 1 with scattered large bi-serrate setae on ventral surface and 1–2 large bi-serrate setae on dorsal surface. Segment 3 apically rounded and with straight or slightly convex inner margin (Figs. 104b,c). Dorsal surface of segment 3 with row of 8 long, sharp setae extending from base to tip of segment (Fig. 104b). Ventral surface of segment 3 with irregular double row of long setae (Fig. 104c). Apex

of segment 2 with short row of 4 long setae (similar to those on segment 3). Rows of setae on segments 2 and 3 meet at joint between segments becoming functionally one row of setae. Setae along inner edge of segment 2 mostly restricted to apical half of segment (Fig. 104c). Crown of galea-lacinia with 8 large pectinate setae (Fig. 104e). Apex of galea-lacinia with 3 canines and 3 large dentisetae flanked by 2 rows of long thin setae with brush-like edges (Fig. 104f).

***Legs.*** **Foreleg:** Dorsal surface of femora with median row of large bi-serrate setae (Fig. 105a). Dorsal edge of femora with irregular double row of large spine-like setae and long bi-serrate setae (Fig. 105a). Ventral edge of femora with irregular rows of spine-like and bi-serrate setae. Ventral apical edge of femora extended as conically shaped projection. Tibiae lacks tibiopatellar suture. Ventral edges of tibiae with numerous large bi-serrate, especially near joint with tarsi (Fig. 105b). Tarsi with large bi-serrate and spine-like setae that extend to base of claw (Fig. 105b). **Foreclaw:** Apex elongate and sharp. Inner surface of claw with 2 patches of small denticles separated by area lacking denticles (Fig. 106). Patches of denticles extend along broad basal part of claw to point where claw tapers toward apex.

***Gills.*** **Mid-Gills (3-5):** Gills typical subcordate form. Gill membranes tinged with yellow-brown (Fig. 107a). Trachea uniformly pigmented dark brown and secondary trachea branch symmetrically from large median trachea. Small hair-like setae occur along periphery of gill lamellae. Ventral sclerotized edge with 2 rows of fine-biserrate setae and scattered spine-like setae (Fig. 107b). Ventral sclerotized edge extends about one third length of lamellae of mid gills, longer on terminal gills 6 and 7 (Fig.107b). Sclerotized mid-rib present on all gills and extend about one third length of gill lamellae. Mid-ribs usually faintly pigmented or unpigmented on some specimens (Fig. 107c).

***Abdomen.*** **Abdominal Color Pattern:** Paired light brown medial marks present near anterior margin of all terga, terga I–V with paired marks lightly over-shaded with brown (Fig. 108). Terga VI–VIII with paired medial marks, posterior triangular brown mark, and brown medial shading color combined forming broad median brown band (Fig. 108). Median brown band distinctive on terga VI–VII, but can be faint on terga II–V. Sublateral dark brown triangular marks on terga I–VIII, brown marks joined across posterior edge of terga forming brown band (Fig. 108). **Setae on Posterior Margin of Abdominal Terga:** Middle of posterior edge of tergite IX with row 7–8 stout spine-like setae, setae often slightly darker than tergite. Posterior margins of terga VII–VIII with few widely separated spine-like, as on tergite IX. On some specimens spine-like setae same color of tergite appearing absent. **Setae on Surface of Abdominal Terga:** Many small hair-like setae broadly distributed over surface of most terga, some stout spine-like setae interspersed among hair-like setae. On tergite X only small light colored spine-like setae were present along lateral edges, large setae were absent from surface and edges. **Setae on Surface of Abdominal Sterna:** Same basic arrangement of setae as described for terga applies to surfaces of abdominal sterna. Posterior edges of sterna lack spine-like setae. **Setae along Lateral Margins of Terga and PLPs-tergite IX:** Lateral margins and PLPs-tergite IX with double row of stout spine-like setae and many thin hair-like setae. Few scattered spine-like setae occur on PLPs-terga VII–VIII. **PLPs-terga V–IX:** Distinct, sharp PLPs on terga VI–IX. Small and blunt PLPs usually present on tergite V, but occasionally absent. PLPs absent from tergite IV. **Left Paraproct:** Numerous long spine-like setae distributed across most of surface, spine-like setae somewhat more dense across apical third of surface and along apical edge (Fig. 109).

***Caudal Filaments.*** Base color yellow-brown, cerci often darker than median terminal filament. Long interfacing setae present along inner edges of cerci (Figs. 110a,b) and edges of median terminal filament. Setae taper toward tips of filaments. Outer edge of annuli of cerci with groups of about 4 dark, flattened, spine-like setae with tips divided into 3 or more points. Groups of flattened spine-like setae occur at junctions of annuli and extend posteriorly about half length of proceeding annulus (Figs. 110a,b). Groups of flattened setae begin on basal annuli and occur along most of outer edge of cerci (Figs. 110a,b), only apical annuli lack flattened setae. Median terminal filament lacks large flattened setae, but small single dorsal setae were present on annuli from midpoint of filament almost to its tip.

***Diagnosis*. Imagos:** Male imagos of *P. midas* can be separated from those of known North American species of *Parameletus* by the following combination of characters: (1) distinctive structure of penes and associated styliger plate (Figs. 89–90), (2) general yellow-brown color of abdomen and color pattern of terga composed of distinctive brown posterior band connected to posterolateral brown marks (Figs. 88a–f), and (3) mostly eastern distribution with all but one population recorded from eastern and northeastern Canada and Maine in USA. The westernmost population near Churchill, Manitoba, Canada (58° N latitude by 095° W longitude) currently stands disjunct from eastern populations with no known populations between it and its closest record (i.e., Ottawa, Ontario) (Fig. 111d, Append. 1). Female imagos can be tentatively separated from those of other species by (1) distinctive pale yellow-brown coloration of thorax and abdomen and brown marks on abdominal terga similar to those of male imago (Figs. 93–94), (2) distinctive

structure of genital openings and associated dark brown marks over sclerotized copulatory pouches (Figs. 92b,c, 97b), dark marks are not completely consistent and were absent on some individuals (Fig. 95c), and (3) mostly eastern distribution with all but one population recorded from eastern and northeastern Canada and Maine in USA. The westernmost population near Churchill, Manitoba, Canada (58° N latitude by 095° W longitude) currently stands disjunct from eastern populations with no known populations between it and closest record (i.e., Ottawa, Ontario) (Fig. 111d, Append. 1).

***Diagnosis.*** **Nymphs**: Nymphs of *P. midas* can be separated from those of all other known North American species of *Parameletus* by the following combination of characters: (1) unique color pattern on abdominal terga VI–VIII (Fig. 108), (2) groups of long, flattened spines on outer edges of cerci with tips divided into 3 or more points, middle point can be longer on setae with only 3 points, on setae with more than 3 points all divisions about equal length (Figs. 110a,b), (3) inner margin of segment 3 of maxillary palp slightly convex or straight, (4) lingua of hypopharynx rectangular with rounded corners and broadly concaved anterior margin (Fig. 101), (5) anterior margin of right mandible between prostheca and molars rough (Fig. 102a), (6) left paraproct with many large spine-like setae, most localized to apical one third of surface and apical edge (Fig. 109), (7) tarsal claws shaped as in Fig. 106, with transition point between broad basal part of claw with denticles and tapering apical portion distinct, denticles in 2 patches that cover much of basal inner surface of claw, and (8) abdominal gills 3–5 subcordate with dorsal edges near bases slightly enlarged (Fig. 107a).

***Comments on Character Variation*. Imagos:** The most common color morph was the yellow-brown form (Figs. 88b,c,d,f), but there was a somewhat less common darker color morph (Fig. 88a,e). The darkest morph was the brown-yellow form, where brown was more pronounced and muddied the yellow base color (Fig. 88a,e); few individuals of this morph were observed. The different color morphs did not seem to be geographically restricted, appearing in samples from both eastern populations and in Manitoba (as judged by voucher images on the BOLD® website). This level of color difference is not uncommon among mayflies with large latitudinal ranges (Burian 1995, 2001) and could be random variation or an ecotypic response to local habitat conditions. However another possibility that should be considered is that the dark morphs might be dispersal forms in the same sense as has been observed in *Dolania americana* Edmunds and Traver (Peters and Peters 1995). In northern Florida an uncommon dark color morph of the female imago preferentially flies away from the emergence site after mating. Ruffieux (1997) showed that the female dark dispersal morphs of *Dolania americana* had higher lipid levels compared to light bodied female imagos, which did not leave the vicinity of the emergence site after mating. This has never been studied in *Parameletus*, but if the dark morphs of *P. midas* were functionally similar to those of *Dolania* Edmunds and Traver, then this could be a highly successful strategy for maintaining stable populations yet occasionally having the capacity to fly long distances to found new ones.

The structure of the male genitalia and associated styliger plate are together the most distinctive diagnostic features of the male imago of *P. midas* and were consistent across eastern populations (Manitoba specimens were not available for study). The most difficult structure of the male genitalia to observe was the membranous projection between the large lobes of the penes because of its small size and potential for being collapsed under the penes (Fig. 89c). The purpose of this structure is unknown.

**Nymphs:** Nymphs of *P. midas* have previously been unidentifiable to species, but despite several structural similarities to nymphs of *P. chelifer* they do have some clear diagnostic characters. For freshly collected specimens, the most useful diagnostic character was the color pattern on abdominal terga VI–VIII. The pattern of *P. midas* is similar in some respects to that of *P. chelifer*, but differences noted for abdominal terga VI–VII concerning the central marks and broad brown band were consistent across all specimens studied. Unfortunately for specimens persevered in alcohol for long periods of time (i.e., decades) these color characters fade to the point of being useless and thus other structural features need to be used. Structural diagnostic characters listed above were effective for mid to late instar nymphs, but early instar nymphs often showed enough variability in some mouthpart and abdominal characters to make positive determination extremely difficult. In some instances (i.e., at the tertiary-level of diagnostic characters) it may be useful to examine the details of the labrum. *Parameletus midas* nymphs from eastern populations all seemed to have a dense brush of stout setae (with finely divided edges) across the entire anterior margin of the labrum (Figs. 99a–c). This differed from nymphs of *P. chelifer* where setae along the anterior margin of the labrum did not form a line and setae of this part of the labrum were generally much thinner (Figs. 18a–c) than those of *P. midas*.

***Biology and Habitat.*** All imagos studied and those in the BOLD® taxonomy system (Sujeevan and Hebert 2007) had collection dates that ranged from May 16 (Quebec) through July 21 (Manitoba). The most

comprehensive series of imagos studied was from the Thunder River in eastern Quebec. Imagos of *P. midas* were recorded at the Thunder River site from 16 May 1930 through 23 June 1930, the majority of collections occurring on June 19, 21, and 23. Records in the BOLD® taxonomy system (Sujeevan and Hebert 2007) showed a male imago *P. midas* from New Brunswick collected 23–25 June 2008 and imagos from Churchill, Manitoba collected 21 July 2008. In Maine (perhaps southernmost part of the range), *P. midas* imagos were collected on 30 May 2008 (far western Maine) and 2 June 1998 (far eastern Maine). The holotype has a collection date of 29 May 1922 (Ottawa, Ontario). Using the dates from all specimen records, which represent virtually all imago occurrences, it is possible to estimate the peak period of emergence across the known range of *P. midas*. Most imagos emerge from mid-May through the end of June. Thus most imago activity occurs over a period of about 6 weeks in the southern and eastern parts of range. In the northwesternmost population (Churchill, Manitoba), emergence occurred later with collections indicating imagos flying in mid-July. The later emergence at the Manitoba site is expected considering the difference in thermal conditions needed for the completion of nymphal development and the maturation of adult tissues at higher latitudes as described by the predictive model presented by Newbold *et al.* (1994). Although the model presented by Newbold *et al.* (1994) does not specifically determine northern emergence dates for *P. midas*, it does for another species that co-occurs with *P. midas* (i.e., *Leptophebia cupida* (Say)) which also has a similar emergence period and is an acceptable analog for *P. midas* in this regard.

In Maine *P. midas* imagos have only been collected from riparian vegetation along the channel of the Narraguagus River south of Rt. 9 (channel width ~21m) in the far eastern part of the State and from the sedge dominated margin of the South Branch of The Dead River (SBDR) in the mountainous western part of the State. Black wing pad nymphs were collected and reared from the SBDR site. The channel width at the SBDR varied from 40–80m. The collection site was a small backwater cove off the main channel. In the small cove, the benthic substrate was dominated by fine mineral sediment and organic detritus. Water temperature ranged from 16.9–17.4°C, being cooler near the opening of the small cove with the main channel and warmer toward the back where less circulation occurred. River water temperatures are not uniform throughout this part of Maine. For example, a short distance away the smaller and swifter Carrabassett River had a water temperature of 14.7°C at the same time the water temperatures in the SBDR were over 2.0°C warmer. In addition, pH was 5.68 and specific conductance was 23 $\mu$S at the SBDR site. In the field, emergence of *P. midas* subimagos began at about 11:00am and continued into the late afternoon. In the lab, black wing pad nymphs collected on 30 May 2008 began emerging about 4:00 pm on 1 June 2008. Using information on emergence at the SBDR obtained in 2008 and from samples collected from this same site in 2007 containing extremely small specimens of *P. midas* (nymphs ~2–4 days old), total development time to emergence was estimated to be ~27–28 days (at the SBDR). Previously the only estimate of total development time was for *P. columbiae* at 16–22 days or less at high elevation in the Rocky Mountains (Edmunds 1957). Although the estimate for the Maine population of *P. midas* is about 5 days longer (at an elevation of 348m AMS), it supports the conjecture that species of Nearctic *Parameletus,* in general, have one of the most rapid developmental strategies known for Nearctic mayflies. The lack of collection records of either mature nymphs or imagos at other times of the year also supports the hypothesis of a univoltine life cycle.

***Distribution.*** The known range for *P. midas* is presented in Fig. 111d, Append. 1. Plotting all records revealed a potentially disjunct distribution between the majority of records in northeastern Canada and Maine, United States and the one western site at Churchill, Manitoba. Presently there are no records for the area between Churchill, Manitoba and Ottawa, Ontario or across the upper part of Quebec. This seems incongruous because both regions that lack records have many suitable habitats and there are records of *P. midas* from Labrador. Therefore it is expected that future surveys in Manitoba, Ontario, and Quebec will confirm the occurrence of *P. midas* broadly across this region and unite the two disjunct parts of its range.

**Acknowledgements**

I am grateful to the following people that generously contributed specimens for this study: Donna Giberson (UPEI, retired), Boris Kondratieff (CSU), Brigid O'Donnell (PSU), Jan Peters (FAMU), Edward DeWalt (INHS), Marcia Seibenmann (Aquatic Biologist-ME), Owen Londsdale (CNC), Derek Sikes (Univ. Alaska–Museum of the North), Philip Clausen (UMN), Richard Lillie (WI-DNR, retired), Robert Dubois (WI-DNR), Beth Swartz (ME Inland Fisheries & Wildlife), David Funk (SWRC), Robert Hood (USGS–NAWQA Voucher Collection), Tom Bansak (FLBS), Heather Proctor (University of Alberta, Strickland Museum), Gino Nearns (PERC), and David Larson (MU- Newfoundland, retired).

**References***

Bauerfeind, E. and T. Soldan. 2012. The Mayflies of Europe (Ephemeroptera). Apollo Books, Ollerup, Denmark. 781 pp.

Bengtsson, S. 1908. Berättelse öfver en resa i entomologiskt syfte till mellersta Sverige Sommaren 1907. K. Svenska Vetenskapsakademiens Årsbok [K. Svenska Vetensk. Akad. Årsb.] **6**: 237–246.

Brinck, P. 1957. Reproductive system and mating in Ephemeroptera. Opuscula Entomol. **22:** 1 –37.

Burian, S.K. 1995. Taxonomy of the eastern Nearctic species of *Choroterpes* Eaton (Ephemeroptera: Leptophlebiidae). p.433–453. *In* Corkum, L.D. and J.H. Ciborowski (eds.). Current Directions in Research on Ephemeroptera. Canadian Scholars' Press Inc. Toronto.

Burian, S.K. 2001. Revision of the genus *Leptophlebia* Westwood in North America (Ephemeroptera: Leptophlebiidae: Leptophlebiinae). Ohio Biological Survey N.S. Vol. 13(3): vi+80p.

Daggy, R.H. 1941. Taxonomic and biologic investigations on Minnesota mayflies Ephemeroptera). Ph.D. dissertation, University of Minnesota, p. 331, plates 1–22.

Edmunds, G.F., Jr. 1952. Studies on the Ephemeroptera: I. The Phylogeny and classification of the Ephemeroptera, with a study of flight mechanics and evolution of their wings; II The taxonomy and biology of the mayflies of Utah. Ph.D. Dissertation, University of Massachusetts, Amherst, 399 p. + 22 plates.

Edmunds, G.F., Jr. 1957. On the life history of *Parameletus columbiae* McDunnough (Ephemeroptera). Uath Academy Proceedings **34**: 25–26.

Edmunds, G.F., Jr., S.L. Jensen, and L. Berner 1976. The Mayflies of North and Central America. University Minnesota Press, Minneapolis. 330 pp.

Esben-Petersen, P. 1916. Ephemerida, Scientific results of the expedition of the Kuznetsov brothers to the Polar Urals in 1909, under command of H. Backlund. Memoirs of the Imperial Academy of Sciences, Series 8, Section of Physics and Mathematics, St. Petersburg, Vol **28**, No. 12: 1–12.

Giberson, D.J., S.K. Burian, and M. Shouldice. 2007. Life history of the northern mayfly *Baetis bundyae* in Rankin Inlet, Nunavut, Canada, with updates to the list of mayflies of Nunavut. Can. Entomol. **139**: 628–642.

Gilpin, B.R. and M.A. Brusven. 1970. Food habits and ecology of mayflies of the St. Maries River, Idaho. Melanderia (Washington State Entomological Society) **4**: 19–40.

Harper, F. and P.P. Harper 1981. Northern Canadian mayflies (Insecta; Ephemeroptera), records and descriptions. Can. J. Zool. **59**: 1784–1789.

Harper, P.P. and F. Harper. 1997. Mayflies (Ephemeroptera) of the Yukon. *In* Danks, H.V. and J.A. Downs (eds.). Insects of the Yukon. Biological Survey of Canada (Terrestrial Arthropods), Canadian Museum of Nature, Ottawa.

Hubbard, M.D., 1977. The validity of the generic name *Parameletus* Bengtsson (Ephemeroptera: Siphlonuridae). Proc. Entomol. Soc. Wash. **79**: 409–410.

Hubbard, M.D. 1995. Toward a standard methodology for the description of mayflies (Ephemeroptera), p. 361–369. *In* Corkum, L.D. and J.J.H Ciborowski (eds.), Current Directions in Research on Ephemeroptera, Canadian Scholars Press, Toronto.

Jensen, S.L. 1966. The mayflies of Idaho (Ephemeroptera). M.S. Thesis, University of Utah, Salt Lake City, p. 365.

Jacobus, L.M. and W.P. McCafferty. 2002. Analysis of some unfamiliar Canadian mayflies (Ephemeroptera). Can. Entomol. **134**: 141–155.

Jacobus, L.M., N.A. Wiersema, and J.M. Webb. 2014. Identification of far northern and western North American mayfly larvae (Insecta: Ephemeroptera), north of Mexico, Joint Aquatic Sciences meeting, Portland, OR, USA, p 176+ suppl., unpublished workshop manual [pdf available from L.M. Jacobus (luke.jacobus@gmail.com)]

Kjærstad, G., J.M. Webb, and T. Ekrem. 2012. A review of the Ephemeroptera of Finnmark –DNA barcodes identify Holarctic relations. Norwegian J. Entomol. **59**: 182–195.

Klubertanz, T.H. 2016. Mayfly Larvae of Wisconsin (G4074). University of Wisconsin-Extension, Cooperative Extension, Cooperative Extension Publishing, Madison, WI.

Kluge, N.Ju., 1994. Pterothorax structure of mayflies (Ephemeroptera) and its use in systematics. Bulletin de la Société Entomologique de France **99**: 41–61.

Kluge, N.Ju., D. Studemann, P. Landolt, and T. Gonser. 1995. A reclassification of the Siphlonuroidea (Ephemeroptera). Bull. Soc. entomol. Suisse **68**: 103–132.

Koss, R.W. 1970. A list of the mayflies (Ephemeroptera) in the Michigan State University Entomology Museum. Michigan Entomol. **3**: 98–101.

Lillie, R.A. 1995. A Survey of Rare and Endangered Mayflies of Selected Rivers of Wisconsin. Wisconsin Dept. of Natural Resources Research Report No. **170**.

McCafferty, W.P. and R.L. Newell. 2007. Insecta, Ephemeroptera: Range extensions and new state records for far western Montana, USA. Check List **3**:260–266.

McCafferty, W.P. and R.P. Randolph. 1998. Canada Mayflies: a faunistic compendium. Proc. Entomol. Soc. Ontario **129**: 47–97.

McCafferty, W.P., R.P. Randolph, and L.M. Jacobus. 2012. The Mayflies of the Intermountain West. Memoirs of the American Entomological Institute (Gainesville, Florida) **85**: 1–317.

McDunnough, J. 1923. New Canadian Ephemeridae with notes. Can. Entomol. **55**: 39–50.

McDunnough, J. 1930. The Ephemeroptera of the north shore of the Gulf of St. Lawrence. Can. Entomol. **62**: 54–62.

McDunnough, J. 1938. New species of North American Ephemeroptera with critical notes. Can. Entomol. **70**: 23–34.

Newbold, J.D., B.W. Sweeney, and R.L. Vannote. 1994. A model for seasonal synchrony in stream mayflies. J. N. Amer. Benthol. Soc. **13**: 3–18.

Newell, R.L. and B.R. Hossack. 2009. Large wetland-associated mayflies (Ephemeroptera) of Glacier National Park, Montana. Western North Amer. Naturalist **69**: 335–342.

Olsson, T. and O. Söderstrom. 1978. Springtime migration and growth of *Parameletus chelifer* (Ephemeroptera) in a temporary stream in northern Sweden. Oikos **31**: 284–289.

Peters, J.G. and W.L. Peters. 1995. Evidence for a dispersal morph in females of *Dolania americana* (Ephemeroptera: Behningiidae). p.253–262 *In* Corkum, L.D. and J.H. Ciborowski (eds.). Current Directions in Research on Ephemeroptera. Canadian Scholars' Press Inc. Toronto.

Ruffieux, L. 1997. Réserves énergétiques et strategies de reproduction chez les Ephéméroptères (Insecta, Ephemeroptera). Thèse Doctorat, University of Lausanne, 168 pp.

Scudder, G.G.E. 1975. An annotated checklist of the Ephemeroptera (Insecta) of British Columbia. Syesis **8**: 311–315.

Shorthouse, David P. 2010. SimpleMappr, an online tool to produce publication-quality point maps. [Retrieved from http://www.simplemappr.net. Accessed August 26, 2016].

Söderstrom, O. 1988. Effects of temperature and food quality on life-history parameters in *Parameletus chelifer* and *P. minor* (Ephemeroptera): a laboratory study. Freshwater Biology **20**: 295–303.

Söderstrom, O. and A. Johansson. 1988. Effects of habitat on development, fecundity, and susceptibility to parasites in *Parameletus chelifer* and *Parameletus minor* (Ephemeroptera). Can. J. Zool. **66**: 2715–2725.

Söderstrom,O. and J. Nilsson. 1986. Redescription of *Parameletus chelifer* Bengtsson and *P. minor* (Bengtsson), with keys to nymphal and adult stages of the Fennoscandian species of Siphlonuridae (Ephemeroptera). Entomlogica scandinavica **17**: 107–117.

Söderstrom,O. and J. Nilsson. 1987. Do nymphs of *Parameletus chelifer* and *P. minor* (Ephemeroptera) reduce mortality from predation by occupying temporary habitats? Oecologia (Berlin) **74**: 39–46.

Studemann, D. and I. Tomka. 1991. European Siphlonuridae (Ephemeroptera): a phylogenetic system for the four genera, p. 103–104. *In* Alba-Tercedor, J. and A. Sanchez-Ortega (eds.), Overview and Strategies of Ephemeroptera and Plecoptera. Sandhill Crane Press, Gainesville, Florida.

Sujeevan, R. and P.N. Hebert. 2007. BOLD: The barcode of life data system (www.barcoding.org ).Molecular Ecol. Notes 7: 355-364 [doi:10.111/ j.1471–8286.2006.01678x].

Spieth, H.T. 1938. Taxonomic studies on Ephemerida. I: description of new North American species. Am. Mus. Novitates **1002**: 1–11.

Traver, J.R. 1935. Part II. North American Mayflies: A systematic account of North American species in both adult and nymphal stages. *In* Needham, J.G., J.R. Traver, and Y. Hsu. The Biology of Mayflies. Comstock Publishing Co., Ithaca, New York.

Tiunova, T.M. 2008. Two species of *Parameletus* Bengtsson 1908 (Ephemeroptera: Siphlonuridae) and notes on other species from far east of Russia. Zootaxa **1725**: 17–26.

Webb, J.M., L.M. Jacobus, D.H. Funk, X. Zhou, B. Kondratieff, C.J. Geraci, R.E. DeWalt, D.J. Baird, B. Richard, I. Philips, and P.D.N. Hebert. 2012. A DNA barcode library for North American Ephemeroptera: Progress and prospects. PLoS One **7**(5): e38063. doi: 10.1371/journal.pone.0038063.

Webb, J.M., D.W. Parker, D.M. Lehmkuhl, and W.P. McCafferty. 2004. Additions and emendations to the mayflies (Ephemeroptera) fauna of Saskatchewan. Entomol. News **115**: 213–218.

*Literature cited also includes citations for records listed in Appendix 1 spreadsheet for all previous published records of Nearctic species of *Parameletus*.

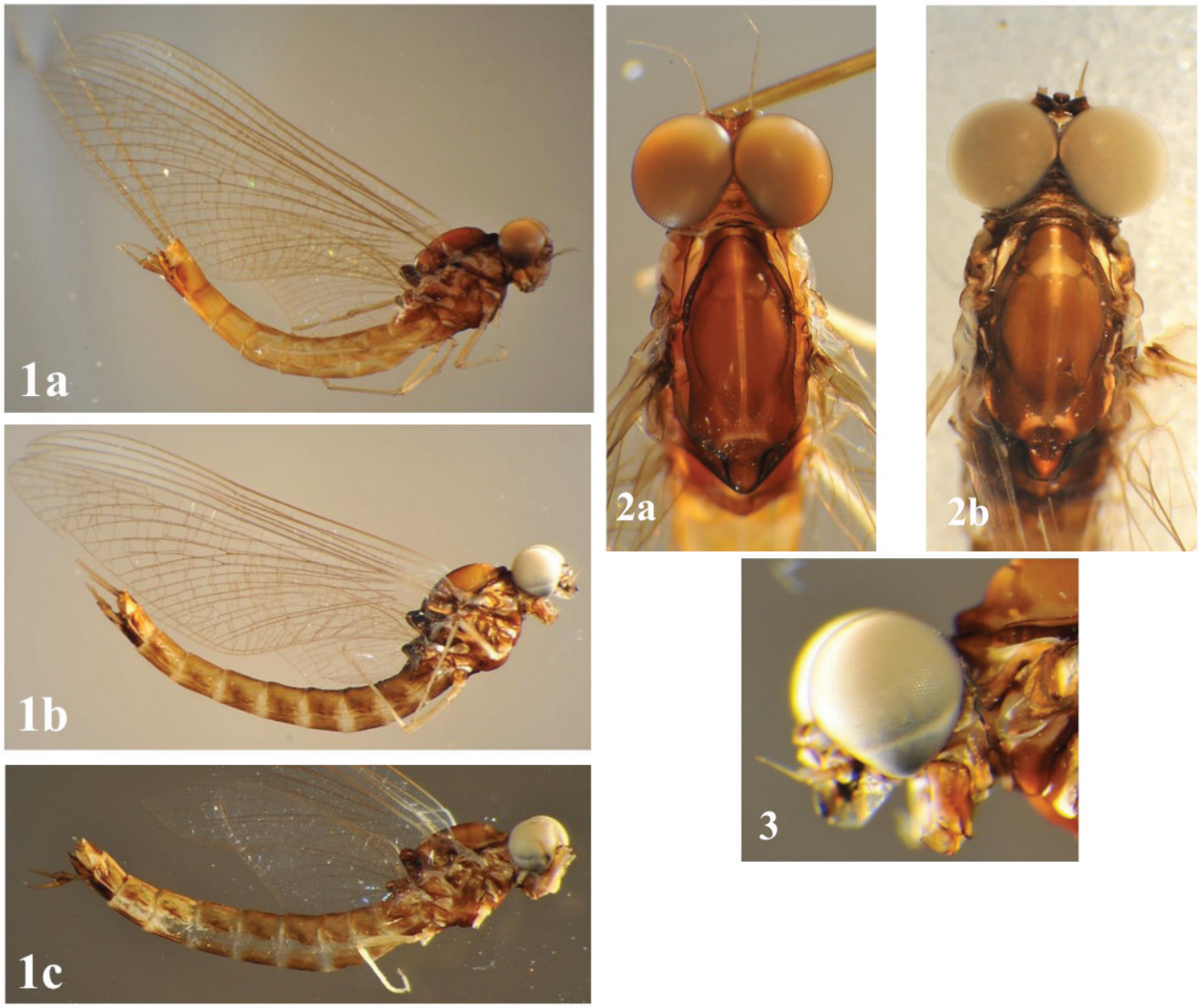


Figs. 1a – c: lateral view of male imago of *P. chelifer*. 1a medium brown color morph, 1b dark brown color morph with minimal interruption of dorsal and ventral brown color along the pleural fold of abdominal segments, 1c dark brown color morph with wide pale area along pleural fold of abdominal segments.

Figs. 2 – 3: dorsal and lateral view of head and thorax of male imago of *P. chelifer*. 2a dorsal view of head and thorax of medium brown color morph, 2b same view as for 2a of dark brown color morph, 3 lateral view of head of dark brown color morph.

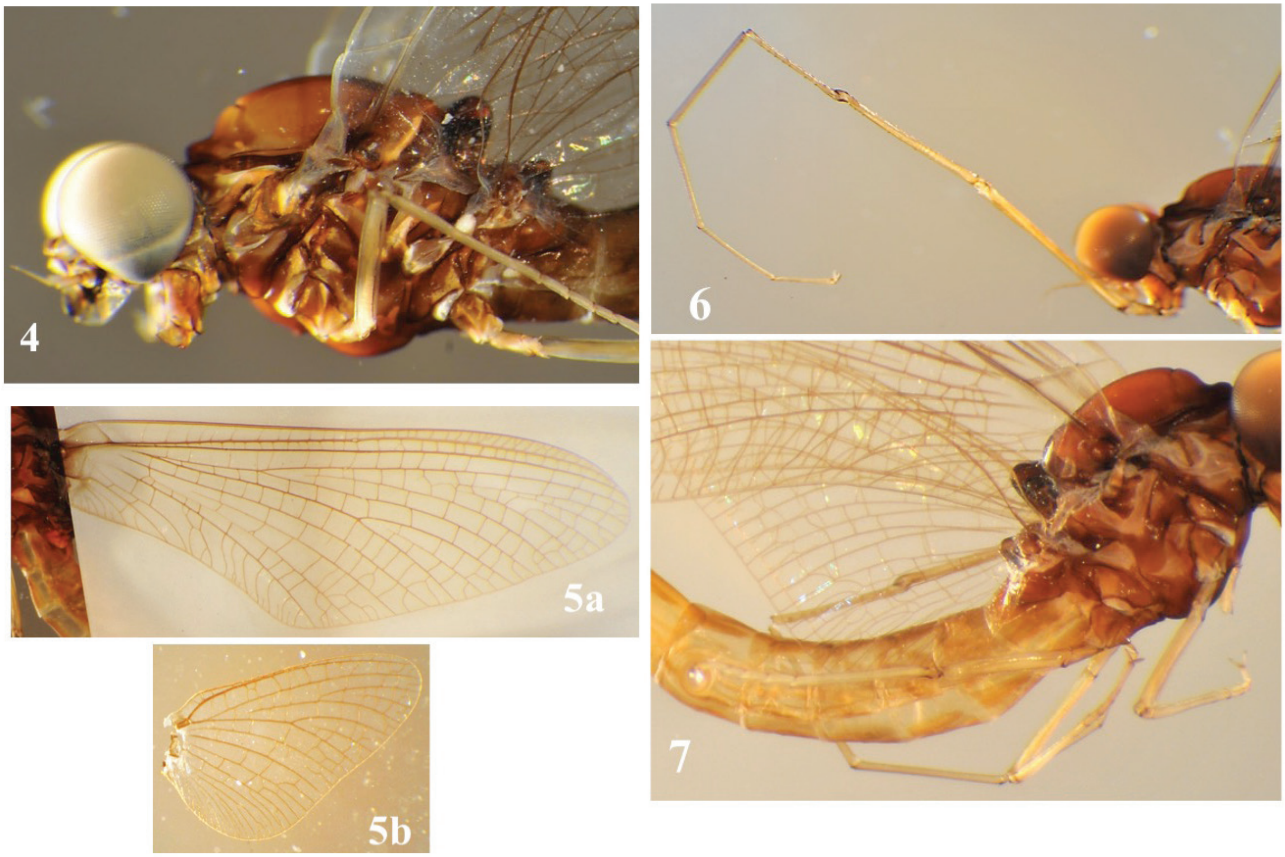


Figs. 4 – 5: lateral view of thorax and wings of male imago of *P. chelifer*. 4 lateral view of thorax of dark brown color morph, 5a forewing, 5b hind wing.

Figs. 6 – 7: thoracic legs of male imago of *P. chelifer*. 6 lateral view of foreleg with blunt spines visible along tarsal segment $T_1$, 7 lateral view of mid and hind legs.

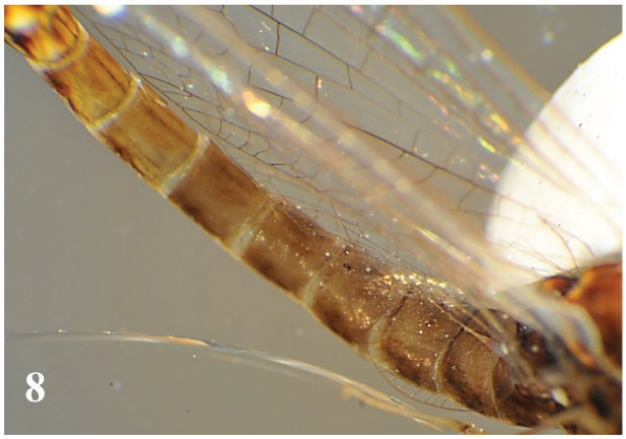




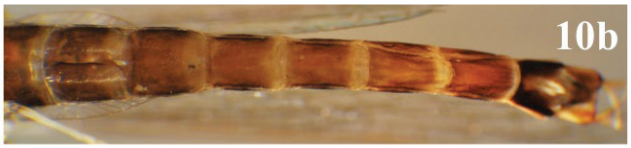




Figs. 8 – 9: abdomen of male imago of *P. chelifer*. 8 dorsal view of abdomen of dark brown color morph, 9 dorsal view of abdomen of medium brown color morph.

Figs. 10 – 11: dorsal and ventral views of abdomens of male imagos of *P. chelifer*. 10a dorsal view of dark brown color morph terga, 10b ventral view of dark brown color morph sterna, 11a dorsal view of slightly faded dark brown color morph terga, 11b ventral view of slightly faded dark brown color morph showing variable coloration of sterna I - VIII.




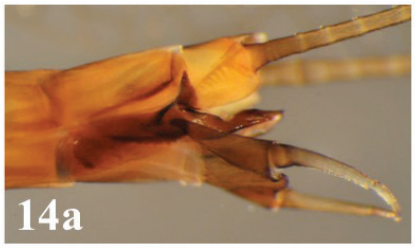







Figs. 12 – 13: male genitalia of *P. chelifer* (slide mounted). 12 dorsal view of penes, 13 dorsal view of penes and forceps.

Figs. 14a – d: male genitalia of *P. chelifer* (intact). 14a lower lateral view of styliger plate, forceps, and penes, 14b dorsal view of tergite X and penes, 14c dorsal view of penes behind styliger plate, 14d ventral view of styliger plate showing median rounded projection on posterior margin between forceps bases and coloration of sternite IX.

Fig. 15: caudal filaments of male imago of *P. chelifer* (intact).

Figs. 16a,b: lateral view of female imago of *P. chelifer*. 16a lateral view of dark brown color morph showing dark shading along edges of abdominal terga, 16b lateral view of abdomen of medium brown color morph with lighter shading along edges of abdominal terga.

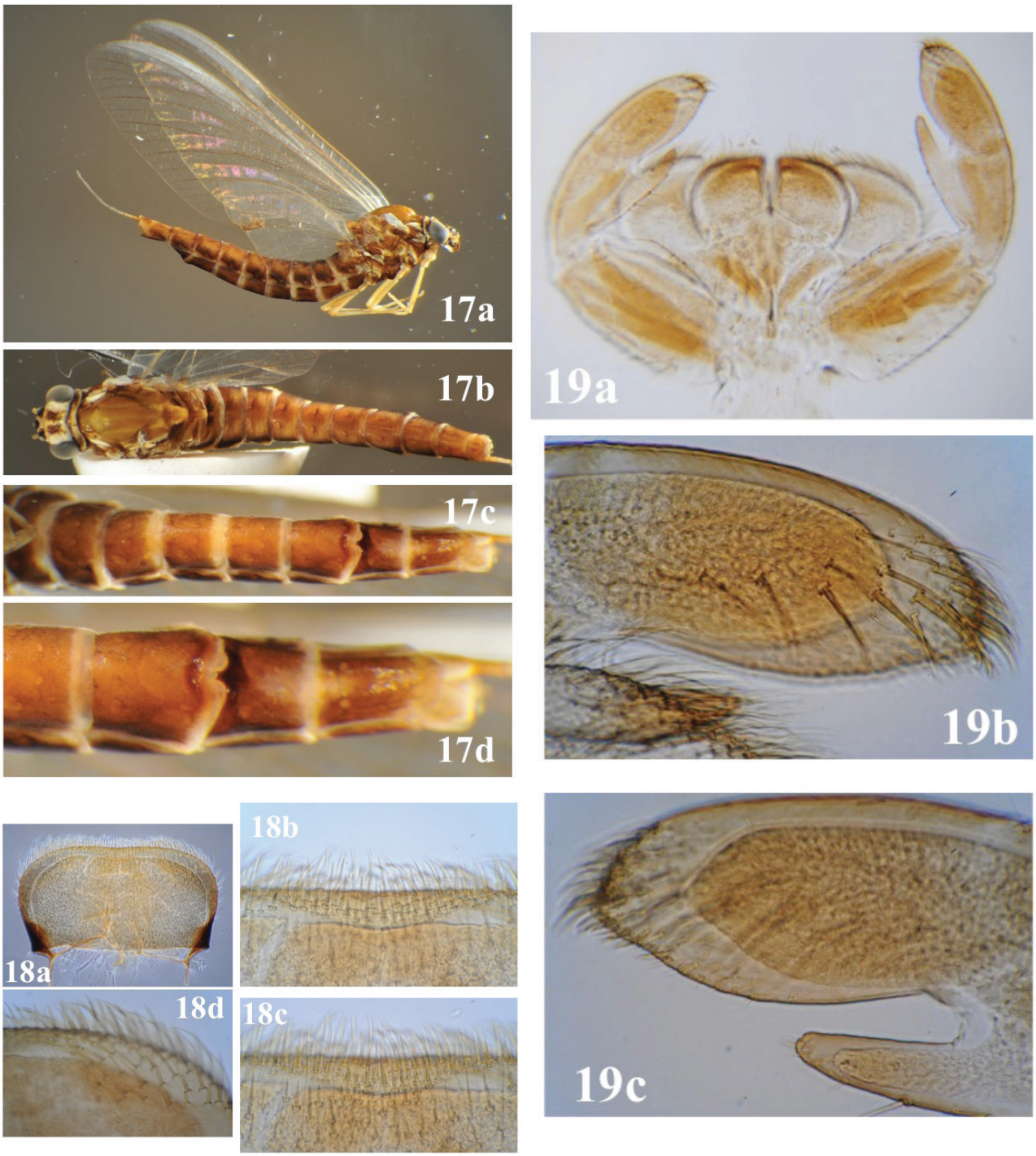


Figs. 17a – d: lateral, dorsal, and ventral view of medium brown color morph of female imago of *P. chelifer*.17a lateral view of body, 17b dorsal view of head, thorax, and abdomen, 17c ventral view of abdominal sterna, 17d detailed view of color pattern of genital sterna VII – VIII.
Figs. 18a – d: labrum of nymph of *P. chelifer*. 18a labrum dorsal view, 18b detailed dorsal view of setae on surface over under-turned anterior margin, 18c detailed view of hair-like setae on medial dorsal surface, 18d ventral view of labrum showing large stout setae below anterior margin.
Figs. 19a – c: labium of nymph of *P. chelifer*. 19a ventral view of labium, 19b detailed view of dorsal surface and inner edge of segment 3 of labial palp, 19c detailed view of ventral surface of segment 3 of labial palp and thumb-like projection of segment 2.

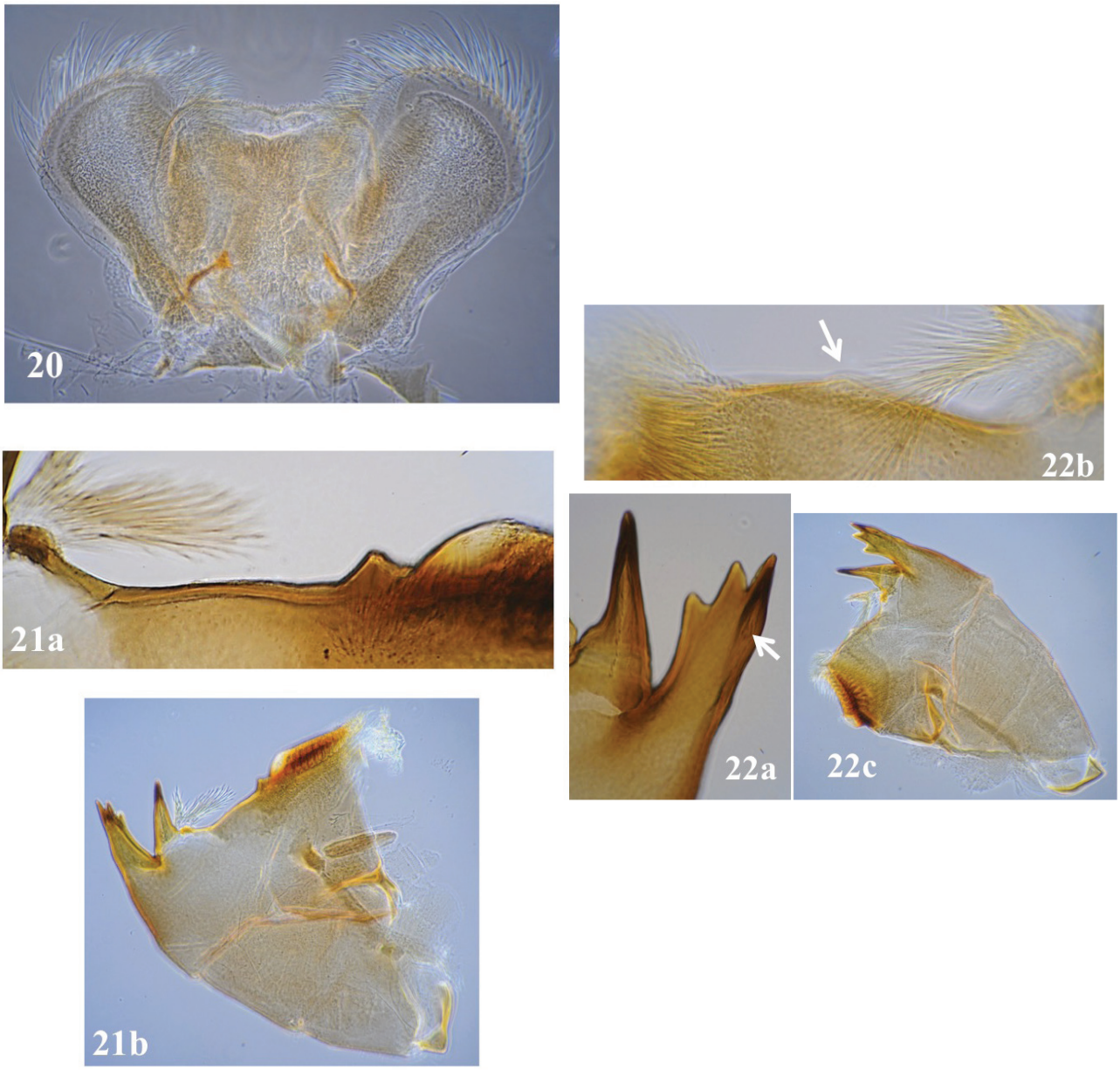


Fig. 20: dorsal view of hypopharynx showing lingua and superlinguae of nymph of *P. chelifer*.

Figs. 21a,b: right mandible of nymph of *P. chelifer*. 21a detailed view of anterior margin between base of prostheca and large projection before molars, 21b ventral view of mandible.

Figs. 22a – c: left mandible of nymph of *P. chelifer*. 22a ventral view of outer incisors with arrow indicating small accessory tooth, 22b detailed view of anterior margin between prostheca and molars with arrow indicating raised area, 22c ventral view of mandible.

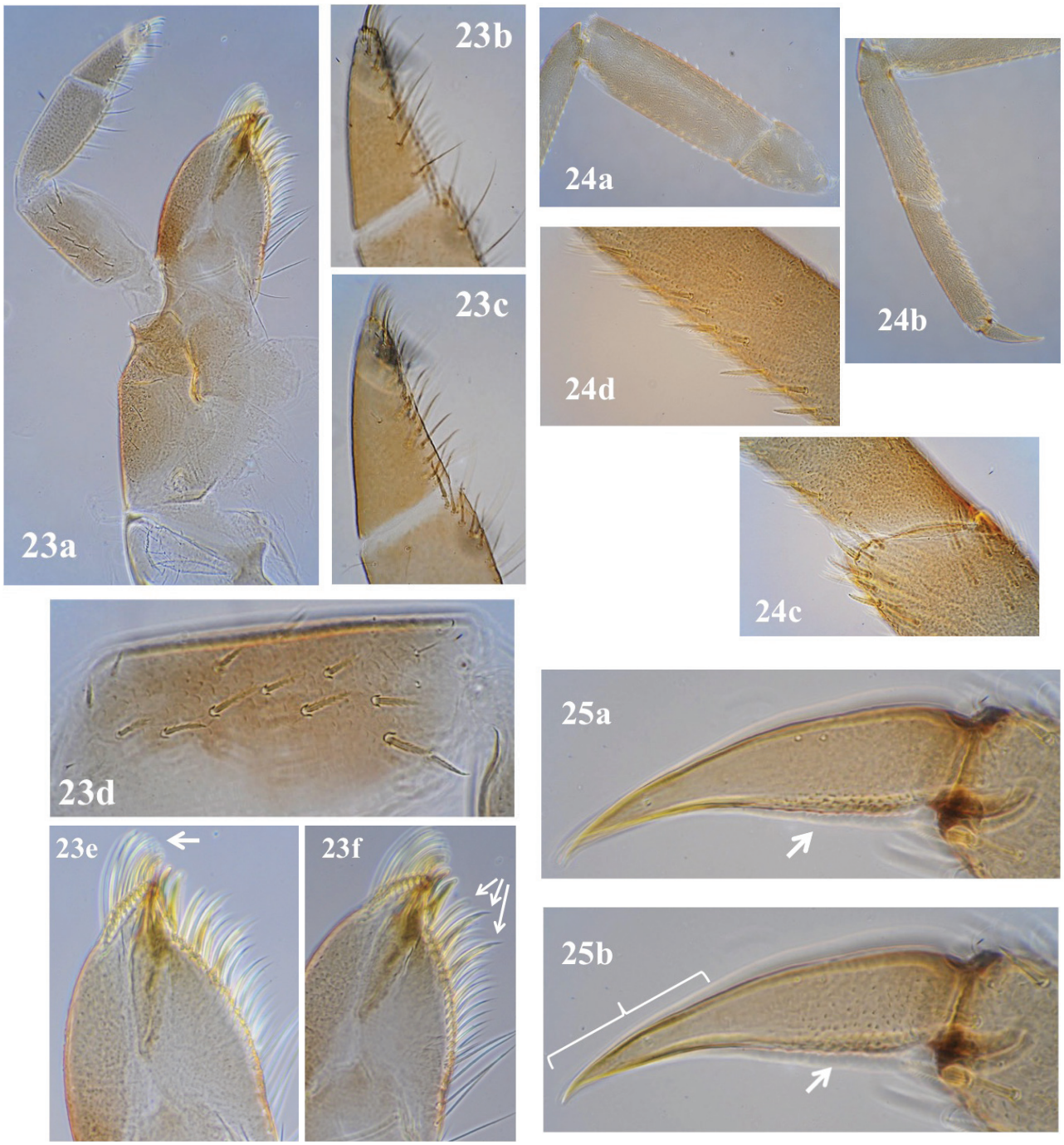


Figs. 23a – d: right maxilla of nymph of *P. chelifer*. 23a ventral view of maxilla, 23b dorsal view of setae on segment 3 of maxillary palp, 23c ventral view of setae on segment 3 of maxillary palp, 23d setae on dorsal surface of segment 1 of maxillary palp.

Figs. 23e,f: apex of right maxilla of nymph of *P. chelifer*. 23e arrow indicates row of long pectinate setae along crown of galea-lacinia, 23f arrows indicate 3 large dentisetae along inner apical edge of galea-lacinia.

Figs. 24a – d: leg segments and surface setae of nymph of *P. chelifer*. 24a dorsal surface of femur, 24b dorsal surface of tibia and tarsus (with claw), 24c setae on inner apical edge of tibia, 24d setae on inner edge of tarsus.

Figs. 25a,b: tarsal claw of nymph of *P. chelifer*. 25a lateral view (base in focus) with arrow indicating surface denticles on basal part of claw, 25b lateral view (apex in focus) with arrow indicating position of denticles on base of claw relative to portion of claw that tapers to apex (indicated by bracket).


Figs. 26a,b: abdominal gill of nymph of *P. chelifer*. 26a lateral view of gill 3, arrow indicates ventral sclerotized edge, 26b view of setae along ventral sclerotized edge.

Fig. 26c: branching pattern of trachea in gill 3, arrow indicates sclerotized mid-rib near the base of the gill.

Figs. 27a,b: color pattern of abdominal terga of nymphs of *P. chelifer* (specimens shown are from the same site in northern Canada). 27a distinctive mid-dorsal pattern of brown spots on terga VI – IX, 27b showing slight variation in mid-dorsal brown spots terga VI – IX.

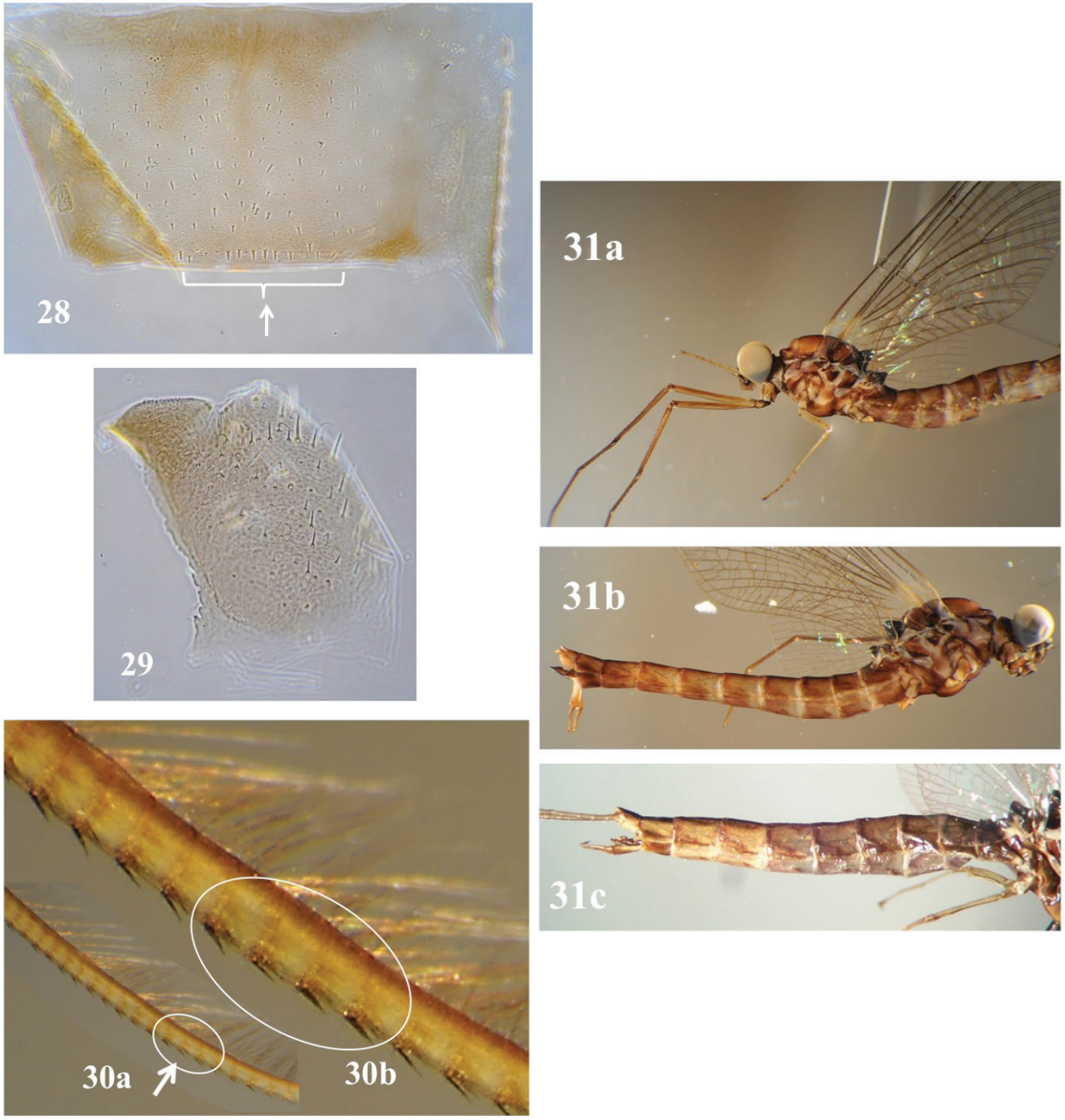


Figs. 28 – 29: setae of tergite IX and paraprocts of nymphs of *P. chelifer*. 28 dorsal view of detached tergite IX showing row of spine-like setae along posterior edge (indicated by bracket and arrow) and on tergite surface, 29 surface of left paraproct showing position and number of large spine-like setae.

Figs. 30a,b: lateral view of left cercus of *P. chelifer* nymph. 30a area indicated by arrow shows groups of large, flat, multi-tipped setae along the outer lateral edges of annuli (finer hair-like setae occur on the opposite side along the inner lateral edges of annuli), 30b close-up of groups of large, flat, multi-tipped setae.

Figs. 31a – c: lateral view of male imago of *P. columbiae*. 31a lateral view of head, thorax, and forelegs, 31b lateral view of thorax and abdomen, 31c lateral view of abdomen and genitalia of holotype (pinned specimen).

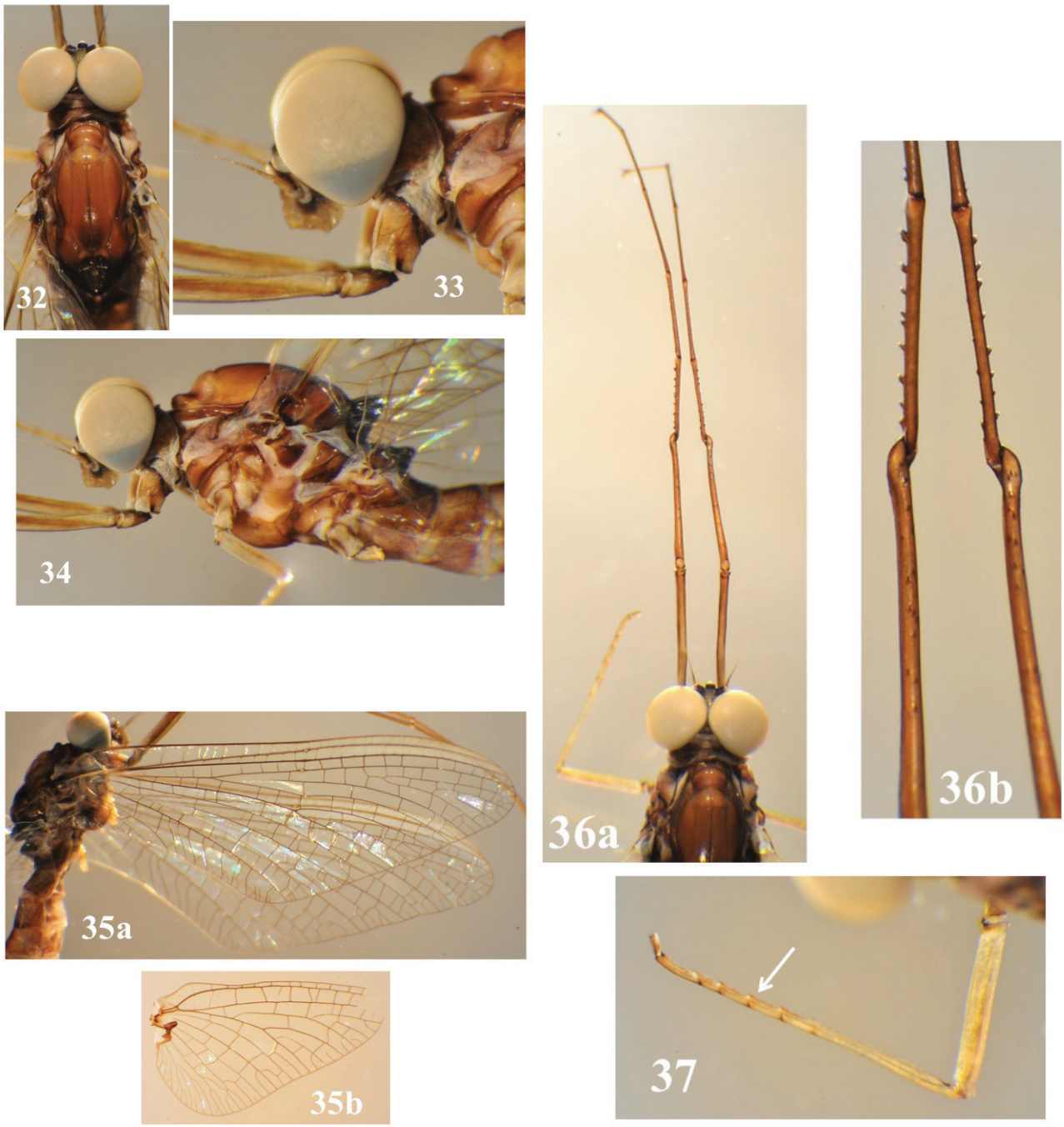


Figs. 32 – 34: head and thorax of male imago of *P. columbiae*. 32 dorsal view of head showing position of compound eyes and details of mesonotum, 33 lateral view of head showing antennae and frons, 34 lateral view of thorax showing wing and leg bases.
Figs. 35a,b: wings of male imago of *P. columbiae*. 35a forewings on intact specimen, 35b hindwing detached, wing apex with small damaged area.
Figs. 36 – 37: legs of male imago of *P. columbiae*. 36a dorsal view of forelegs, 36b detailed view of tibiae and tarsal segment $T_1$ showing blunt spines and knobs, 37 mid leg showing ventral edge of tarsal segments indicated by arrow, only 4 tarsal joints visible (joint of fused segment $T_1$ indistinct).

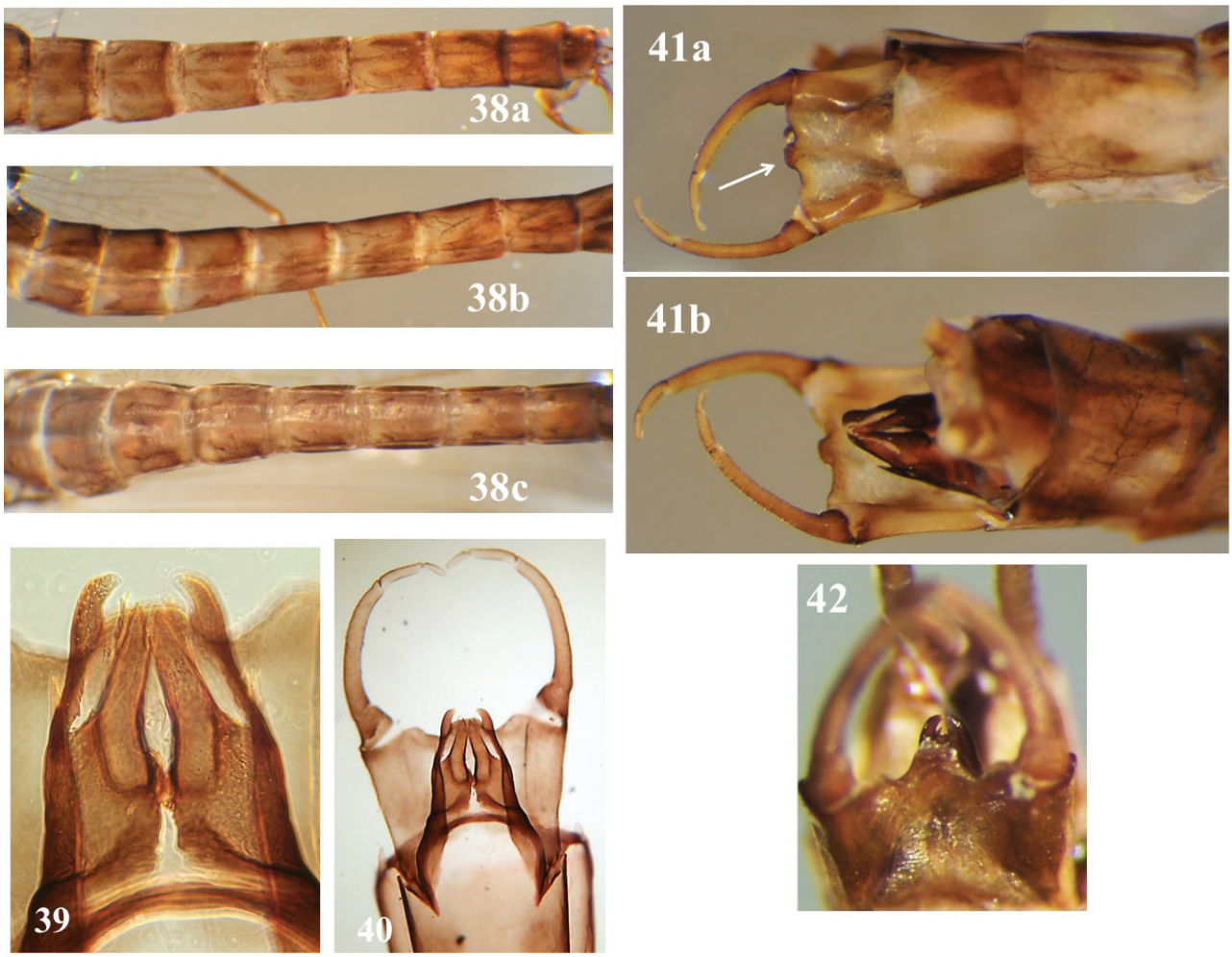


Figs. 38a – c: abdomen of male imago of *P. columbiae*. 38a dorsal view of abdominal color pattern on terga, 38b lateral view of abdominal segments showing the pleural color pattern, 38c ventral view of color pattern of abdominal sterna.
Figs. 39 – 40: male genitalia of paratype of *P. columbiae* (slide mounted). 39 dorsal view of penes showing accessory spines, 40 dorsal view of penes and forceps.
Figs. 41 – 42: male genitalia of *P. columbiae* (intact). 41a ventral view showing projection on posterior margin of styliger plate between forceps bases, indicated by arrow, 41b dorsal view of penes relative to styliger plate and tergite X, 42 ventral view of styliger plate showing median projection and tips of penes (holotype – pinned specimen).

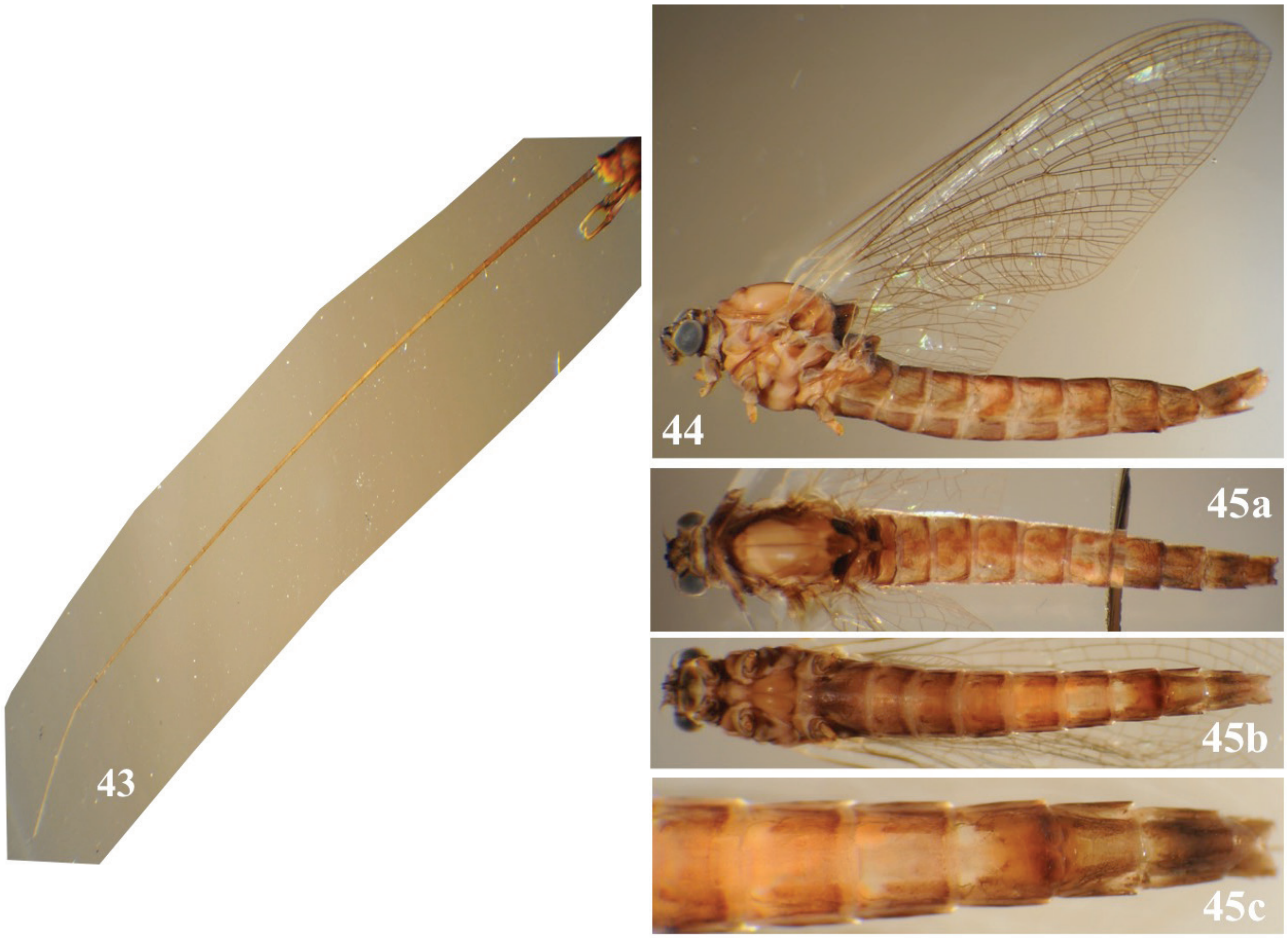


Fig. 43: lateral view of intact caudal filament of male imago of *P. columbiae*.

Figs. 44 – 45: body of dark brown color morph of female imago of *P. columbiae*. 44 lateral view of head, thorax, and abdomen, 45a dorsal view of color patterns of head, thorax, and abdomen, 45b ventral view of color patterns of head, thorax, and abdomen, 45c ventral view of color patterns of genital sterna VII – VIII.

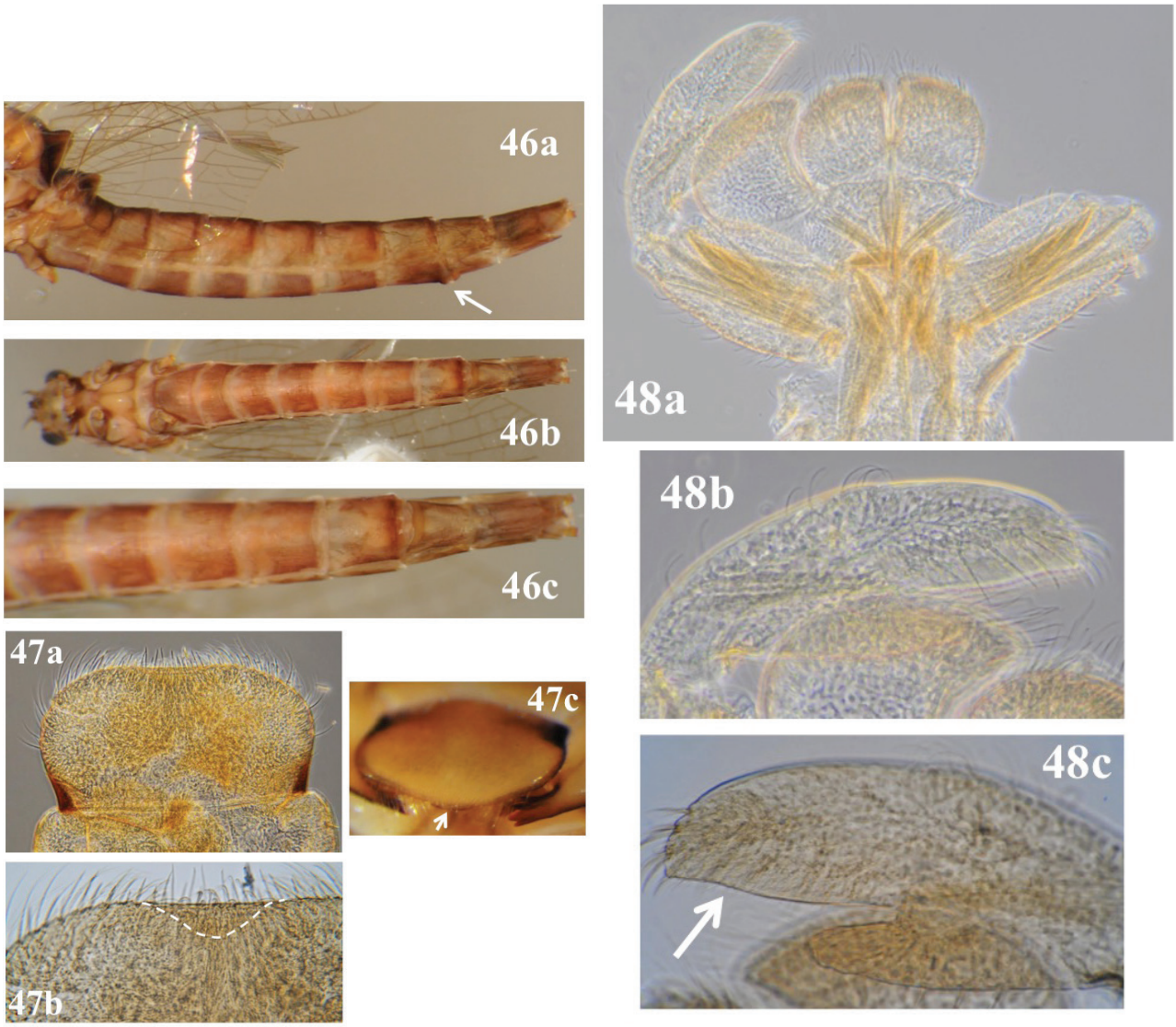


Figs. 46a – c: body of light brown color morph of female imago of *P. columbiae*. 46a lateral view of color patterns of abdominal segments and appearance of genital opening (indicated by the arrow), 46b ventral view showing color patterns of abdominal sterna, 46c ventral view of color patterns of genital sterna VII – VIII.

Figs. 47a – d: labrum of nymph of *P. columbiae*. 47a dorsal view of labrum, 47b detailed dorsal view of setae and medial under-turned lip of anterior margin (shape and width lip indicated by dotted line), 47c frontal view of labrum with arrow indicating under-turned lip.

Figs. 48a – c: labium of nymph of *P. columbiae*. 48a ventral view of labium, 48b view of dorsal setae on surface of segment 3 of labial palp, 48c view of the shape of inner edge of segment 3 and thumb-like projection of segment 2 of labial palp.

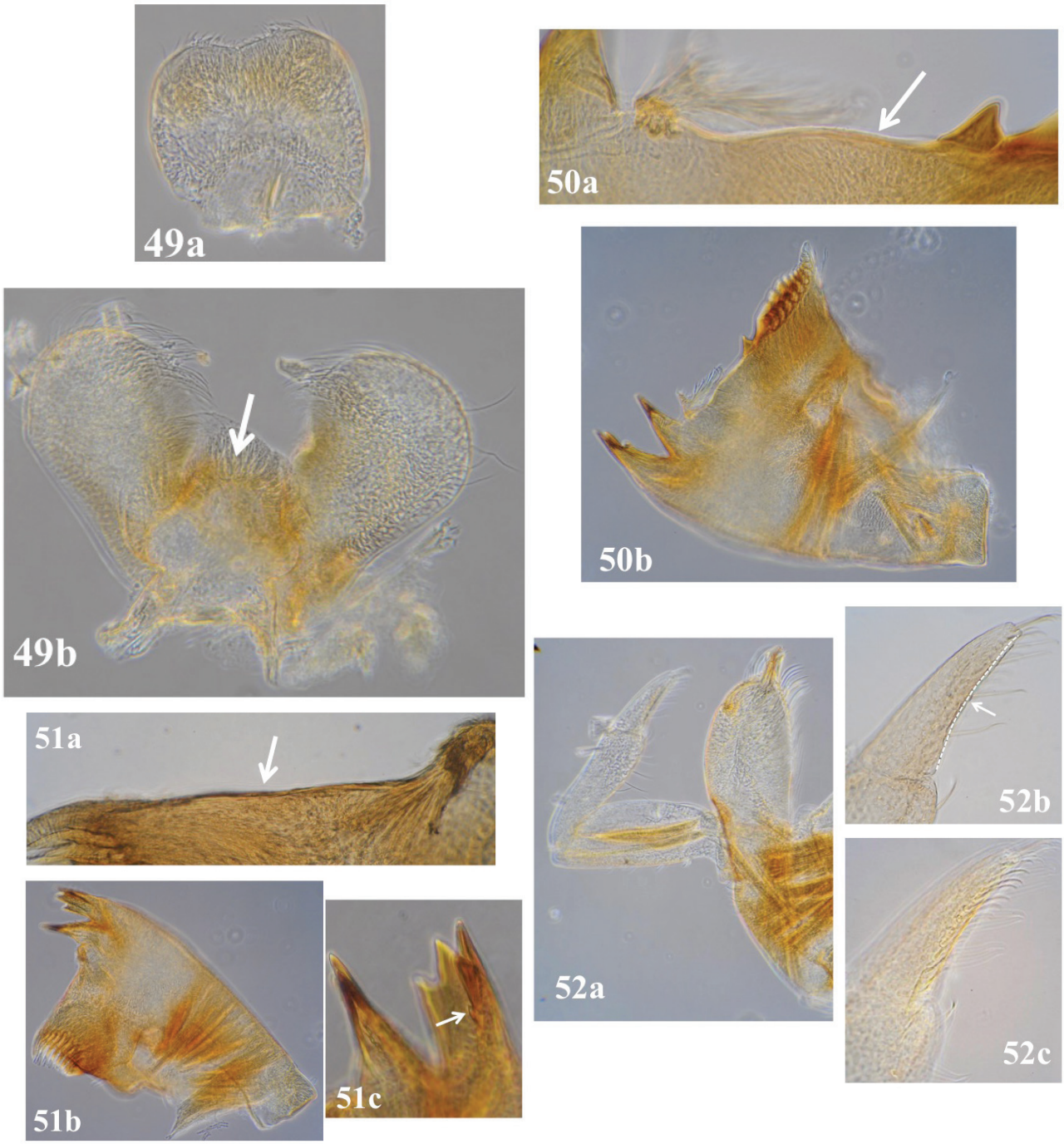


Figs. 49a,b: hypopharynx of nymph of *P. columbiae*. 49a dorsal view of detached lingua, 49b dorsal view of superlinguae with arrow indicating where detached lingua should be positioned.

Figs. 50a,b: right mandible of nymph of *P. columbiae*. 50a view of anterior margin of mandible between base of prostheca and large projection before molars (margin indicated by arrow), 50b ventral view of right mandible.

Figs. 51a – c: left mandible of nymph of *P. columbiae*. 51a view of anterior margin of mandible between base of prostheca and large projection before molars (margin indicated by arrow), 51b ventral view of left mandible, 51c ventral edge of outer incisors, arrow indicates position of small accessory tooth.

Figs. 52a – c: right maxilla of nymph of *P. columbiae*. 52a ventral view of maxilla, 52b dorsal view of setae on segment 3 of maxillary palp, dotted line indicates concave inner margin, 52c ventral view of setae on segment 3 of maxillary palp.

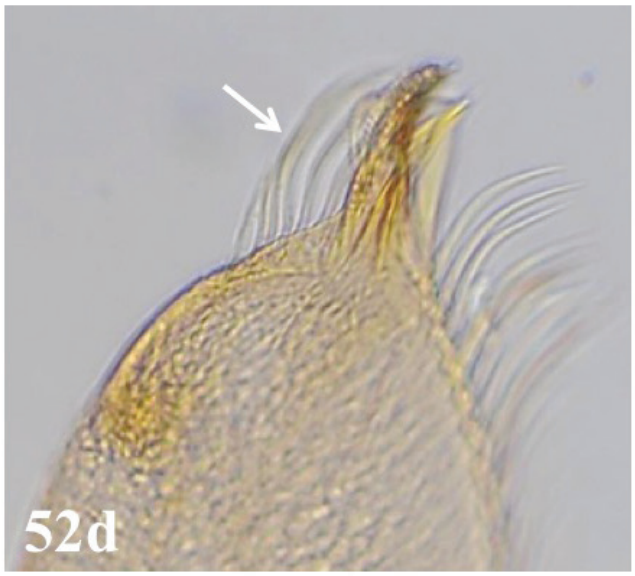


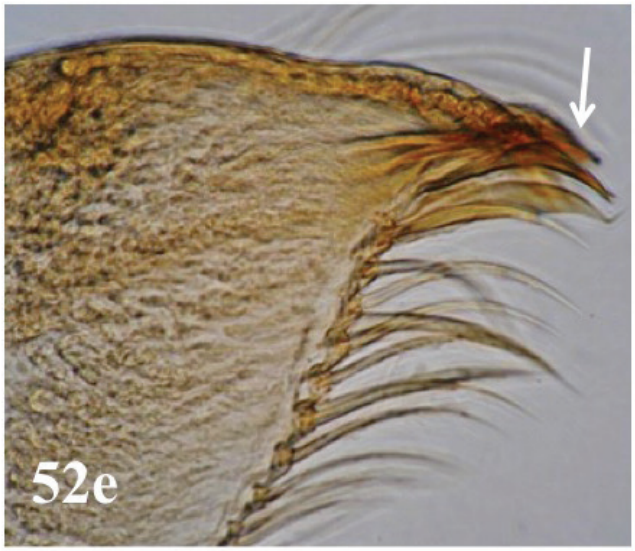



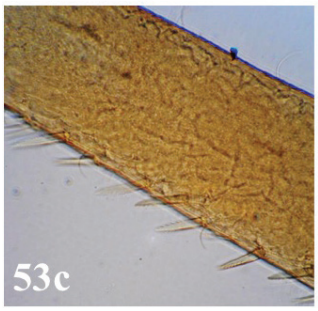


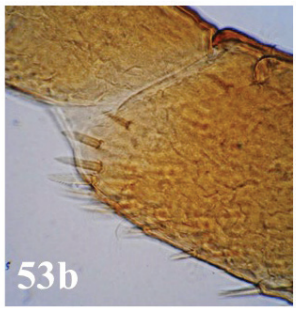



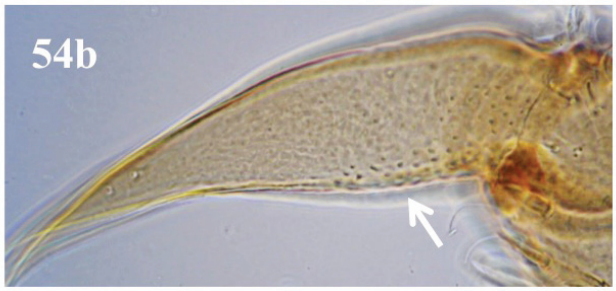


Figs. 52d,e: apex of right maxilla of nymph of *P. columbiae*. 52d arrow indicates short row of large pectinate setae on crown of galea-lacinia, 52e apex of galea-lacinia showing large canines (indicated by arrow) and dentisetae along inner edge below canines.

Figs. 53a – c: leg of nymph of *P. columbiae*. 53a dorsal view of all leg segments, 53b lateral view of apex of tibia showing large setae at joint with tarsus, 53c lateral view of setae along inner edge of tarsus.

Figs. 54a,b: tarsal claw of nymph of *P. columbiae*. 54a lateral view of claw with arrow indicating position of minute denticles at base of claw, bracket indicates the extent of the claw that lacks denticles and gradually tapers to the apex, 54b lateral view of claw with arrow indicating the areal extent of minute denticles.

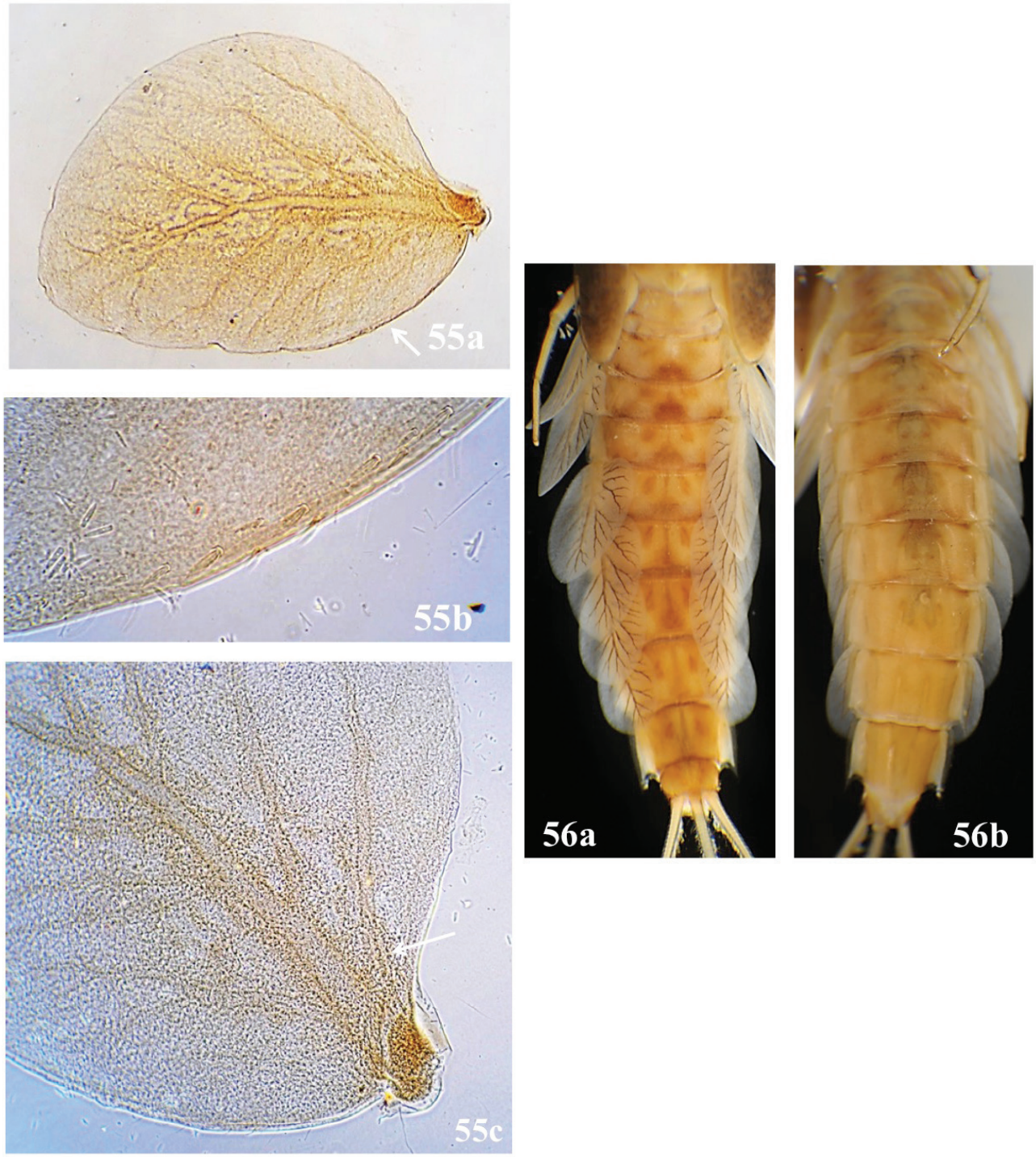


Figs. 55a,b: abdominal gill of nymph of *P. columbiae*. 55a lateral view of gill 3 with arrow indicating ventral sclerotized edge, 55b detailed view of setae along ventral sclerotized edge.

Fig. 55c: detailed view of branching pattern of trachea in gill 3, arrow indicates position of sclerotized mid-rib near base of gill.

Figs. 56a,b: abdominal color patterns of nymph of *P. columbiae*. 56a dorsal view of abdomen showing pattern of paired brown spots on terga II -X, 56b ventral view of abdomen showing pattern of faint brown spots and posterior band on sterna II – VI and faint paired spots on sterna VII - IX.

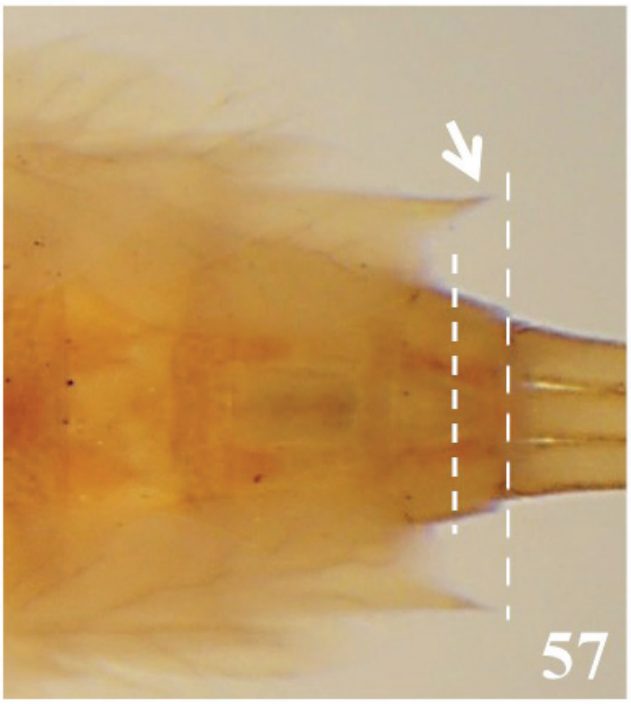


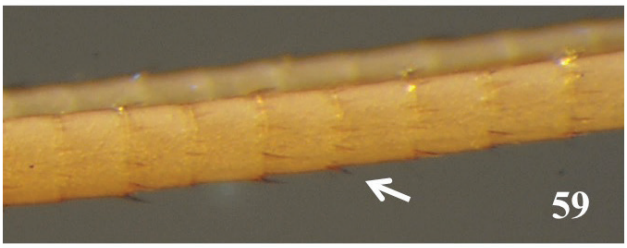





Figs. 57 – 58: features of abdominal segment IX and paraprocts of nymph of *P. columbiae*. 57 relative length of PLPs tergite IX to the overall length of tergite X, thick dotted line marks midpoint of tergite X and the thin dotted line marks the extent of the tips of PLPs tergite IX, 58 left paraproct showing distribution of large spine-like setae on surface.

Fig. 59: view of setae along the outer edges of cerci of nymph of *P. columbiae*, arrow indicates dark thin setae restricted to posterior edges of annuli.

Figs. 60a,b: lateral view of male imago of *P. croesus*. 60a lateral view of head, thorax, and abdomen of specimens from St. Croix River MN/WI border, 60b lateral view of the head, thorax, and abdomen holotype (pinned specimen).

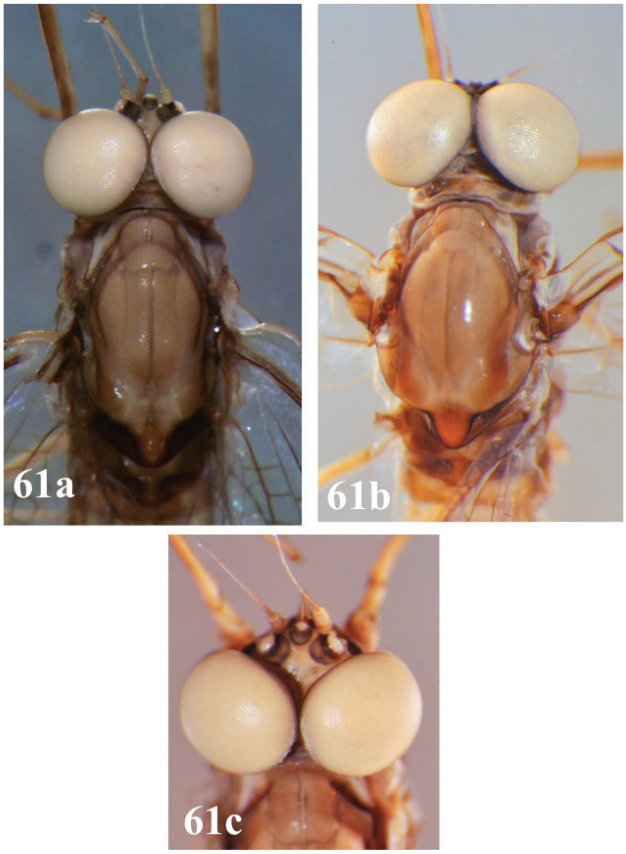


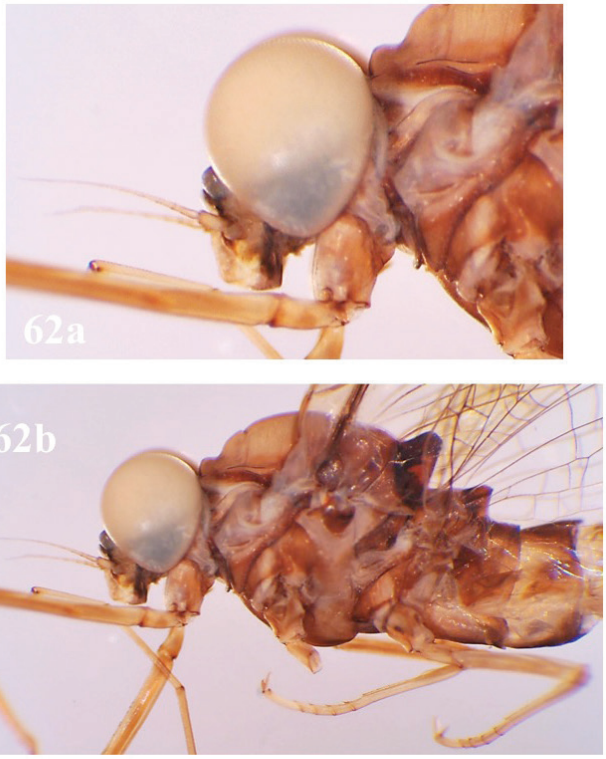


Figs. 61a – c: head and thorax of male imago of *P. croesus*. 61a dorsal view of dark color morph, 61b dorsal view of lighter color morph, 61c view of head showing position and color of compound eyes, ocelli, and antennae.
Figs. 62a,b: lateral view of head and thorax of male imago of *P. croesus*. 62a lateral view of head showing frons and antennal bases, 62b lateral view of thorax showing wing and leg bases as well as dark shading on meso- and metanotum.

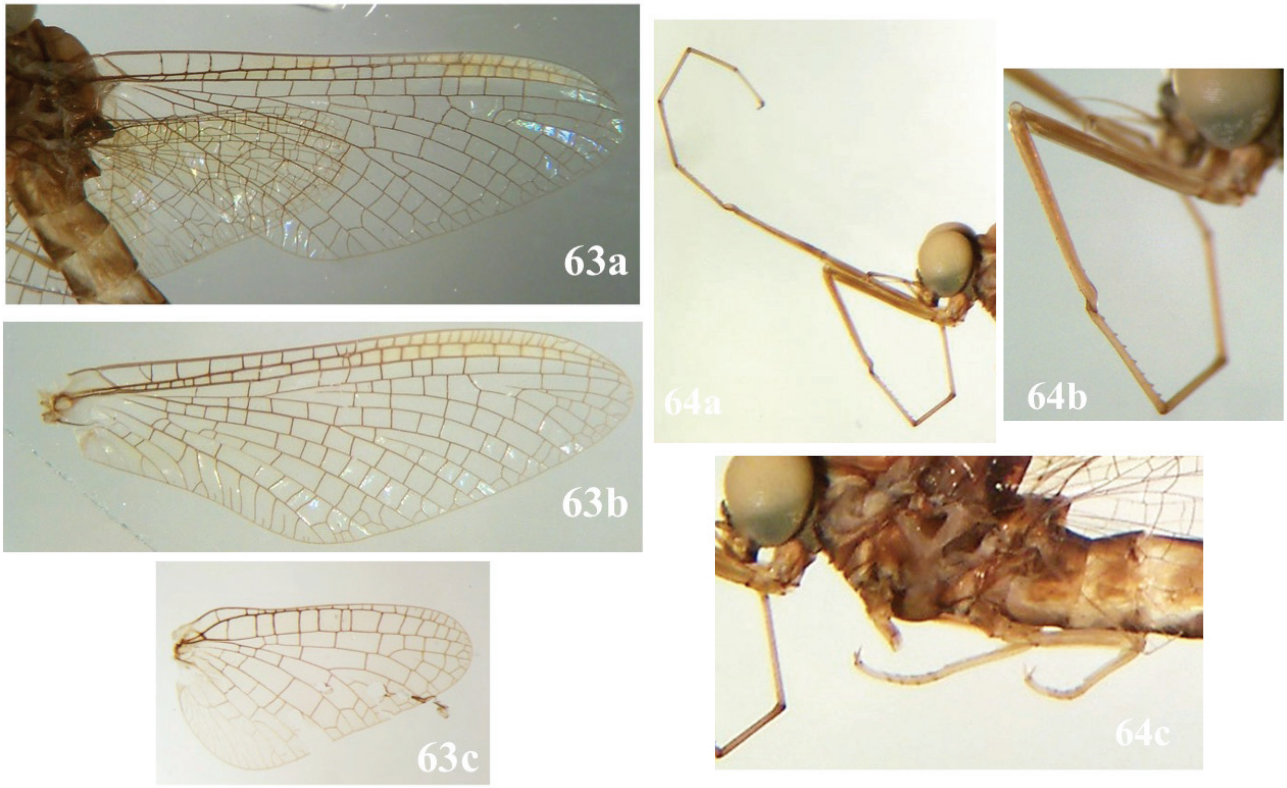


Figs. 63a – c: wings of male imago of *P. croesus*. 63a intact wings of male imago (MN/WI specimen), 63b forewing detached and flattened under glass slide, 63c hind wing detached and flattened under glass slide with small damaged area along hind margin.
Figs. 64a – c: legs of male imago of *P. croesus*. 64a lateral view of foreleg, 64b lateral view of foretibia and tarsal segment $T_1$ showing blunt spines, 64c lateral view of mid and hind legs.

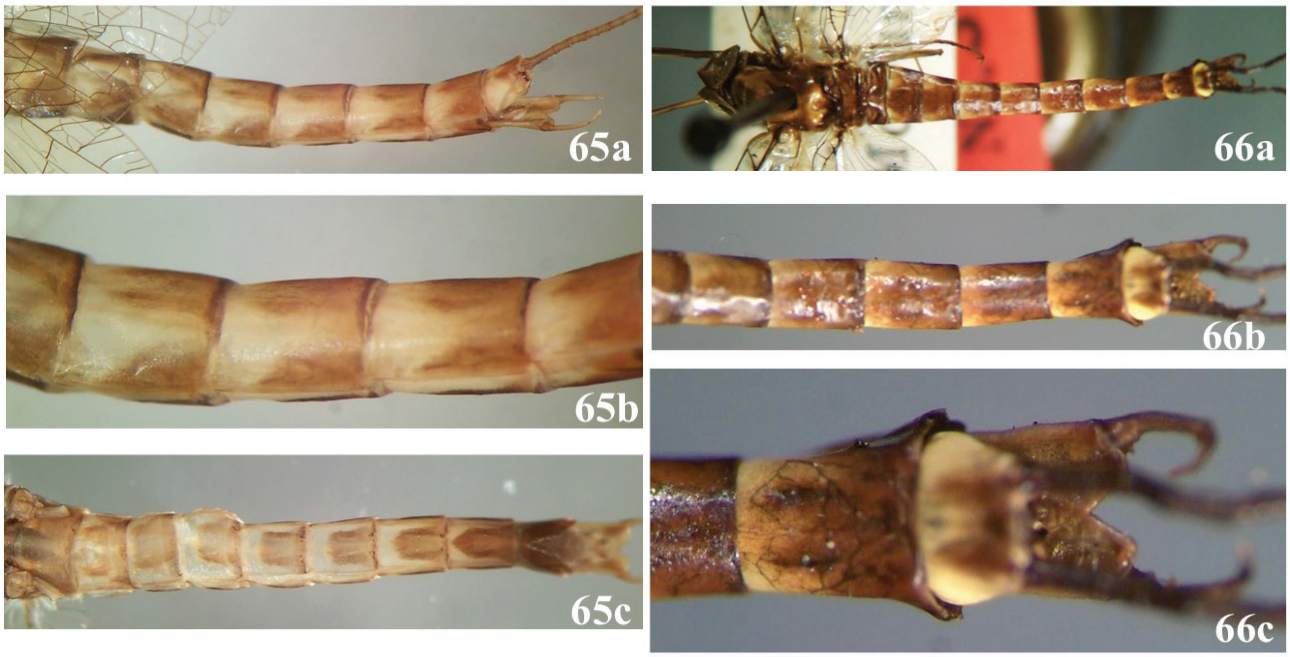


Figs.65a – c: abdomen of male imago of *P. croesus* (MN/WI specimen). 65a dorsal and lateral view of abdomen and genitalia, 65b view of abdominal terga VI – IX, 65c ventral view of abdominal sterna I – IX.
Figs. 66a – c: abdomen of male imago of *P. croesus* (holotype). 66a dorsal view of head, thorax and abdomen, 66b dorsal view of abdominal terga V – X, 66c dorsal view of abdominal tergite IX and deep v-shaped notch in posterior margin of the styliger plate of sternite IX, forceps arising from edges of styliger plate.

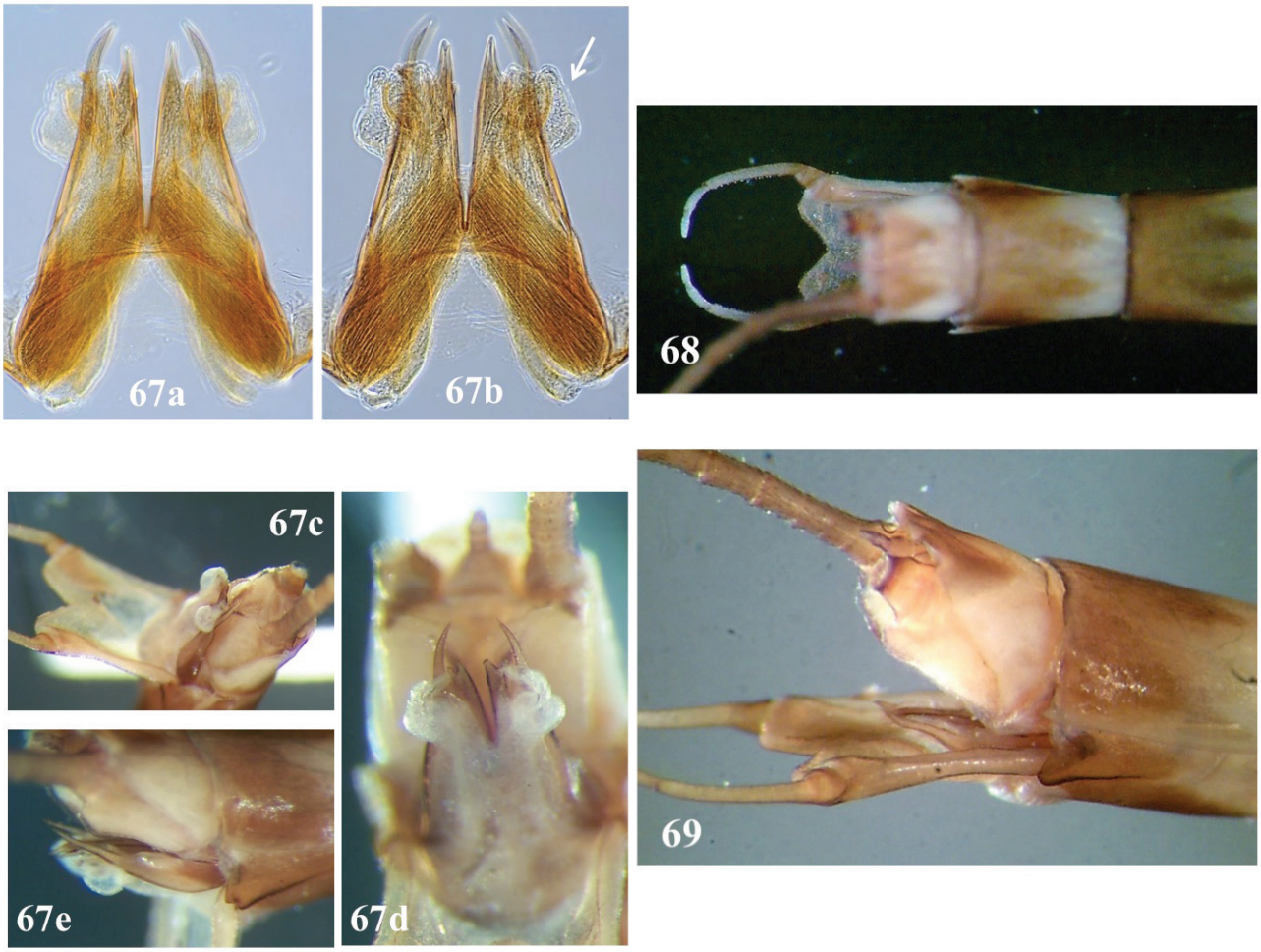


Figs. 67a,b: male genitalia of *P. croesus* (slide mounted). 67a dorsal view of penes, 67b ventral view of penes, arrow indicates membranous intromittent organs.

Figs. 67c – e: male genitalia of *P. croesus* (intact). 67c apical view of penes with styliger plate positioned ~90º to midline of abdomen, 67d ventral view of penes and inflated membranous intromittent organs, 67e lateral view of penes showing position of dorsal spines and ventral membranous intromittent organs.

Figs. 68 – 69: male genital segments of abdomen of *P. croesus*. 68 dorsal view of styliger plate and forceps showing deep v-shaped median notch in posterior margin of styliger plate, 69 lateral view of abdominal segment X and position of styliger plate and penes roughly parallel to midline of abdomen.

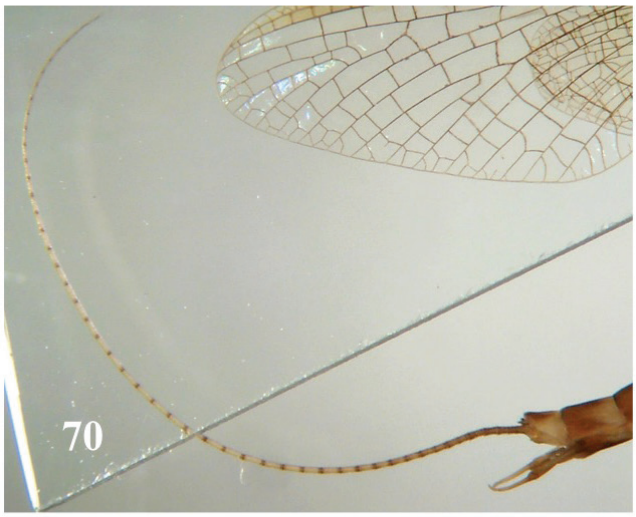



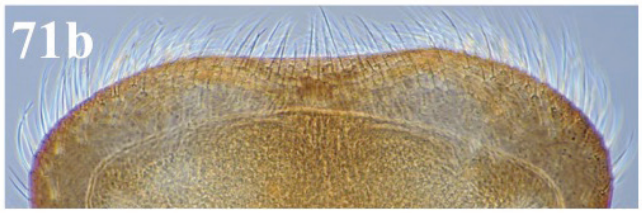


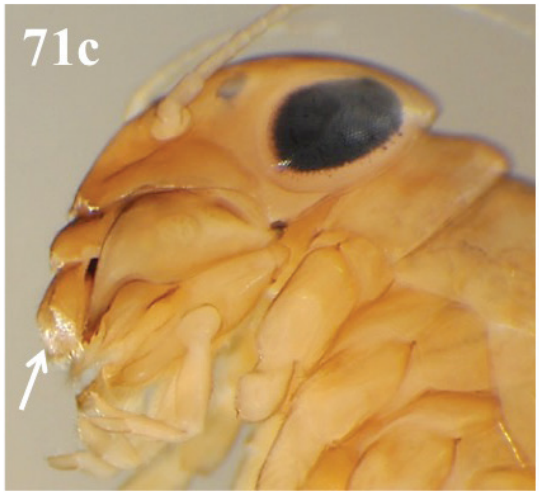


Fig. 70: lateral view of intact caudal filament of male imago of *P. croesus*.

Figs. 71a – c: labrum of nymph of *P. croesus*. 71a dorsal view of labrum and surface setae, 71b detailed dorsal view of setae and under-turned anterior edge, 71c lateral view of labrum, arrow indicates the angled anterior edge and raised dorsal surface.



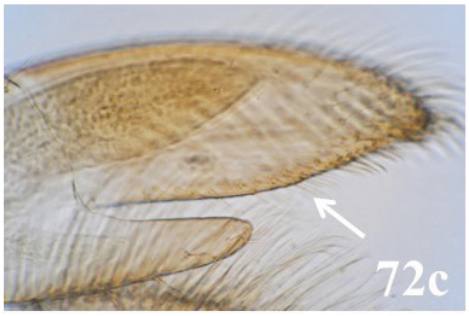




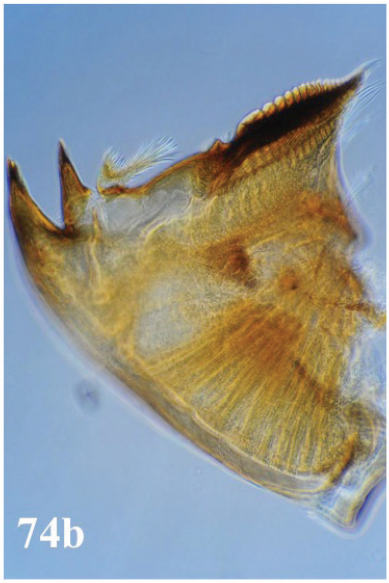


Figs. 72a – c: labium of nymph of *P. croesus*. 72a ventral view of labium, 72b view of dorsal surface setae on segment 3 of labial palp, 72c view of setae along ventral edge of segment 3 of labial palp, arrow indicates shape of inner edge.

Fig. 73: dorsal view of hypopharynx showing lingua and superlinguae of nymph of *P. croesus*.

Figs. 74a,b: right mandible of nymph of *P. croesus*. 74a view of anterior margin of mandible between base of prostheca and projection before molars, arrow indicates rough surface texture, 74b ventral view of right mandible.

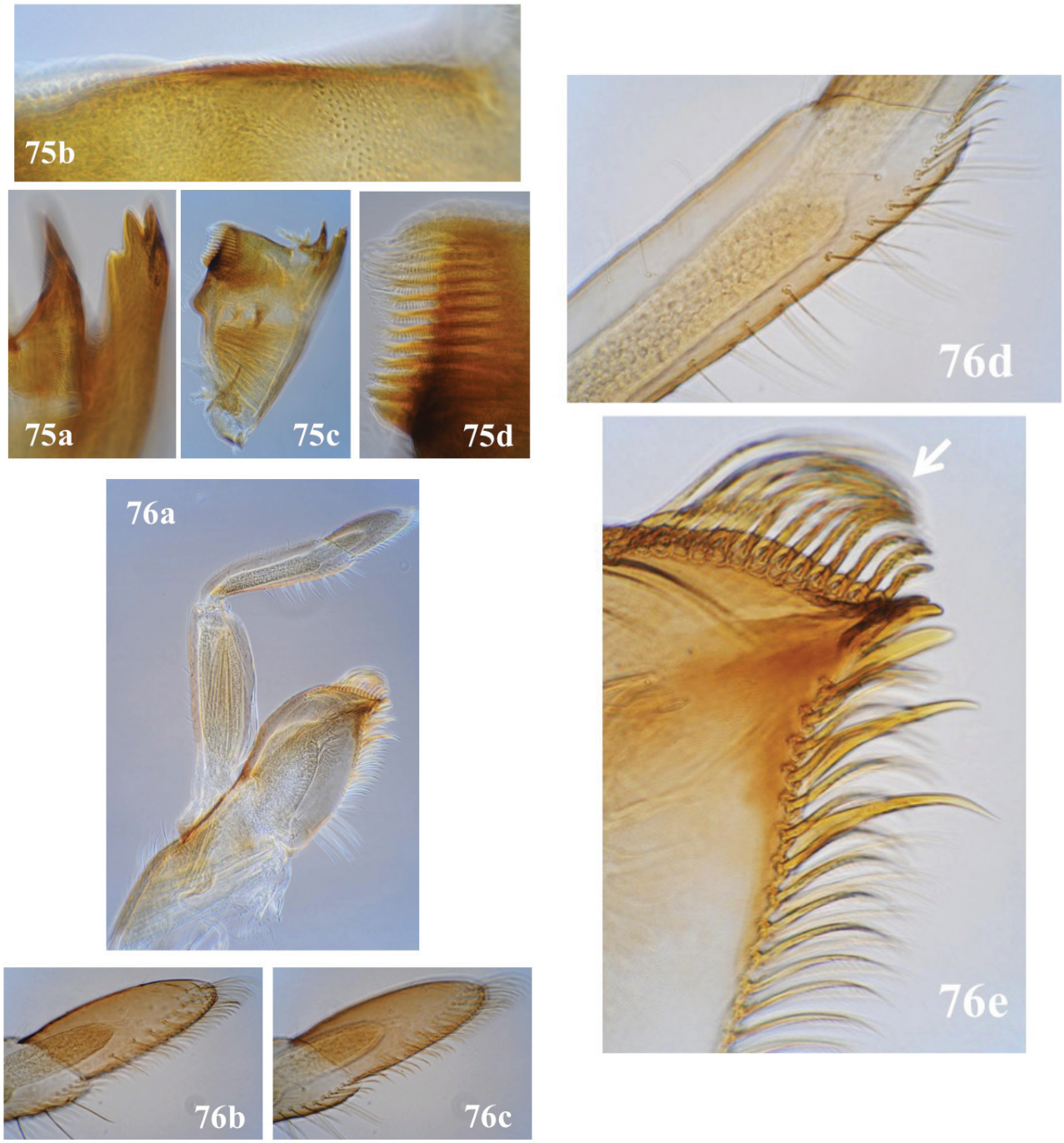


Figs. 75a – d: left mandible of nymph of *P. croesus*. 75a view of ventral edge of outer incisor, 75b view of anterior margin of mandible between base of prostheca and projection before molars, arrow indicates rough surface texture, 75c ventral view of left mandible, 75d ventral view of molar surface.

Figs. 76a – c: right maxilla of nymph of *P. croesus*. 76a ventral view of maxilla, 76b dorsal view of row of widely spaced long setae on segment 3 of maxillary palp, 76c ventral view of row of closely spaced setae on segment 3 of maxillary palp.

Figs. 76d,e: right maxilla of nymph of *P. croesus*. 76d view of long setae along ventral edges of segment 2 of maxillary palp, 76e crown of galea-lacinia with row of large pectinate setae (indicated by arrow), apex of galea-lacina with 3 large canines and 3 dentisetae below canines.

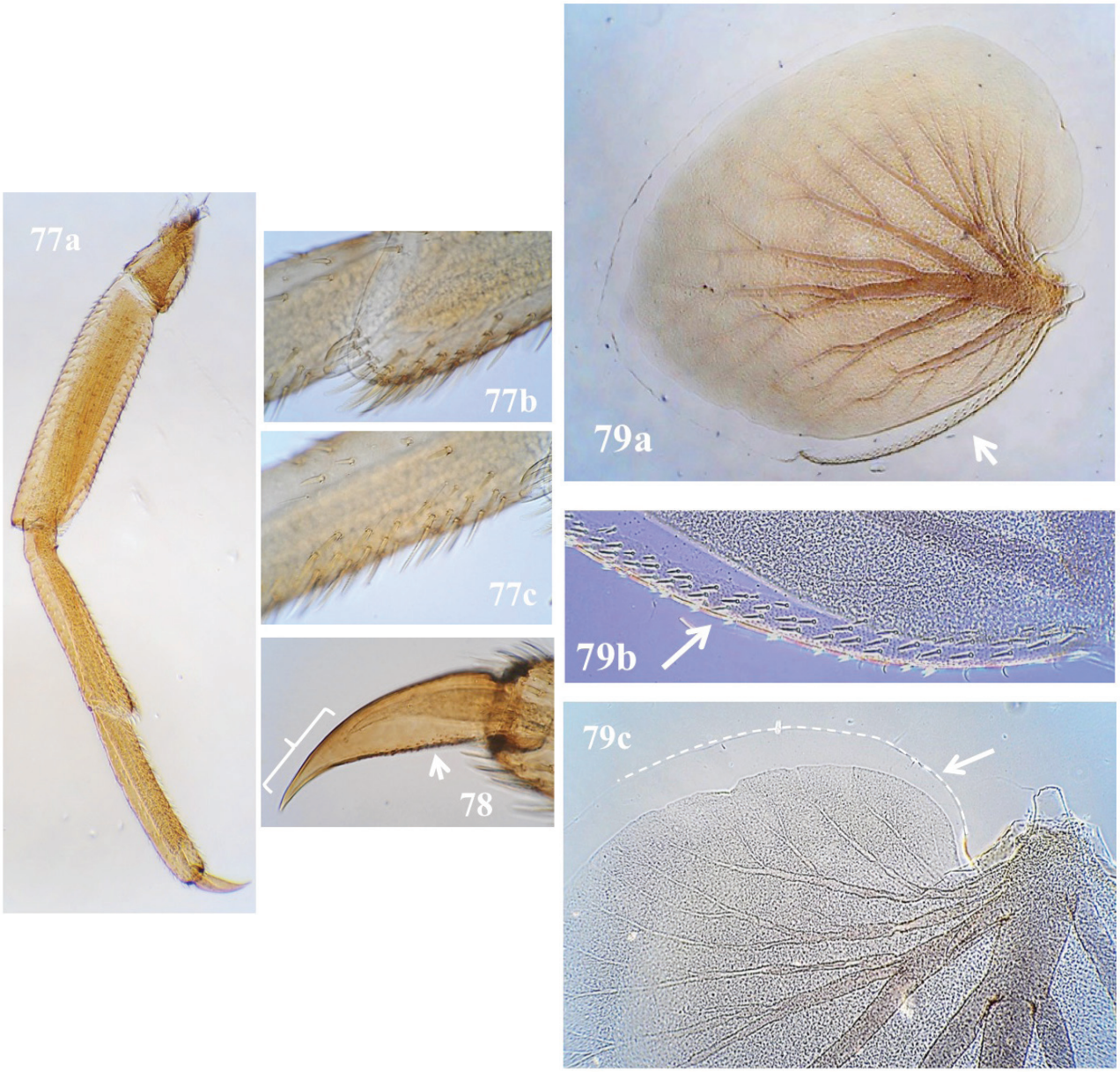


Figs. 77a – c – 78: leg of nymph of *P. croesus*. 77a dorsal view of all leg segments, 77b lateral view of apex of tibia showing large setae at joint with tarsus, 77c lateral view of setae along inner surface of tarsus, 78 lateral view of tarsal claw, arrow indicates areal of small denticles at base of claw in relation to portion of claw that tapers to apex (indicated by bracket).

Figs. 79a,b: abdominal gill of nymph of *P. croesus*. 79a lateral view of gill 3, arrow indicates ventral sclerotized edge, 79b view of setae along ventral sclerotized edge of gill 3.

Fig. 79c: view of dorsal lobe-like edge of gill 3 (dotted line follows the edge of the gill lamella), basal branching pattern of secondary trachea, and virtually transparent mid-rib.




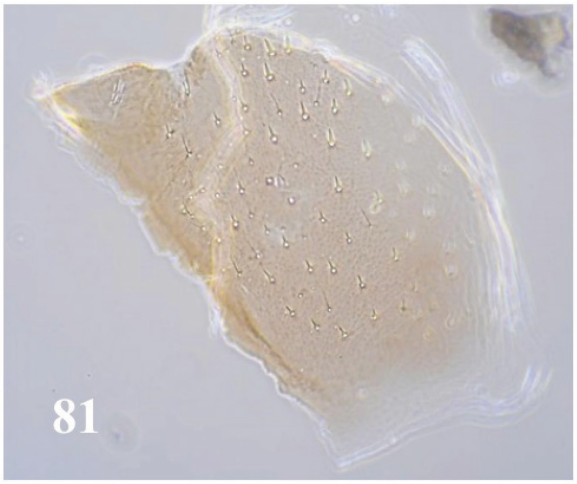


Fig.80a: dorsal view of abdomen of nymph of *P. croesus*, arrows indicate PLPs-terga I – IX (where not covered by gills).
Figs. 80b,c: color patterns of abdomen of nymph of *P. croesus*. 80b dorsal view of color patterns on terga, 80c ventral view of color patterns on sterna, dark median brown areas visible through the cuticle on sterna VII – IX actually occur on the male subimago developing within this last instar male nymph.
Fig. 81: surface of left paraproct of nymph of *P. croesus* showing distribution of large spine-like setae.

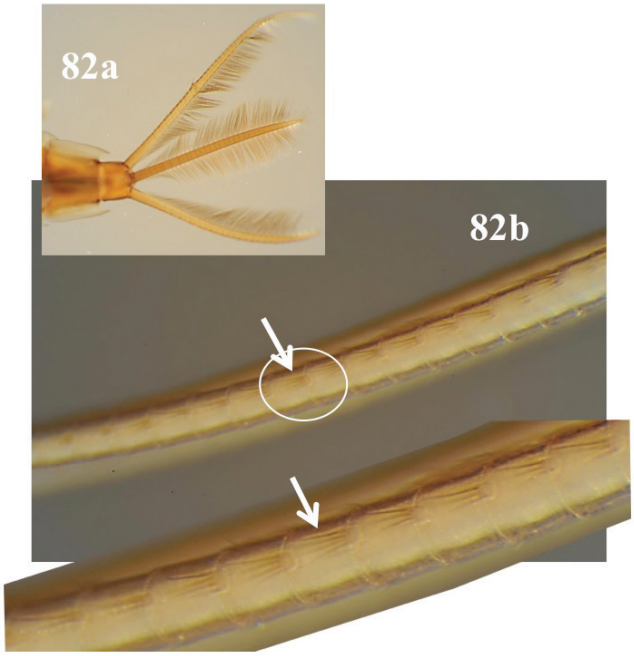






Figs. 82a,b: caudal filaments of nymph of *P. croesus*. 82a dorsal view of all 3 caudal filaments, 82b outer edge of cerci, circle and arrow indicate group of large thick setae (some with divided tips) typical of posterolateral edges of most annuli.
Fig. 83: dorsal-lateral view of male imago of *P. midas* (Maine specimen).
Figs. 84a – c: head and thorax of male imago of *P. midas*. 84a dorsal view of head and thorax of light yellow-brown color morph, 84b dorsal view of head showing ocelli, antennae, and color of vertex between compound eyes, 84c ventrolateral view of head showing coloration of gena and frons.

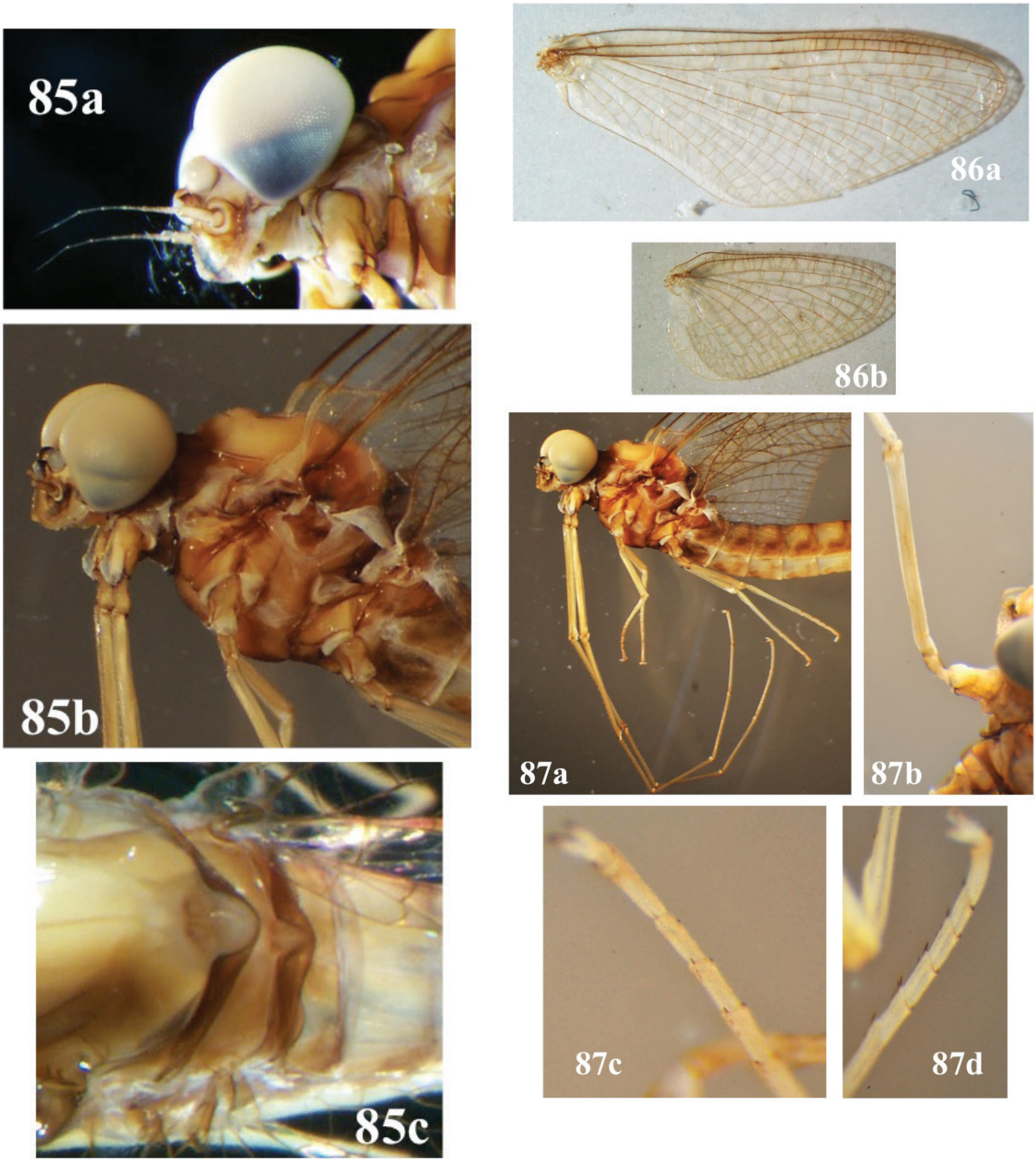


Figs. 85a – c: lateral view of head and thorax of male imago of *P. midas*. 85a lateral view of head, 85b lateral view of head and thorax, 85c dorsal view of SL and ISL of meso- and metanotum.
Figs. 86a,b: wings of male imago of *P. midas*. 86a forewing detached and flattened under glass, 86b hind wing detached and flattened under glass.
Figs. 87a – d: legs of male imago of *P. midas*. 87a lateral view of fore, middle, and hind legs, 87b dorsal view of femur of foreleg, 87c ventral view of tarsal segments of mid leg showing ventral spines, 87d lateral view of tarsal segments of hind leg.


Figs. 88a,b: abdomen of male imago of *P. midas*. 88a full lateral view of color pattern of abdominal terga and sterna of darker brown-yellow color morph, 88b lateral view of color pattern of abdominal terga and sterna of typical yellow-brown color morph.
Figs. 88c – f: abdominal color pattern variation among male imagos of *P. midas*. 88c dorsal view of abdominal terga of typical yellow-brown color morph, 88d ventral view of abdominal sterna of typical yellow-brown color morph, 88e dorsal-lateral view of abdominal terga of darker brown-yellow color morph, 88f full lateral view of the abdomen of typical yellow-brown color morph.

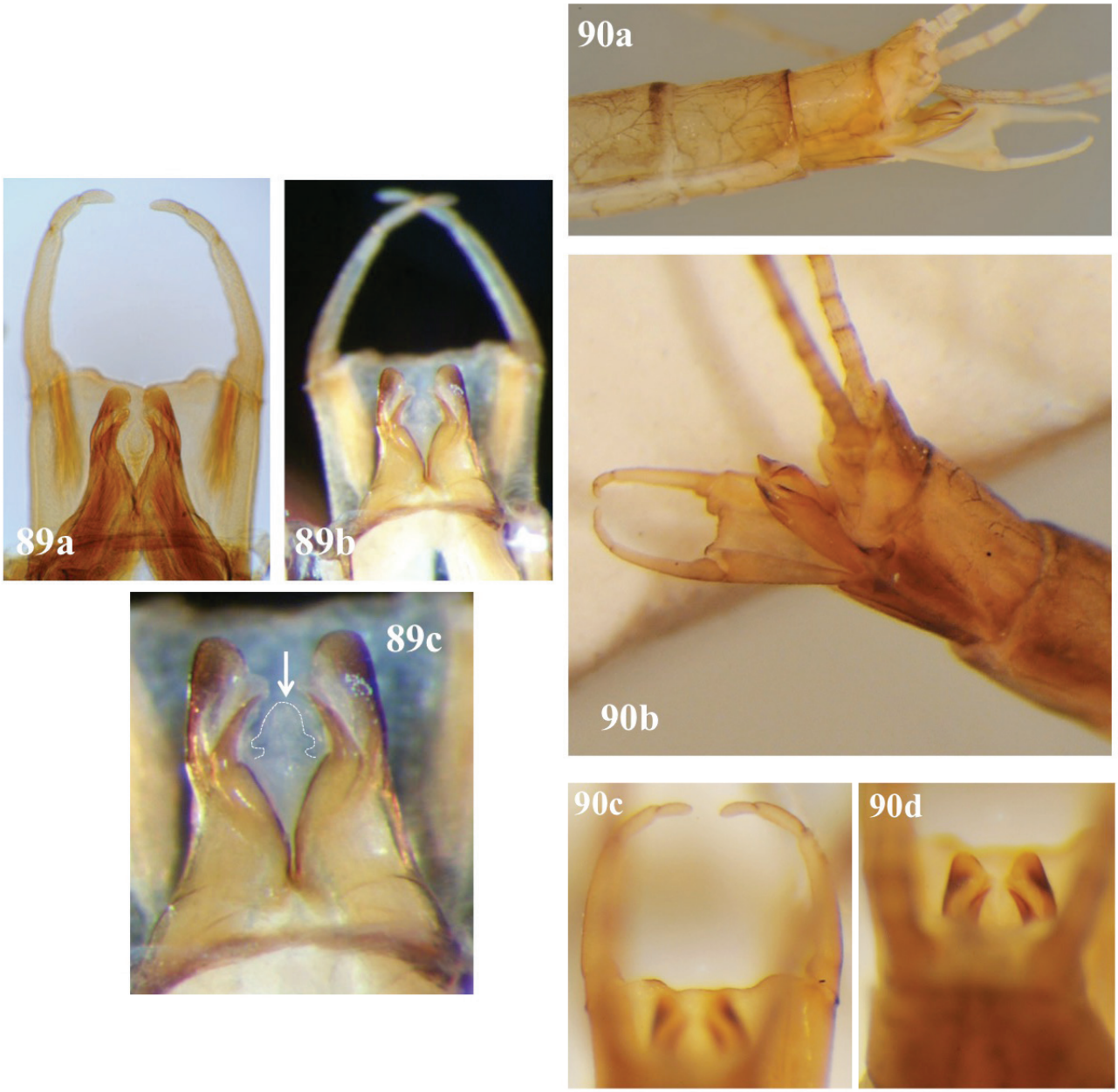


Figs. 89a – c: male genitalia of *P. midas*. 89a dorsal view of penes and styliger plate with forceps (slide mounted), 89b dorsal view of penes and styliger plate with forceps (intact specimen), 89c detailed dorsal view of penes, white dotted line and arrow indicate location of medial membranous projection (intact specimen).

Figs. 90a,b: male genital segments of *P. midas*. 90a dorsal lateral view of styliger plate, penes, and forceps of typical yellow-brown color morph, 90b dorsal lateral view of styliger plate, penes, and forceps of darker brown-yellow color morph.

Figs. 90c,d: styliger plate and penes of *P. midas*. 90c ventral view of posterior margin of styliger plate between forceps bases, 90d dorsal view showing position of tips of penes relative to posterior margin of styliger plate (styliger plate in background, out of focus).




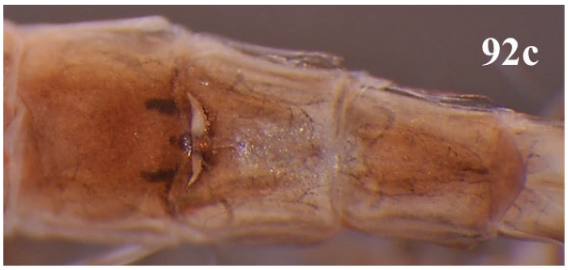


Fig. 91: lateral view of intact caudal filaments of male imago of *P. midas*.

Figs. 92a – c: lateral and ventral view of female imago of *P. midas*. 92a lateral view of head, thorax, and abdomen of most common color pattern with yellow-brown body and dark brown lateral marks, 92b ventral view of abdominal sterna of specimen shown in 92a, 92c ventral view of abdominal sterna VII – IX showing brown marks on copulatory pouches.


Figs. 93a – c: lateral, dorsal, and ventral view of female imago of *P. midas*. 93a lateral view of head, thorax, and abdomen of specimen with pale body and light brown lateral marks, 93b dorsal view of head, thorax, and abdomen of specimen shown in 93a, 93c ventral view of abdominal sterna I – VIII, no dark brown marks on copulatory pouches.

Figs. 94a,b: close-up view of abdomen of female imago of *P. midas* shown in Fig 93. 94a dorsal view of abdominal terga IV – VII (indicated by numbers) showing medial brown shading over underlying dorsal vessel, 94b detailed ventral view of abdominal sterna VII – IX showing uniform light brown shading and no dark marks on sternite VII.



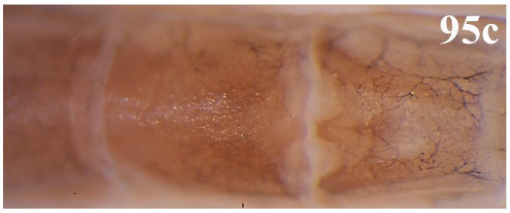




Figs. 95a – c: lateral and ventral view of female imago of *P. midas*. 95a lateral view of head, thorax, and abdomen pale body and dark brown lateral marks, 95b ventral view of abdominal sterna I – IX showing uniform light brown shading, 95c ventral view of sterna VII – IX showing pale color and no dark marks on copulatory pouches.

Figs. 96a – b: lateral view of female imago of *P. midas*. 96a lateral view of head, thorax, and abdomen of lightest cream colored form with light brown lateral marks, 96b view of broad pale area of pleural region of abdominal segments, brown areas much less distinct.


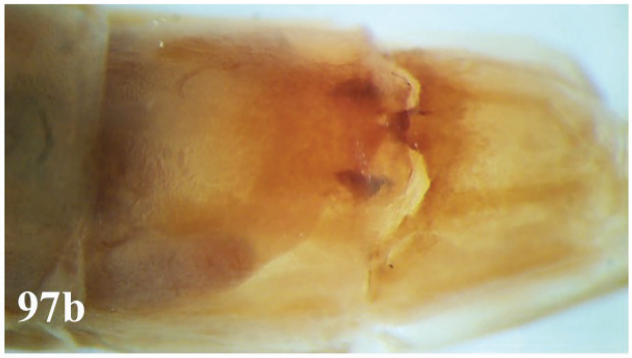


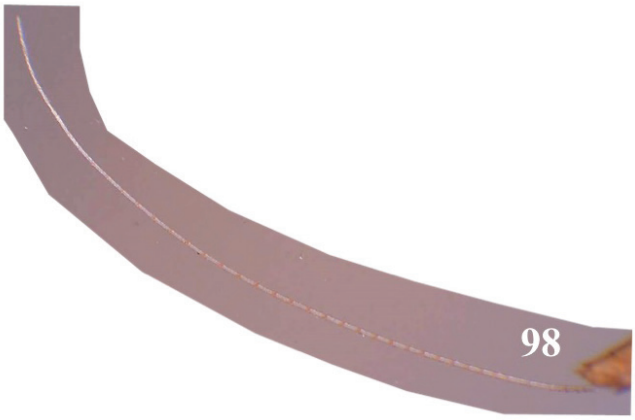


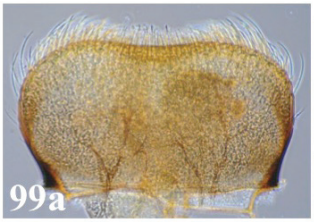


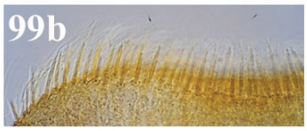


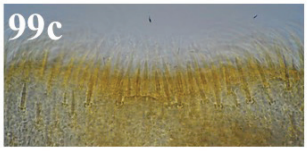





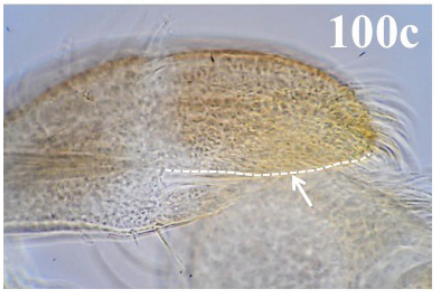


Figs. 97a – b: detailed views of genital segments of lightest cream colored female imago of *P. midas.* 97a detailed ventral view of sterna VI – IX, 97b detailed view of dark posterior margin and dark marks on copulatory pouches and bridge between pouches.

Fig. 98: lateral view of intact caudal filament of female imago of *P. midas*.

Figs. 99a – d: labrum of nymph of *P. midas*. 99a labrum dorsal view, 99b view of dense row of stout bi-serrate setae from outer corner to middle of anterior margin of labrum, 99c view of dorsal setae present across middle of anterior margin of labrum, 99d view of more widely spaced thinner setae dominant across middle of labrum.

Figs. 100a – c: labium of nymph of *P. midas*. 100a ventral view of labium, 100b view of setae on dorsal surface of segment 3 of labial palp, 100c view of ventral edge and associated setae of segment 3 of labial palp, shape of inner edge indicated by the arrow.

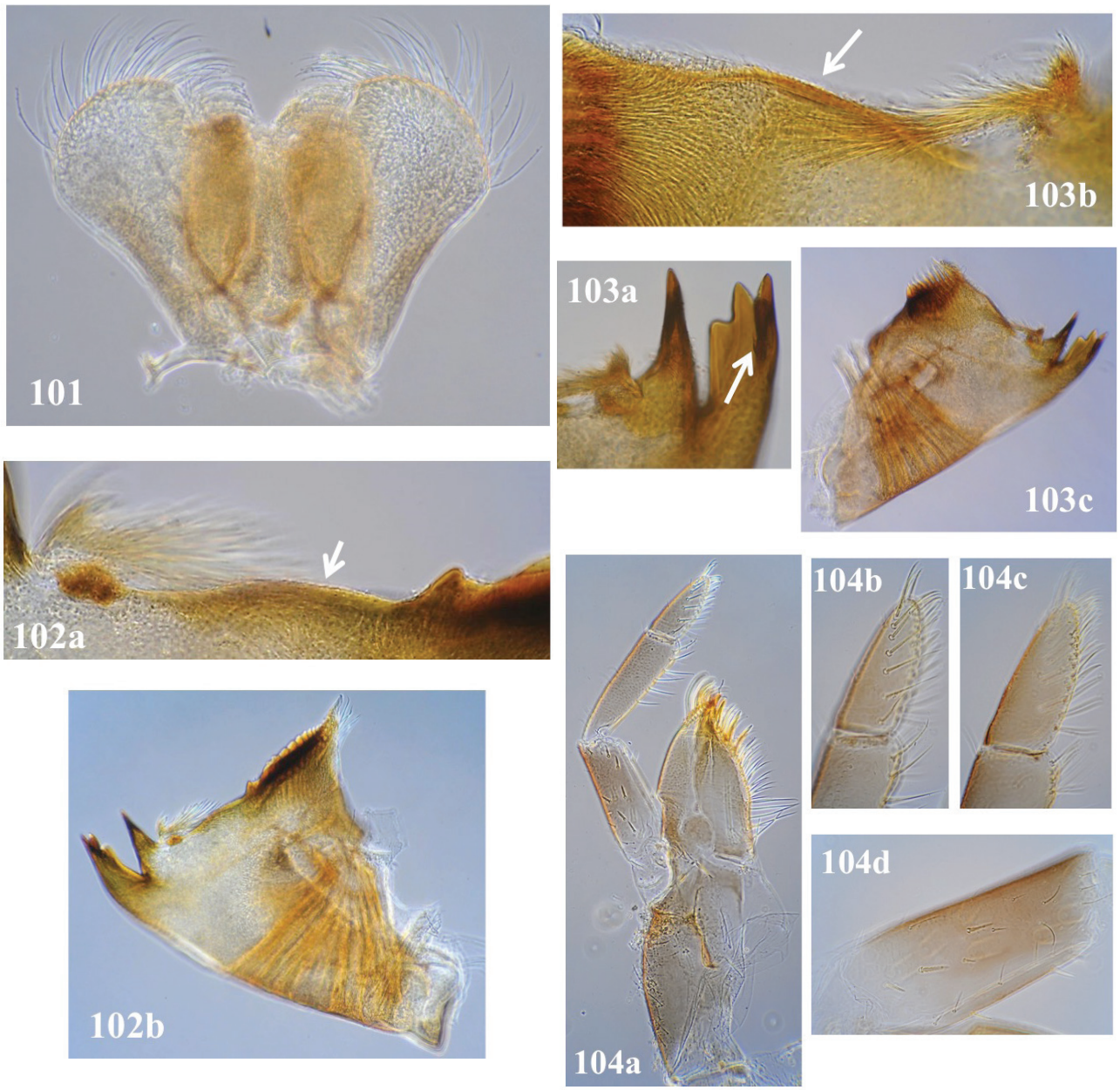


Fig. 101: dorsal view of hypopharynx showing lingua and superlinguae of nymph of *P. midas*.

Figs. 102a,b: right mandible of nymph of *P. midas*. 102a view of anterior margin of mandible between base of prostheca and projection at beginning of molars, arrow indicates rough surface texture, 102b ventral view of mandible.

Figs. 103a – c: left mandible of nymph of *P. midas*. 103a view of ventral edge of outer incisor with arrow indicating accessory tooth, 103b view of anterior margin of mandible between base of prostheca and molars, arrow indicates rough surface texture, 103c ventral view of mandible.

Figs. 104a – d: right maxilla of nymph of *P. midas*. 104a ventral view of maxilla, 104b dorsal view of widely spaced long setae on segment 3 of maxillary palp, 104c ventral view of row of closely spaced setae along edge of segment 3 of maxillary palp, 104d dorsal view of setae on surface of segment 1 of maxillary palp.

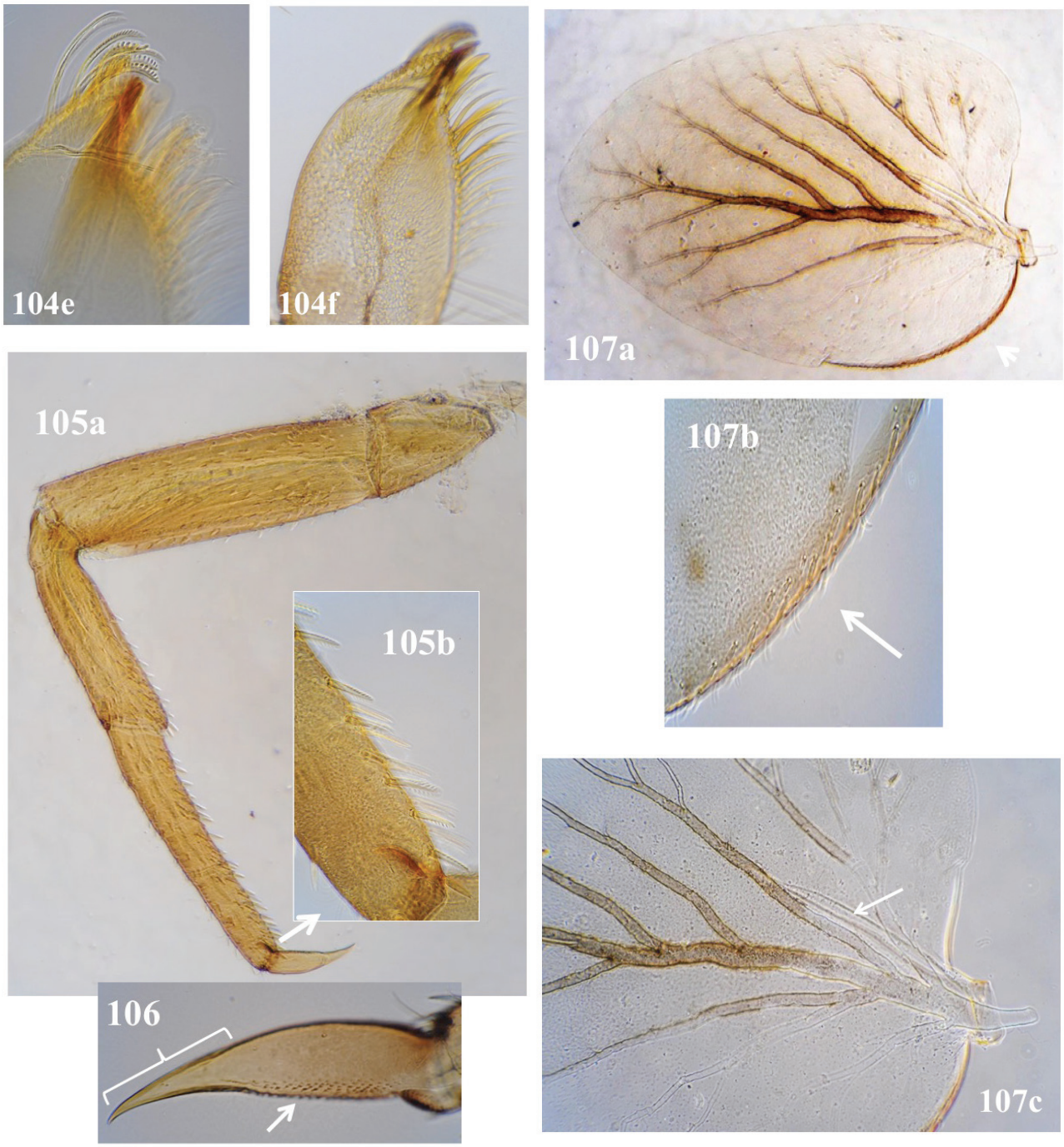


Figs. 104e,f: right maxilla of nymph of *P. midas*. 104e view of long pectinate setae at apex of galea-lacinia, 104f view of apex of galea-lacinia showing canines and dentisetae along inner edge.

Figs. 105 – 106: foreleg of nymph of *P. midas*. 105a dorsal view of all leg segments and tarsal claw, 105b lateral view of inner edge of tarsus near claw showing bi-serrate setae, 106 lateral view of tarsal claw, arrow indicates areal of small denticles at base of claw in relation to portion of claw that tapers to apex (indicated by bracket).

Figs. 107a,b: abdominal gill of nymph of *P. midas*. 107a lateral view of gill 3, arrow indicates ventral sclerotized edge, 107b view of setae along ventral sclerotized edge of gill 3.

Fig. 107c: view of basal trachea branching pattern of gill 3, arrow indicates sclerotized mid-rib at base of gill (mid-rib transparent).


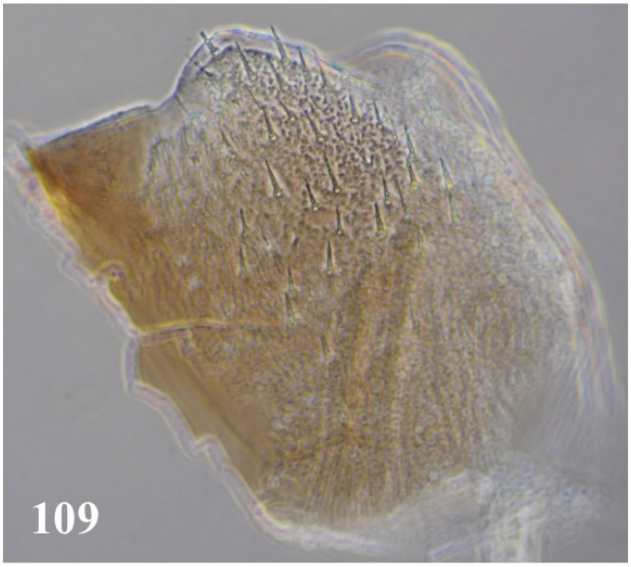


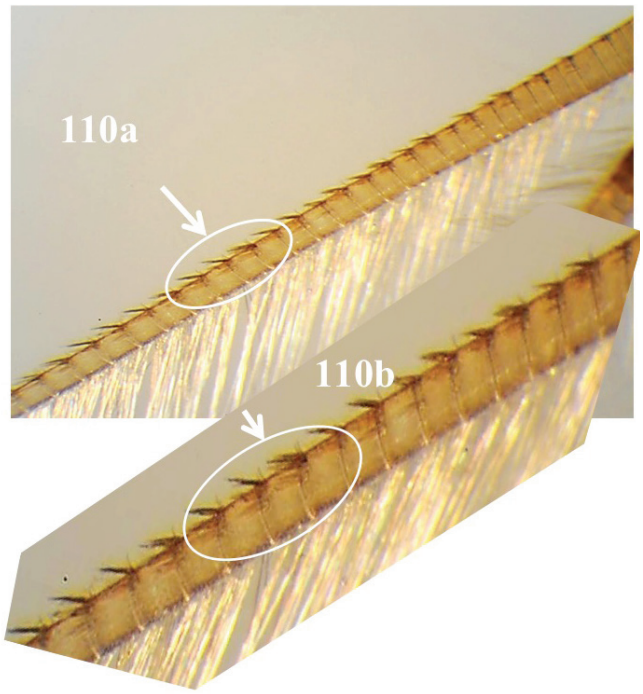


Fig. 108: color pattern of abdominal terga I – X of final instar nymphs of *P. midas*.
Fig. 109: left paraproct showing distribution of large, spine-like setae across surface.
Figs. 110a,b: lateral view of cercus of nymph of *P. midas*. 110a arrow and oval indicates typical groups of large, flat, multi-tipped setae that occur along the outer lateral edges of most annuli (fine hair-like setae occur on the inner edge of cercus), 110b close-up of groups of large, flat, multi-tipped setae.

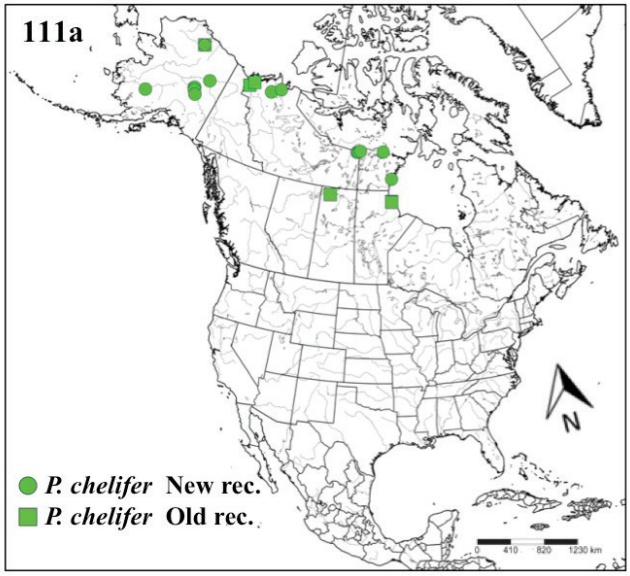


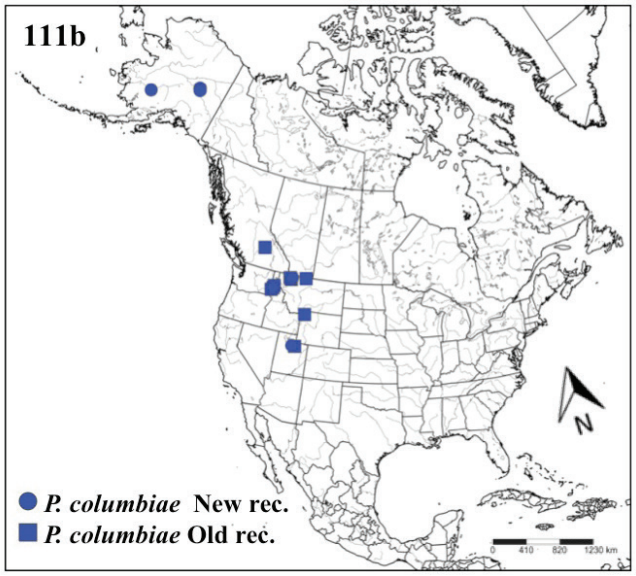


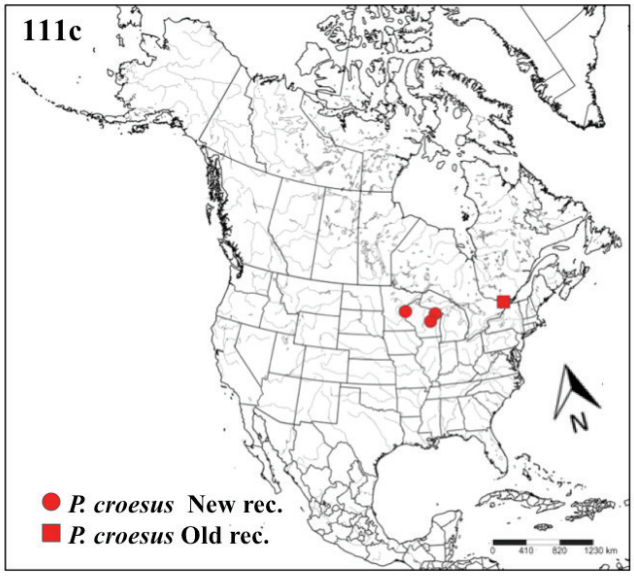


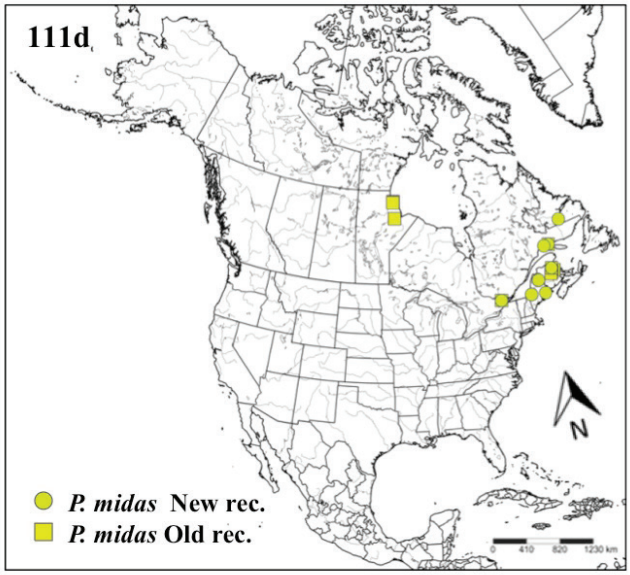


Figs. 111a: distribution of North American *Parameletus chelifer* showing the location new records and all previously published records (Append. 1).

Figs. 111b: distribution of North American *Parameletus columbiae*, showing the location of new records and all previously published records (Append. 1).

Figs. 111c: distribution of North American *Parameletus croesus*, showing the location of new records and all previously published records (Append. 1).

Figs. 111d: distribution of North American *Parameletus midas*, showing the location of new records and all previously published records (Append. 1).